7-21-2016

Linear Inlet Optimization for Capture of River Kinetic Energy

Chiu P. Yan

LINEAR INLET OPTIMIZATION FOR CAPTURE OF RIVER KINETIC ENERGY

by

Chiu Pang Yan

A Thesis

Submitted in Partial Fulfillment of the

Requirements for the Degree of

Master of Science

Major: Mechanical Engineering

The University of Memphis

July 2016

Dedication

This thesis is dedicated to my mother, my father for giving me the opportunity to succeed and supported me throughout my life, and to those who believed in me.

Acknowledgments

I would like to thank Dr. Teong Tan and Dr. Jeffrey Marchetta for serving as members of my Master Thesis Committee. Also I would like to thank each of the faculty members and graduate students in Mechanical Engineering Department for being very supportive throughout the years of my studies.

This research would not be possible without the support of Convergent Science, and their technical support on CFD: their professionalism is truly unparalleled. Also the support of the HPC department, namely Ed Koshland and Philip Barnett, and the University of Memphis IT department, namely Martha Harrell, made this research possible. Thank you.

A special thank you to the Chair of my Committee, Dr. John Hochstein. Although it has been a long year working on this research, words could not describe how lucky I consider myself to be able to work with one of the most knowledgeable faculty members on this floor. I am thankful that even when I was about to give up, you were able to continue to show optimism toward this project. I would not be here today without your guidance, and it has truly been a great roller coaster ride.

Abstract

Yan, Chiu P. MS. The University of Memphis. July, 2016. Linear Inlet Optimization for Capture of River Kinetic Energy. Major Professor: John I. Hochstein, Ph.D.

The kinetic energy in a flow such as a river or ocean current can be harvested by a partially or fully submerged turbine. Placing the turbine within a carefully designed channel has the potential to significantly increase the amount of energy that can be harvested. Computational Fluid Dynamic simulations have been performed to study the influence of the channel inlet geometry on the kinetic energy flow rate through the throat of the channel.

These simulations show that placing the turbine within a converging-diverging flow channel can significantly increase the performance of the machine. For a design space constrained by the approximate dimensions of a lower-Mississippi River barge and limited to flow channels with 2D inlets with plane walls, a 2:1 contraction ratio with an inlet half-angle of approximately 15 degrees maximizes the power available to drive the turbine.

Table of Contents

Table of Figures

Table of Tables

Nomenclature

$\dot{KE}_{n-1}$	kinetic energy flow rate from the previous iteration
$\dot{KE}_{n}$	kinetic energy flow rate from the current iteration
n	number of iteration
ρ	density
A	area
V	velocity
Δt	change of time, size of time step
AR	area ratio
Athroat	cross sectional area of the flow at the throat of the machine
Amouth	cross sectional area of the flow at the mouth of the machine

I. Background

A. Motivation

Humans have been using the force of moving river water for centuries for their benefit, as many early civilizations relied on the moving water to provide power for their machines (i.e. gristmills). As civilization progressed, more and more people realized the need for electricity, and hydroelectricity became desirable for power generation. From the mid-nineteenth century to the present, many small to large-scale power plants consisting of dams, reservoirs and turbomachinery appeared all around the world and became economic successes. Today, many hydroelectric systems face environmental challenges. [1]

Since traditional hydroelectricity is facing a scarcity of suitable installation sites, there is an increasing need for alternative forms of producing hydroelectric energy. One alternative is kinetic hydropower. This form of energy can be harvested using turbines submerged into the river. The advantage of using river turbines for electricity generation is that it does not require large infrastructure, and with no reservoir or spillways, it can be deployed in a relatively short time with a minimal amount of environmental impact. [2]

Although the river turbine technology has many advantages, there are a few disadvantages: for example, the low energy density in a typical flow makes economic viability challenging. The focus of the present research is to investigate the feasibility of increasing the flow's energy density by incorporating a carefully shaped channel into the energy capture machine as proposed by Willingham. [3]

In addition to increasing the energy density, increasing the fluid velocity at the entrance to the turbine allows for an increase in turbine rotational speed, and thereby reduces structural challenges resulting from the transmission of power at low rotational speeds.

The research started with a simple goal: create a sustainable energy system that operates without pollution. Looking around the city of Memphis, there lies the Mississippi River, the second longest river in North America. [4] In order to take advantage of the flowing river nearby, it's logical to consider using a water turbine to extract its nearly endless supply of kinetic energy.

B. Relevant Literature

At the University of Buenos Aires (FIUBA), the ISEP Research Lab developed a floating water-current turbine (WCT) concept which uses a channeling device integrated into the floatation system (Figure 1). [2]

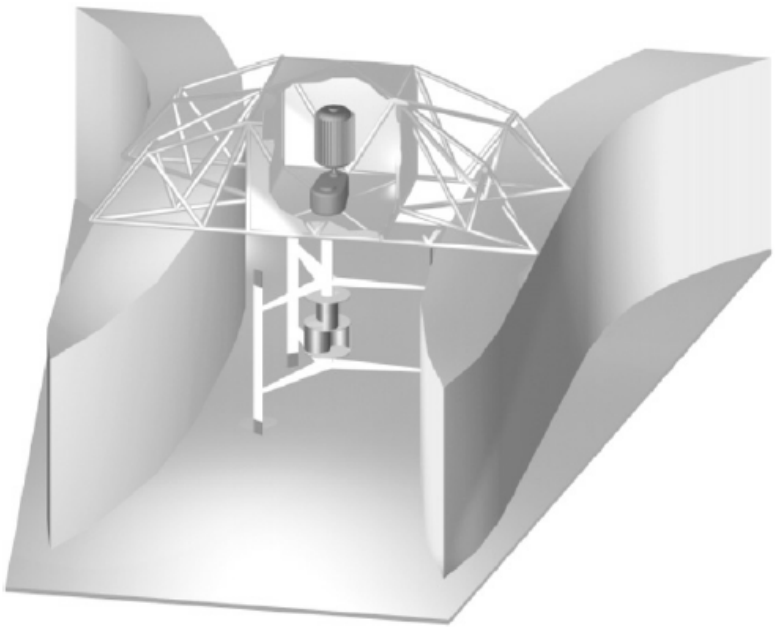

Figure 1. Perspective view of the FIUBA's diffuser-augmented floating WCT. [5]

The channeling geometry is shaped in such a way as to form a variable section open channel that helps to increase flow speed in the neighborhood of the turbine. It functions as an amplifier for the rotor's power input, or retains the same power output with smaller rotor, which in turn simplifies the design process and reduces initial cost of the unit. Ponta et al. built 24 different scale models and tested them in towing-tank facilities. Their experimental results confirmed the advantages of using a channeling device: the flow speed in the neighborhood of the rotor increased compared to the WCT without the channeling device (Figure 3). [2] [5]

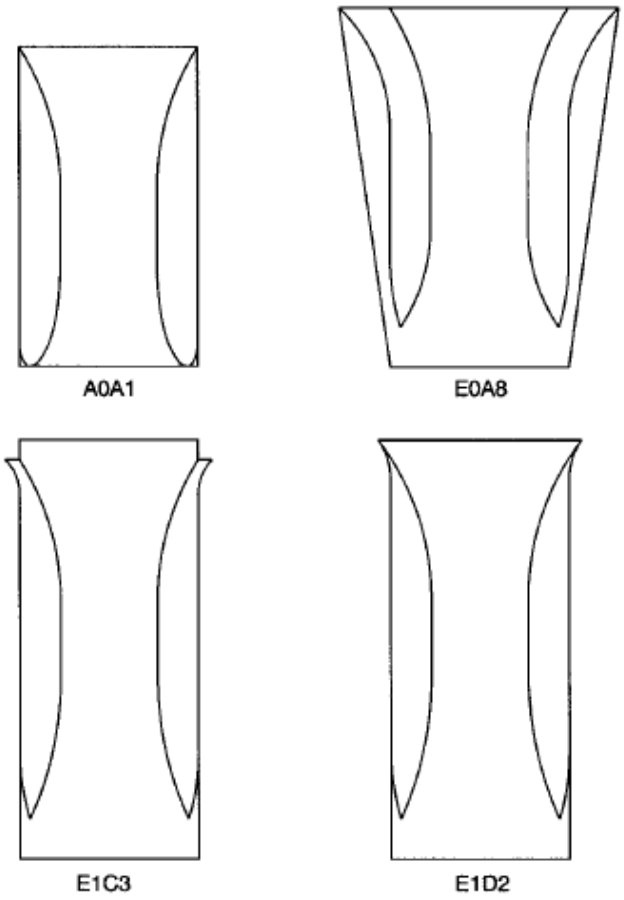

Figure 2. Four examples of channels being tested by Ponta et al.'s research. [5]

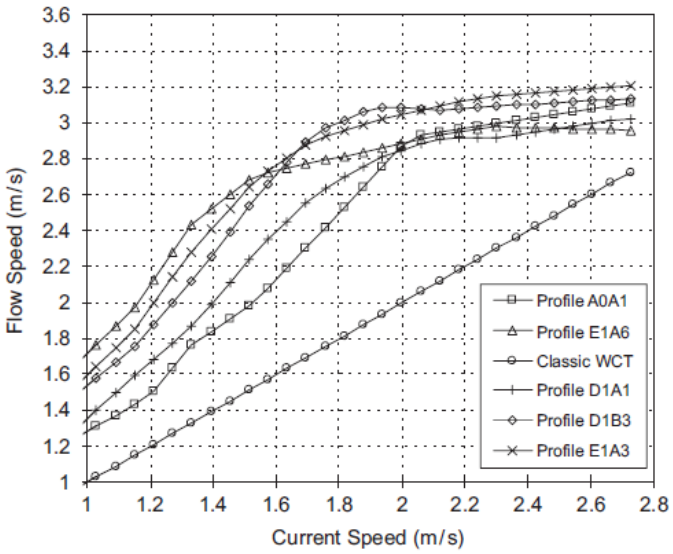

Figure 3. Flow speed versus current speed for different profiles of the channeling device [2]

C. Research Objective

Although a complete computational model of a hydro-kinetic power machine including the flow channel, turbine, generator, and river is very desirable, it would be very costly in terms of both human effort (build, verify validate, use) and computational effort (CPU, RAM, storage, run-time). With the exception of the research cited in the preceding section, nothing could be found in the open literature relating to the performance of the flow channel of interest: a converging, constant-are (throat), diverging channel immersed within a larger stream. Therefore, there is much of value that can be learned from study of just flow through the channel without the other components of the machine. The research objective of the present study is to gain an understanding of the relationship between Area-Ratio ($AR=A_{throat}/A_{mouth}$) of a simple linear inlet and the rate of kinetic energy flow through the constant-area section of the channel. It is expected that a decrease in AR will result in an increase in the throat velocity and will also result in a decrease in the mass flow rate into the channel because there is more resistance to the flow. It is precisely this “bypass

flow" that distinguishes the flow of interest from the vast open-channel flow literature in which all flow is confined to the channel. Maximizing the kinetic energy flow rate will maximize the rate at which the machine can harvest energy. The 1st Law of Thermodynamics shows that in the absence of heat transfer, the rate of kinetic energy flow into the turbine is the theoretical maximum amount of power that the turbine can provide at its output shaft. This equivalency can also be seen by examining the units used to specify the magnitude of the quantities: Kinetic energy = joule, kinetic energy flow rate = joule/s = watt = power. Therefore, to emphasize the relationship one more time, maximizing the kinetic energy flow rate in the throat maximizes the amount of power that can be produced by the machine. The present research seeks to verify the assumed qualitative performance relationship and to begin quantifying relationships between parameters of interest.

II. Methodology

A. Characteristics of the Flow of Interest

The river turbine and the channeling device are designed to float at the river surface. In order to have a good understanding of the flow physics and how to model the flow of interest, the first step is to identify the flow system and determine the features to be included in the Computational Fluid Dynamics (CFD) simulation. The flow system can be described as an open channel, three-dimensional, turbulent, and incompressible flow. Looking ahead to details of the research conducted, the Froude number computed using minimum throat area to be studied and the flow speed approaching the machine of interest is approximately 0.4. Therefore, even if the flow speed in the throat is twice that of the approach flow, the flow through the throat will still be subcritical. In the future, there will be a need for a CFD software that is capable of modeling a moving rigid solid boundary. The CFD software used for this research is CONVERGE by Convergent Science because it is a well-established tool for some applications, it includes all models identified as being important for the present study, a very expensive academic license was made available, and both training and support were provided at no cost.

B. Computational Fluid Dynamics Software

CONVERGE is a multipurpose computational fluid dynamics program developed by the engine simulation experts of Convergent Science. The primary motivation for developing this commercial code was to simulate flow inside internal combustion engine applications. An initial computational mesh is generated in converge given a specific geometry and specification of mesh control parameter values. To accommodate large changed in domain geometry during a simulation,

the software includes an Adaptive Mesh Refinement (AMR) feature as well as the ability for the user to provide specific instructions for mesh modification as a function of simulation time. [6]

Although Converge has not previously been used to simulate open channel flow, it has models for each feature identified above as being important for simulating the flow of interest.

- Free Surface - The Volume of Fluid (VOF) model in CONVERGE may be used to simulate flows with identifiable multi-fluid interfaces such as a free-surface. [6]
- Turbulent flow - CONVERGE offers many turbulence models for different applications: Standard k-ε, Renormalization Group (RNG) k-ε, Rapid Distortion RNG k-ε, Realizable k-ε, and various k-ω models. The present study used the standard k-ε model [6]

C. Computational Setup

The present study uses the flow domain dimensions identified in Table 1. These values were chosen to approximate the installation of the flow channel in a typical lower-Mississippi River barge.

Table 1. Dimensions of the machine.

Overall Channel Length	200 ft.
Overall Channel Width	60 ft.
Channel Draught	9 ft.
Power Section Length	40 ft.
Base Plate Thickness	1 in.

The channeling device features three main sections: the inlet section, the power or “throat” section, and the discharge section with a diffuser. The power section length is the same for all simulations in the present study. Since the research is focused on the inlet geometry and its effect on the flow inside the power section, the diffuser angle is unchanging across all simulations in an attempt to minimize the influence of the diffuser on channel performance. Figure 4 shows the geometry of the flow channel and the nomenclature used to describe it. In order to determine the kinetic energy flow rate near the turbine location, an evaluation plane was located at the midpoint of the throat section to record flow data for the study.

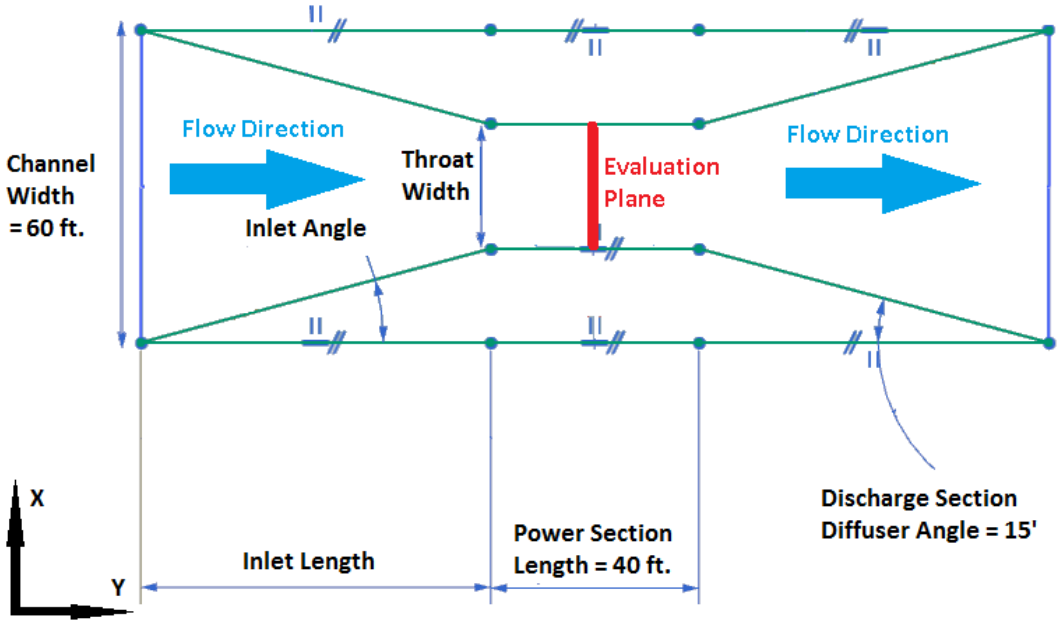

Figure 4. Basic dimensions of the machine from the top view.

Unlike typical open-channel flows, the river flow approaching the machine can either flow through the channel or around the machine. It was expected that decreasing the channel's Area Ratio, ($AR = A_{throat}/A_{mouth}$), would both increase the velocity in the throat and increase the resistance to flow. Using the term "bypass" to indicate flow that would have gone through the channel for AR=1 but does not for values of AR <1, it is expected that the bypass flow will

increase with decreasing values of AR. Therefore, AR was identified as the primary parameter of interest for the present study.

Although it is expected that an inlet with curved solid boundaries will maximize machine performance, curved surfaces significantly increase the size of the design space as compared to simple flat planes. For plane surfaces, for any AR, there are only two related parameters in the design space: inlet angle and inlet length. It was decided to conduct two families of simulations: one to study the influence of inlet angle on performance and the other to study the influence of inlet length on performance. For both families, AR was varied from 90% to 30% to show the dependence of machine performance on this parameter. Table 2 presents the dimensions for the constant inlet angle families and Table 3 presents the dimensions for the constant inlet length families. Figure 6 and Figure 7 provide a sense of the range of channel shapes simulated.

Table 2. Model geometry data for case study #1A and #1B with constant inlet angle.

Study #1A	Inlet angle = 15°		Study #1B	Inlet angle = 30°	
Area Ratio	Throat width (ft.)	Inlet length (ft.)	Area Ratio	Throat width (ft.)	Inlet length (ft.)
90%	54.00	11.20	90%	54.00	5.20
80%	48.00	22.39	80%	48.00	10.39
70%	42.00	33.59	70%	42.00	15.59
60%	36.00	44.78	60%	36.00	20.78
50%	30.00	55.98	50%	30.00	25.98
40%	24.00	67.18	40%	24.00	31.18
30%	18.00	78.37	30%	18.00	36.37

Table 3. Throat width and inlet angle data for case study #2 with constant inlet length.

Study #2A	Inlet length = 30 ft.		Study #2B	Inlet length = 60 ft.	
Area Ratio	Throat width (ft.)	Inlet angle (deg.)	Area Ratio	Throat width (ft.)	Inlet angle (deg.)
90%	54.00	5.71	90%	54.00	2.86
80%	48.00	11.31	80%	48.00	5.71
70%	42.00	16.70	70%	42.00	8.53
60%	36.00	21.80	60%	36.00	11.31
50%	30.00	26.57	50%	30.00	14.04
40%	24.00	30.96	40%	24.00	16.70
30%	18.00	34.99	30%	18.00	19.29

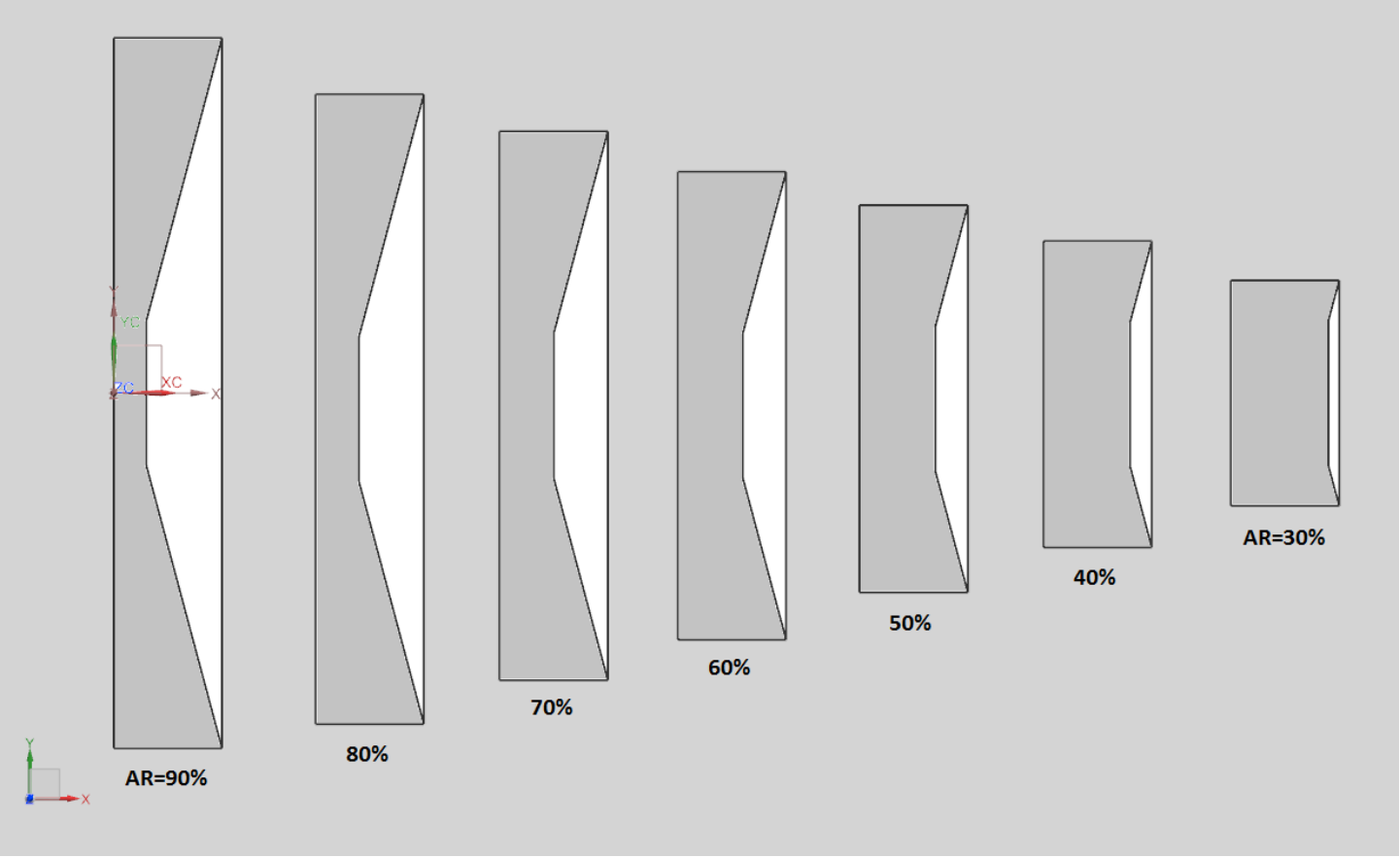

Figure 5. Channel size comparison for 15 degree inlet angle with different AR.

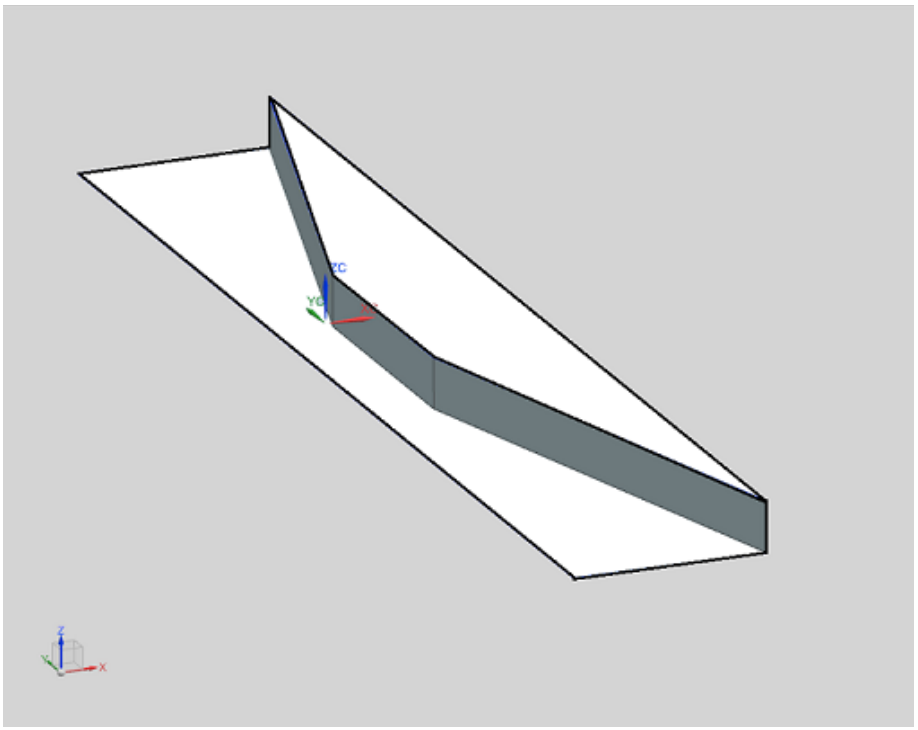

Figure 6. Channel model for 15 degree inlet angle (same scale as Figure 7).

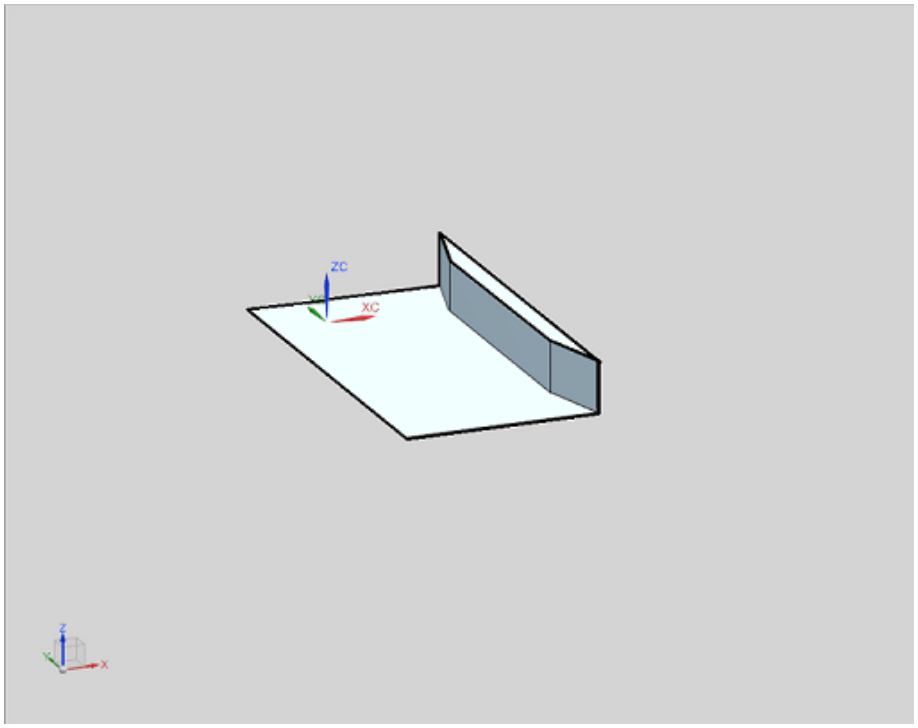

Figure 7. Channel model for 15 degree inlet angle (same scale as Figure 6).

Since this is the first time Converge CFD being used to simulate river flow, considerable effort was required to determine appropriate and usable boundary conditions. Table 4 and Table 5 summarize a lengthy process during which many boundary conditions were tried in search of boundary condition combinations that both accurately specify the flow and produce a useful computational simulation.

Table 4. The different boundary conditions setup for the flow simulation and its outcome.

Boundary Condition	Initial setup	Trial boundary condition #1	Trial boundary condition #2
Water Inflow	Boundary Type = Inflow Velocity Boundary Condition = (0 , 2 , 0) m/s	Boundary Type = Inflow Velocity Boundary Condition = (0 , 2 , 0) m/s Pressure Boundary Condition = Neumann	Boundary Type = Inflow Velocity Boundary Condition = (0 , 2 , 0) m/s
Water Outflow	Boundary Type = Outflow Velocity Boundary Condition = Neumann Pressure Boundary Condition = Neumann	Boundary Type = Outflow Velocity Boundary Condition = Neumann Pressure Boundary Condition = Neumann	Boundary Type = Outflow Velocity Boundary Condition = specific mass flow rate in kg/s
Water side	Boundary Type = Wall Slip Boundary Condition	Boundary Type = Outflow Velocity Boundary Condition = Neumann Pressure Boundary Condition = Neumann	Boundary Type = Outflow Velocity Boundary Condition = (0 , 2 , 0) m/s
Water Bottom	Boundary Type = Wall Slip Boundary Condition	Boundary Type = Outflow Velocity Boundary Condition = Neumann Pressure Boundary Condition = Dirichlet with calculated pressure in Pa	Boundary Type = Outflow Velocity Boundary Condition = (0 , 2 , 0) m/s
Air Inflow	Boundary Type = Inflow Velocity Boundary Condition = (0 , 0.1 , 0) m/s	Boundary Type = Inflow Velocity Boundary Condition = (0 , 0.1 , 0) m/s	Boundary Type = Inflow Velocity Boundary Condition = (0 , 2 , 0) m/s
Air Outflow	Boundary Type = Outflow Velocity Boundary Condition = Neumann Pressure Boundary Condition = Neumann	Boundary Type = Outflow Velocity Boundary Condition = Neumann Pressure Boundary Condition = Neumann	Boundary Type = Outflow Velocity Boundary Condition = Neumann Pressure Boundary Condition = Neumann
Air side	Boundary Type = Wall Slip Boundary Condition	Boundary Type = Outflow Velocity Boundary Condition = Neumann Pressure Boundary Condition = Neumann	Boundary Type = Outflow Velocity Boundary Condition = (0 , 2 , 0) m/s
Air top	Boundary Type = Inflow Pressure Boundary Condition = Atmospheric pressure	Boundary Type = Inflow Pressure Boundary Condition = Atmospheric pressure	Boundary Type = Inflow Pressure Boundary Condition = Atmospheric pressure
Outcome	Water surface rises over time in the flow region.	Water drained from the bottom, significantly causing the water surface to be lowered.	Water surface remains steady in the flow region, but abnormal surface waves significantly slow down simulation.
Note: For Velocity Boundary Condition, it is required to specify the velocity of the flow in the format of (u, v, w) where the river flow is aligned with the y-direction so the value of the v-component is the river velocity.			

Table 5. Additional boundary conditions setup for the flow simulation and its outcome.

Boundary Condition	Trial boundary condition #3	Final setup
Water Inflow	Boundary Type = Inflow Velocity Boundary Condition = (0 , 2 , 0) m/s	Boundary Type = Inflow Velocity Boundary Condition = (0 , 2 , 0) m/s
Water Outflow	Boundary Type = Outflow Velocity Boundary Condition = Neumann Pressure Boundary Condition = Neumann	Boundary Type = Outflow Velocity Boundary Condition = (0 , 2 , 0) m/s
Water side	Boundary Type = Outflow Velocity Boundary Condition = (0 , 2 , 0) m/s Pressure Boundary Condition = Neumann	Boundary Type = Outflow Velocity Boundary Condition = (0 , 2 , 0) m/s
Water Bottom	Boundary Type = Outflow Velocity Boundary Condition = (0 , 2 , 0) m/s	Boundary Type = Outflow Velocity Boundary Condition = (0 , 2 , 0) m/s
Air Inflow	Boundary Type = Inflow Velocity Boundary Condition = (0 , 2 , 0) m/s	Boundary Type = Inflow Velocity Boundary Condition = (0 , 2 , 0) m/s
Air Outflow	Boundary Type = Outflow Neumann Boundary Condition	Boundary Type = Outflow Velocity Boundary Condition = (0 , 2 , 0) m/s
Air side	Boundary Type = Outflow Velocity Boundary Condition = (0 , 2 , 0) m/s	Boundary Type = Outflow Velocity Boundary Condition = (0 , 2 , 0) m/s
Air top	Boundary Type = Outflow Velocity Boundary Condition = (0 , 2 , 0) m/s Pressure Boundary Condition = Neumann	Boundary Type = Inflow Pressure Boundary Condition = 100000 Pa
Outcome	Water surface decreases over time in the flow region.	Water surface remains steady in the flow region.

The flow channel and the boundary conditions describing the river flow are all symmetric about a vertical plane aligned with the flow direction and located at the centerline of the channel. A large savings in the computational effort required for each simulation can be realized by simulating the ½-field instead of the full field. This is accomplished by imposing boundary conditions at the geometric symmetry plane that enforce flow symmetry at that plane. Therefore, all simulations performed for the present research are ½-field simulations: any predictions of kinetic energy flow rate, or machine power, should be doubled to obtain estimates of the performance for a real machine.

The same steps were followed to prepare and perform each of simulation. The ½-field geometry was defined using CAD software in the mechanical engineering department's Computer-Aided Design laboratory, and exported from that software in a STL-format file. That file was imported into Converge Studio running on a workstation in the mechanical engineering department's Flow Research Center (FRC). With the specification of additional spatial parameters, (e.g., the boundaries of the computational domain, definition of distinct and named regions with that domain), Converge Studio generated an initial computational mesh. This software also provides mechanisms for initializing every aspect of the computational field and the boundary conditions to be enforced. This entire process is detailed in Appendix C.

After simulation initialization was completed, a relatively brief simulation was run on the workstation to expose any gross errors in simulation definition. After this test was successful, the set of input files was sent to the University of Memphis High-Performance Computing Center (HPC) and along with a script that inserted a request to run the simulation in the job queue. The architecture of the HP is that of a modern computing cluster with 97 compute nodes, (3,360 Opteron 6274 cores & 12,299 NVIDIA Tesla M2090 GPU cores), that have access to

more than 15,000 GB of RAM. This facility provides an efficient environment for running Converge which was craft to be highly parallelizable.

Once the simulation has completed, the output files are sent back to the FRC workstation. Converge has arranged for a specialized version of EnSight visualization software that is bundled with Converge. This software was used to produce all of the flow visualizations presented and it computed "integral quantities" of interest, (e.g., kinetic energy flow rate through the evaluation plane).

D. Mesh Convergence Study

A mesh convergence study must be performed to ensure that the simulation results are independent of computational domain size and mesh refinement choices. A sequence of simulations were performed to ensure mesh independence for the simulation using the longest channel model (15 degree inlet angle with 30% AR). The sequence of simulations examined the influence of the mesh parameters in the following order:

1. The distance between the air and water outlet boundary and the machine.
2. The distance between the air and water inlet boundary and the machine.
3. The distance between the flow region side boundary and the machine.
4. The distance between water boundary bottom and the machine.
5. The number of fixed embedding layers inside the machine.
6. The size of the base grid (the biggest cell allowed).
7. The influence of k-ε turbulence model convergence tolerance value

The geometry of the 15 degree inlet angle with 30% AR is presented in Table 6.

Table 6. Dimension of the machine used in the mesh convergence study (15deg,AR=0.3).

Length=	60	m
Width=	9.14	m
Height=	4.5	m
Depth=	2.4	m

The initial distance of each boundary from the channel is presented in Table 7.

Table 7. The initial distances between the channel and different boundaries.

Distance between channel discharge and outlet boundary	Distance between the mouth and inlet boundary	Distance between channel bottom and bottom boundary	Distance between machine and side boundary
120 m	70 m	12.6 m	51 m

The convergence criterion used for the present study to determine that a good approximation to steady-state flow has been reached is presented in Equation 2.1.

$$\text{Convergence Criterion} = \left| \left(\frac{\dot{\text{KE}}_{n-1} - \dot{\text{KE}}_{n}}{\dot{\text{KE}}_{n}} \right) / \Delta t \right| \tag{2.1}$$

where $\dot{\text{KE}}$ is the kinetic energy flow rate, and $\dot{\text{KE}}_{\text{n-1}}$ is the kinetic energy flow rate from the previous time step, and Δt is the time difference between iterations. When the value of this criterion remains small, it is concluded that the simulation has reached steady-state.

Distance from the channel discharge to the downstream mesh boundary was the first parameter investigated to start the mesh convergence study. Table 8 presents the mesh parameter

values used for this investigation: the values for the parameter of interest are highlighted in the table. Looking forward to the eventual application of dimensional analysis for performance predictions, the distance parameters describing the mesh have been normalized by division by the machine length (ML) when presented in Table 8 below. Figure 8 displays the kinetic energy flow rate through the throat as a function of time and Figure 9 presents the value of the convergence criterion as a function of time. It should be noted for this investigation, and the others in the mesh convergence study, that much of the oscillation seen in the value of the kinetic energy flow rate after the initial start-up is due to waves passing through the channel. It should also be noted that fluctuations of the kinetic energy flow rate, (ρAV^3), are amplified as compared to the fluctuations in the mass flow rate, (ρAV).

Table 8. Mesh convergence study flow region parameters for the distance between the channel discharge section and the outlet boundary.

	Case 0		Case 1		Case 2	
Parameter	Distance(m)	ML	Distance(m)	ML	Distance(m)	ML
To inlet	70	1.17	70	1.17	70	1.17
To outlet	**120**	**2.00**	**135**	**2.25**	**150**	**2.50**
To bottom	12.6	0.21	12.6	0.21	12.6	0.21
To side	51	0.85	51	0.85	51	0.85
Cell size(m)	2x2x2		2x2x2		2x2x2	

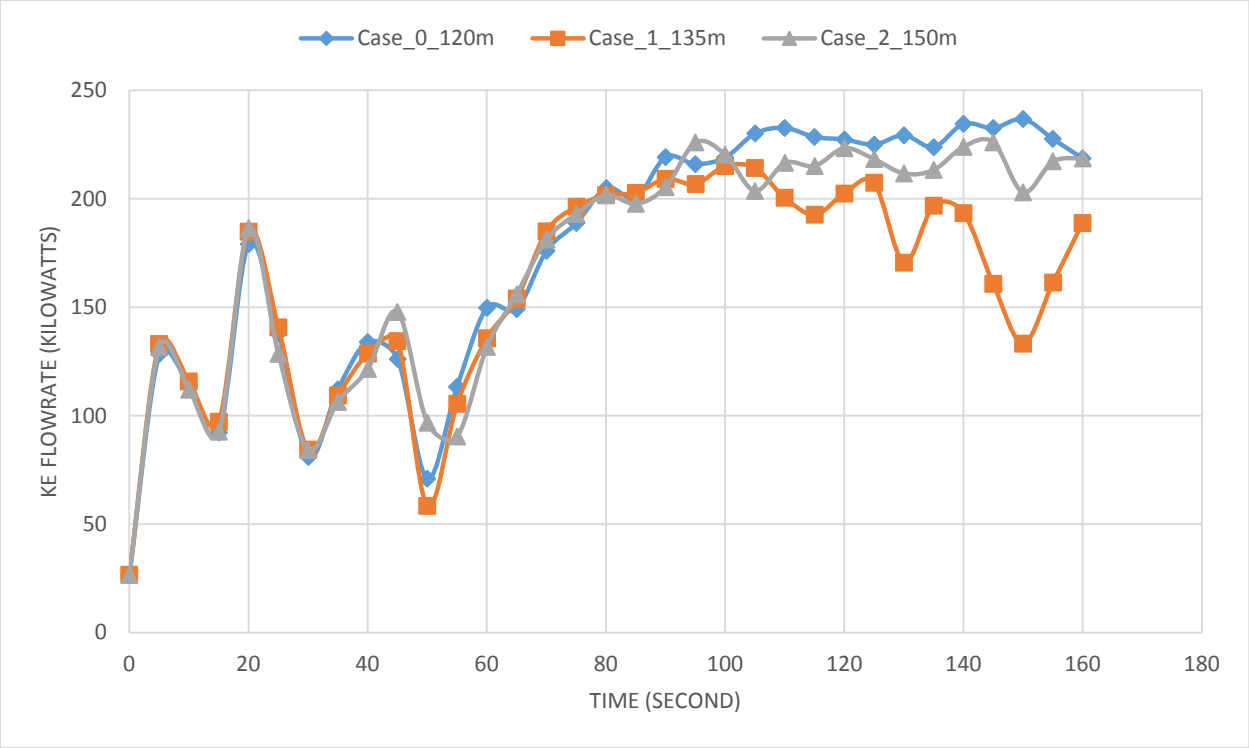

Figure 8. Kinetic energy flow rate in kilowatts vs time for outlet mesh independent study.

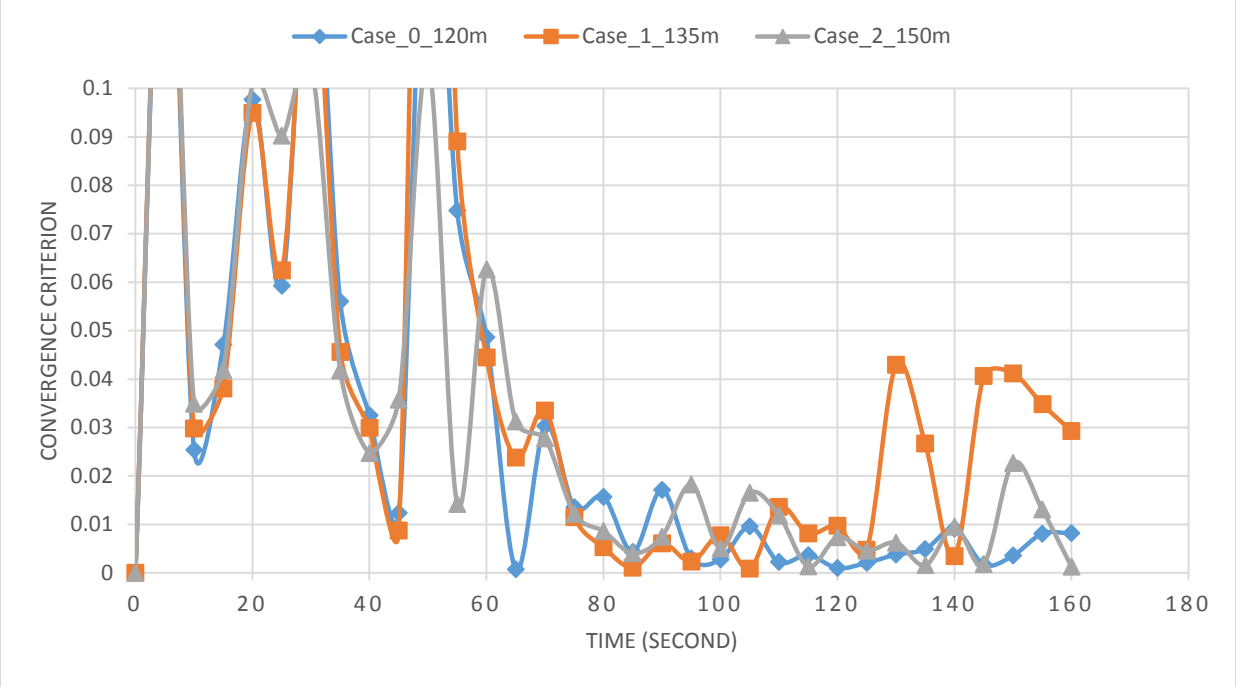

Figure 9. Convergence criterion vs time for outlet mesh independent study.

The value of the convergence criterion drops below 0.05 shortly after 60 seconds of elapsed simulation time and remains below that threshold for all three cases for the duration of the simulation. The simulation was terminated at an elapsed time of 160 seconds because of the value of the convergence criterion for all three cases is below 0.03 and seems likely to not get larger. At simulation termination, the kinetic energy flow rates are: [case 0, 219 kW], [case 1, 189 kW], [case 3, 219kW]. There is no question that the value of the key parameter of interest for present research, kinetic energy flow rate, is virtually identical for cases 0 and 2. When normalized by the value for case 2, the difference between the value for case 2 and the value for case 1 is less than 15%. Looking at the history of this parameter for case 1 leads to the conclusion that it is likely to approach the value for the other two cases with additional simulation time as viscosity dampens the surface waves. Therefore, it was concluded that a distance of 120 m from the channel discharge to the mesh downstream boundary was adequate to ensure a mesh independent simulation and was used for all simulations in the study.

Distance from the upstream mesh boundary to the mouth of the machine was the second parameter investigated for the mesh convergence study. Table 9 presents the mesh parameter values used for this investigation: the values for the parameter of interest are highlighted in the table. Figure 10 displays the kinetic energy flow rate through the throat as a function of time and Figure 11 presents the value of the convergence criterion as a function of time.

Table 9. Mesh convergence study flow region parameters for the distance between the mouth of the machine and the inlet boundary.

	Case 3		Case 4		Case 5		Case 6	
Parameter	Distance(m)	ML	Distance(m)	ML	Distance(m)	ML	Distance(m)	ML
To inlet	**70**	**1.17**	**90**	**1.5**	**105**	**1.75**	**60**	**1**
To outlet	120	2.00	120	2.00	120	2.00	120	2.00
To bottom	12.6	0.21	12.6	0.21	12.6	0.21	12.6	0.21
To side	51	0.85	51	0.85	51	0.85	51	0.85
Cell size(m)	2x2x2		2x2x2		2x2x2		2x2x2	

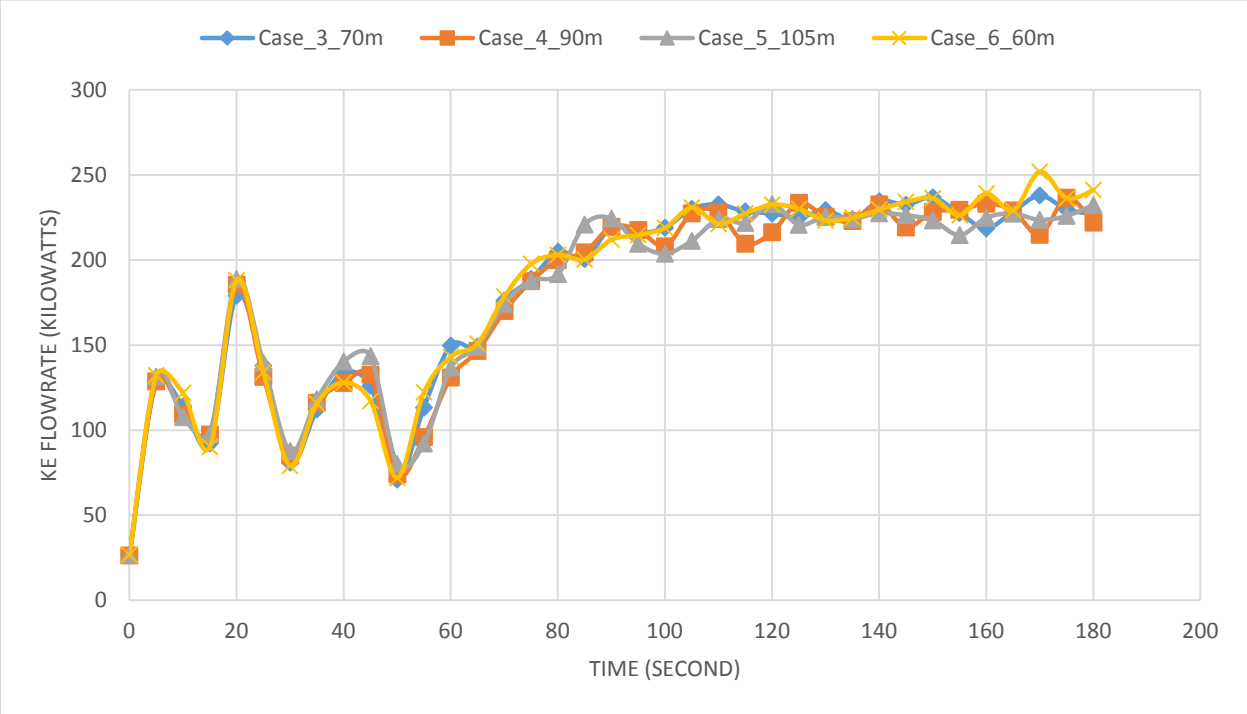

Figure 10. Kinetic energy flow rate in kilowatts vs time for inlet mesh independent study.

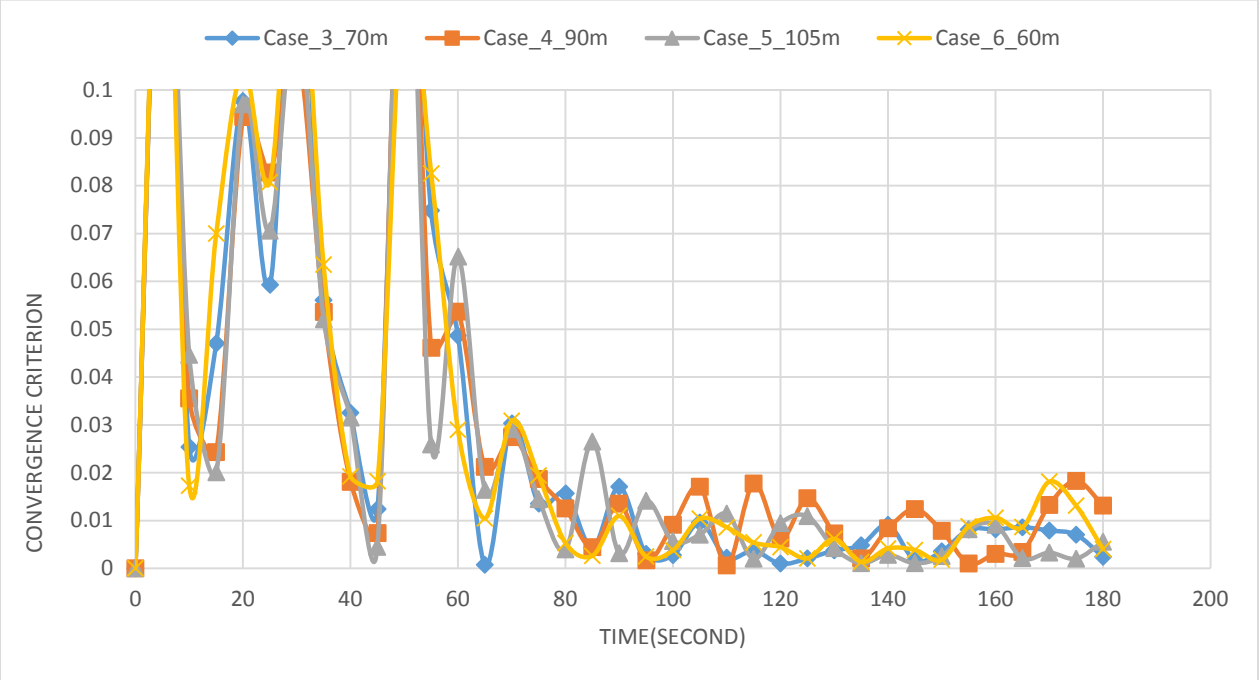

Figure 11. Convergence criterion vs time for inlet mesh independent study.

The time history of the convergence criterion displayed in Figure 11 supports the conclusion that the simulation has reached approximately steady-state conditions after 180 seconds of simulation time. At this time, the values of the kinetic energy flow rate at the evaluation plane are: [case 3, 227kW], [case 4, 222kW], [case 5, 232kW], [case 6, 241kW]. With the exception of case 6 in which the distance from inlet boundary to channel mouth is the smallest, the values of kinetic energy flow rate are tightly grouped. This indicates that the distance for case 6 is insufficient to produce a mesh independent solution and that the distance used for any of the other cases would produce a mesh independent solution. Therefore, a distance of 70 m from the inflow boundary to the channel mouth was used for all simulations.

Distance from the side mesh boundary to the side of the machine was the third parameter investigated for the mesh convergence study. Table 10 presents the mesh parameter values used for this investigation: the values for the parameter of interest are highlighted in the table. Figure 12 displays the kinetic energy flow rate through the throat as a function of time and Figure 13 presents the value of the convergence criterion as a function of time.

Table 10.Mesh convergence study flow region parameters for the distance between the machine and the side boundary.

	Case 7		Case 8		Case 9	
Parameter	Distance(m)	ML	Distance(m)	ML	Distance(m)	ML
To inlet	70	0.58	70	1.17	70	1.17
To outlet	120	2.00	120	2.00	120	2.00
To bottom	12.6	0.21	12.6	0.21	12.6	0.21
To side	**51**	**0.85**	**60**	**1**	**69**	**1.15**
Cell size(m)	2x2x2		2x2x2		2x2x2	

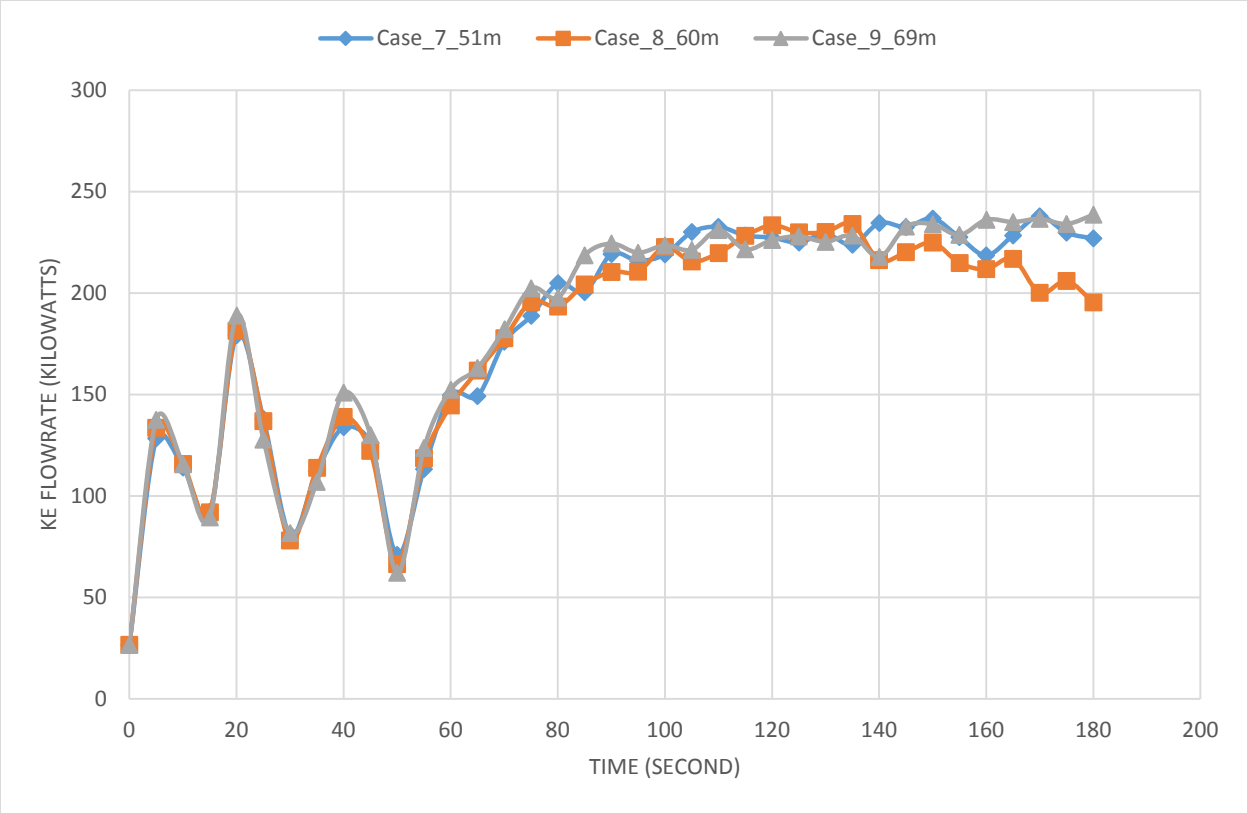

Figure 12. Kinetic energy flow rate in kilowatts vs time for side mesh independent study.

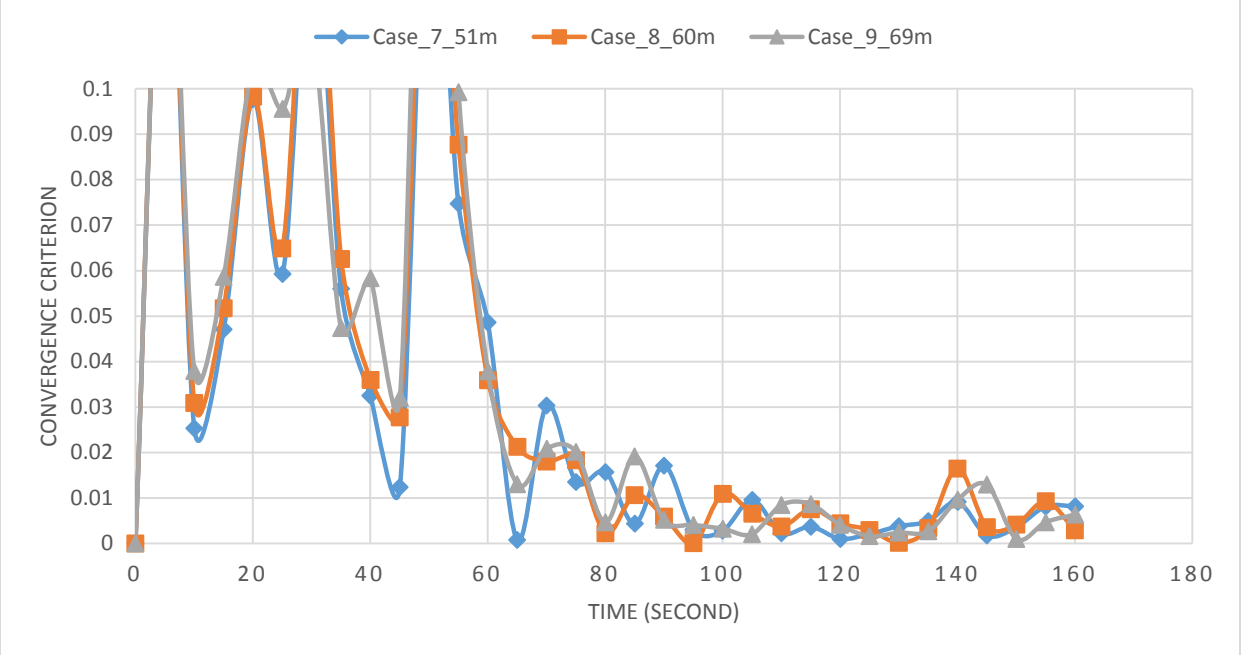

Figure 13. Convergence criterion vs time for side mesh independent study.

After the completion of simulations, the values of the kinetic energy flow rate at the evaluation plane are: [case 7, 227kW], [case 8, 195kW], [case 9, 239kW]. Figure 13 shows that the convergence criterion for all three cases remains after 100 seconds of simulation time. The time-history for case 7 and case 9 are in close agreement whereas the kinetic energy flow rate for case 8 seems to be drifting to lower value toward the end of the simulation. This is surprising as the parameter value under investigation is between that of case 7 and case 9. It is believed that this difference is due to surface elevation oscillations similar to those predicted when simulation time was extended for a later study (case 10, 11, 12). It is expected that as the value for case 8 would rebound with an extension of simulation time. The conclusion drawn from the simulations of cases 7, 8, and 9 is that a distance of 51 meter from the machine side to the side mesh boundary will ensure that the results of simulations for the present research will be mesh independent.

Distance from the bottom mesh boundary to the bottom of the machine was the fourth parameter investigated for the mesh convergence study. Table 11 presents the mesh parameter values used for this investigation: the values for the parameter of interest are highlighted in the table. Figure 14 displays the kinetic energy flow rate through the throat as a function of time and Figure 15 presents the value of the convergence criterion as a function of time.

Table 11. Mesh convergence study flow region parameters for the distance between the machine and the bottom boundary.

	Case 10		Case 11		Case 12	
Parameter	Distance(m)	ML	Distance(m)	ML	Distance(m)	ML
To inlet	70	0.58	70	1.17	70	1.17
To outlet	120	2.00	120	2.00	120	2.00
To bottom	**12.6**	**0.21**	**17.4**	**0.29**	**22.2**	**0.37**
To side	51	0.85	51	0.85	51	0.85
Cell size(m)	2x2x2		2x2x2		2x2x2	

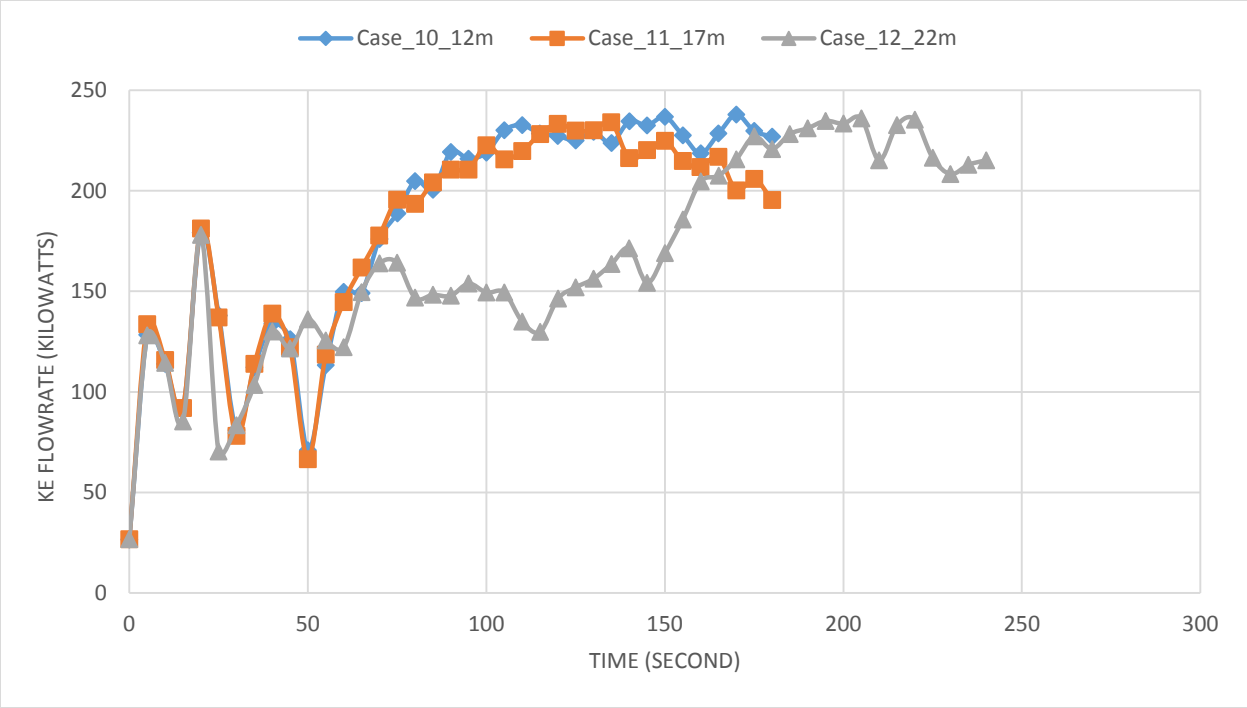

Figure 14. Kinetic energy flow rate in kilowatts vs time for depth mesh independent study.

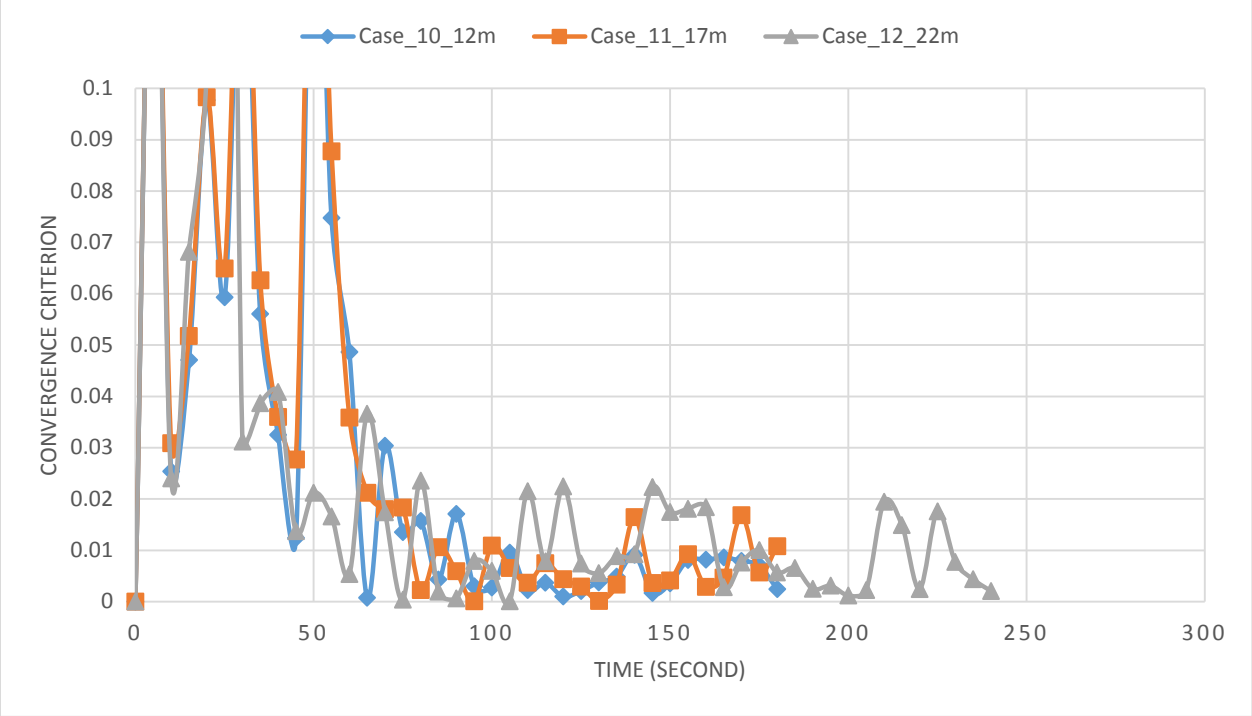

Figure 15. Convergence criterion vs time for depth mesh independent study.

After the completion of simulations, the values of the kinetic energy flow rate at the evaluation plane are: [case 10, 227 kW], [case 11, 195 kW], [case 12, 215 kW]. The time-history of the convergence criterion suggests that all three cases have approached a steady-state flow after 180 seconds. Although the time-history of kinetic energy flow rate for cases 10 and 11 are very similar, and there is a tight grouping of the kinetic energy flow rate predicted by each of the three simulations, the time-history for case 12 appears to be significantly different than that of the other two. To be specific, the value seems to still be changing significantly near termination. To determine if termination of the case 12 simulation was premature, the simulation was extended to a termination at 240 seconds. Although oscillations in kinetic energy flow rate persist during the extended simulation, the value remain bracketed by the termination value predicted for the other two cases. It is reasonable to conclude that further extension of the case 12 simulation will not alter the conclusion of this parameter study. A distance of 12.6 meter from the bottom of the machine to the bottom of the mesh was used for all subsequent simulations.

Fixed embedding is a tool that refines the grid near a specific location in the domain where finer resolution is critical to the accuracy of the simulation by adding layers of smaller cells near the specified boundary. Figure 16 shows how increasing the number of embedding layers in the throat increases the number of cells appearing in a transverse plane in the throat and thereby improves the simulation accuracy. Table 12 presents the mesh parameter values used for this investigation. Figure 17 displays the kinetic energy flow rate through the throat as a function of time and Figure 18 presents the value of the convergence criterion as a function of time.

Table 12.Mesh convergence study for the fixed embedding layers inside the channel.

	Case 13	Case 14	Case 15	Case 16
Fixed embedding layers	0	3	5	7

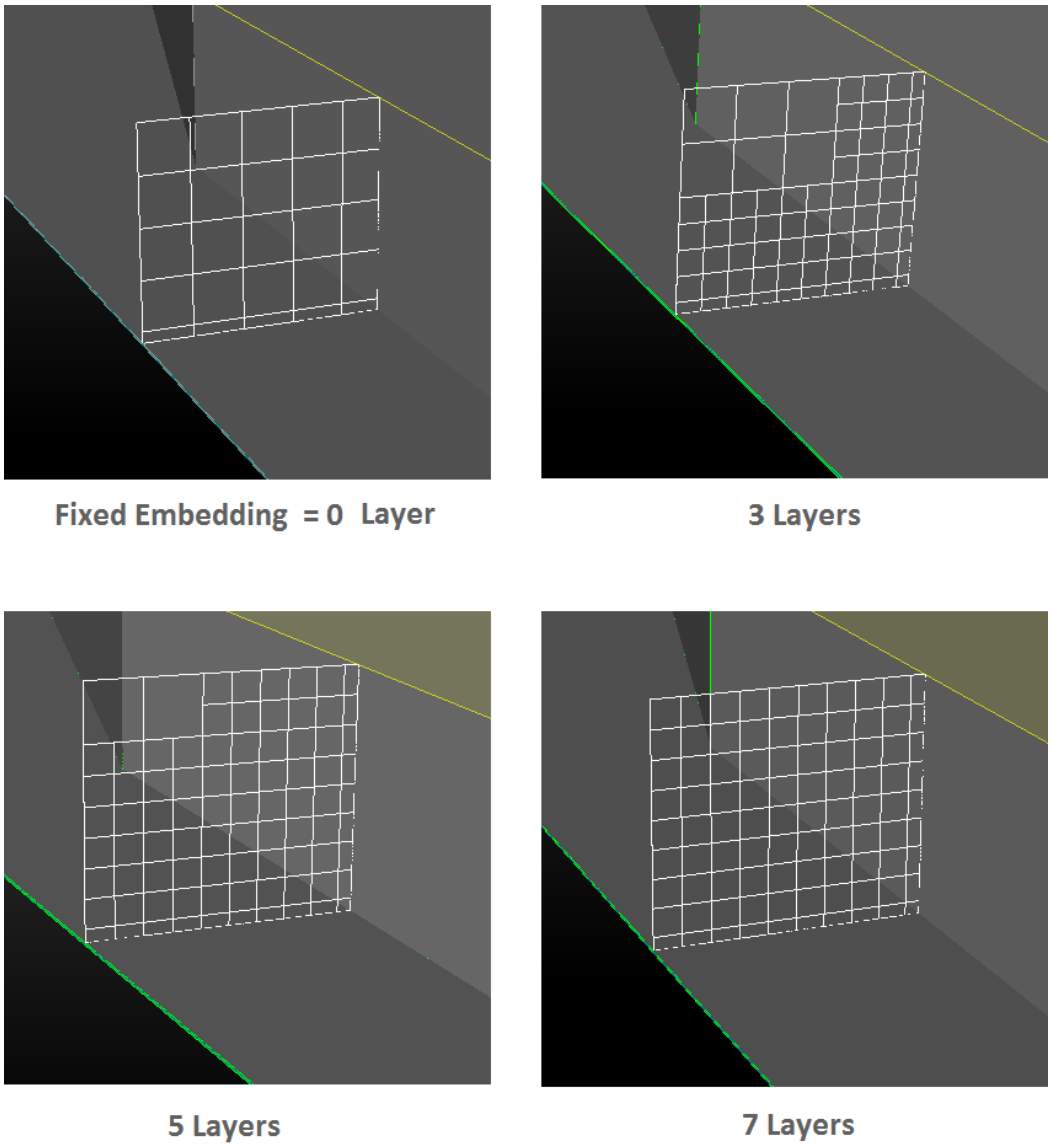

Figure 16. The comparison between different fixed embedding layer setup.

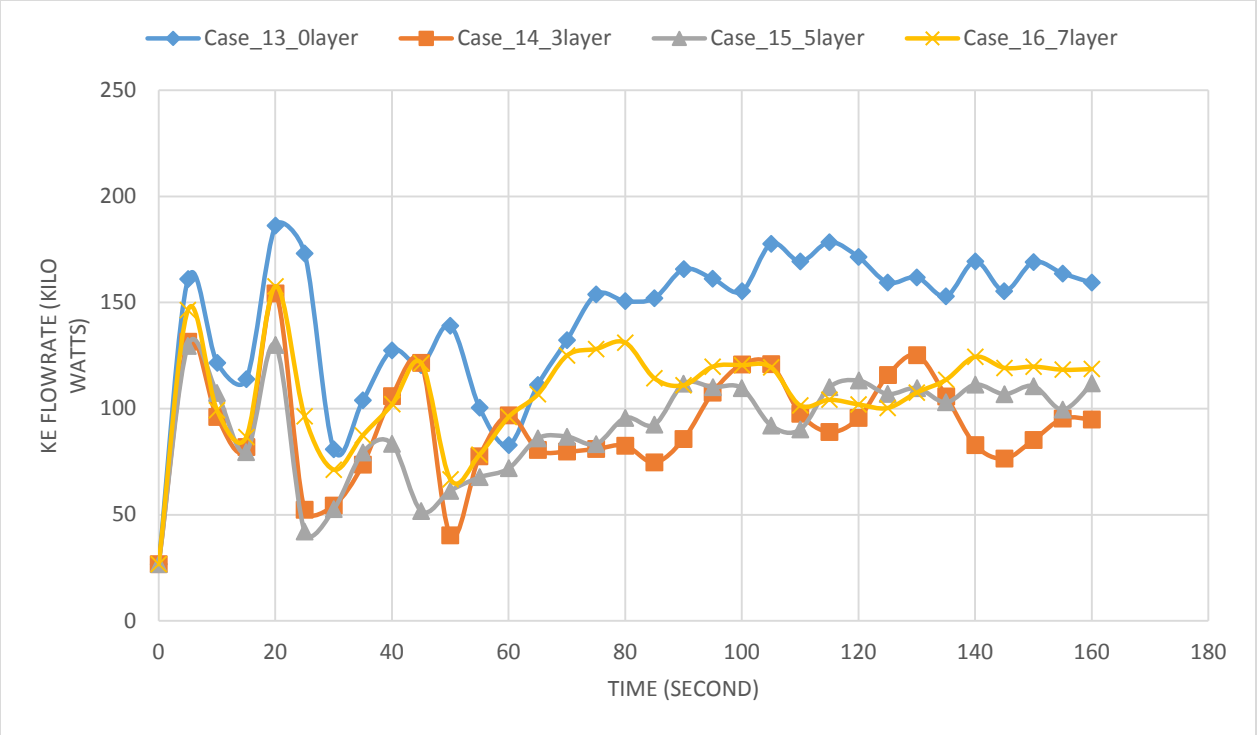

Figure 17. Dependence on number of fixed embedding layers.

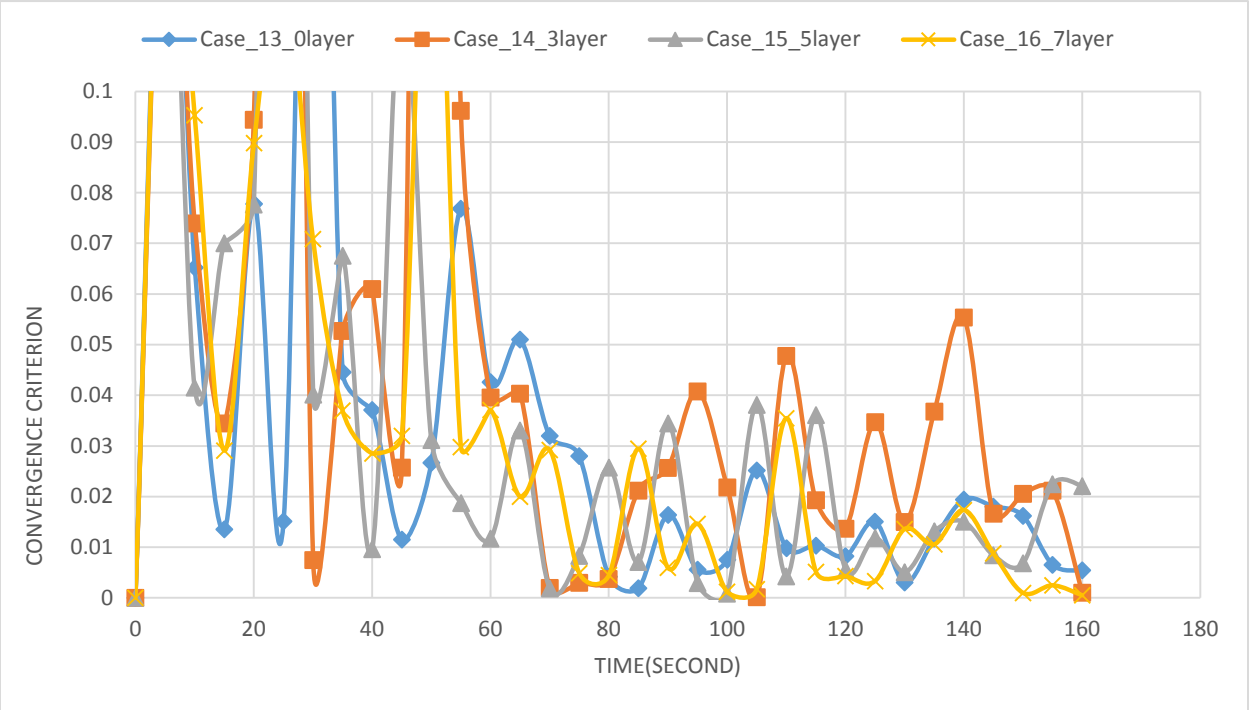

Figure 18. Convergence criterion vs time for fixed embedding layer independent study.

After the completion of simulations, the values of the kinetic energy flow rate at the evaluation plane are: [case 13, 159kW], [case 14, 94kW], [case 15, 112kW], [case 16, 118kW]. For these simulations, the convergence criterion remains below 0.02 after a simulation time of 145 seconds. The only case for which the predicted kinetic energy flow rate at termination is significantly different from the others is the unrefined case, case 13. Case 14 has a greater fluctuation after 80 seconds of simulation time compared to case 15 and case 16. While the kinetic energy flow rate from case 15 and case 16 is closely matched, case 16 took a lot longer to run due to the extra layers of mesh. It was concluded that 5 layers of fixed embedding should be used for the remainder of the cases in the present research.

The “base grid” input parameter specifies the size of the largest cells to be used in the mesh. Mesh refinement is accomplished by repeatedly halving the cell sizes. In this investigation, the general size of the cells in the flow region is being investigated for base grid size sensitivity. Table 13 presents the mesh parameter values used for this investigation. Figure 19 displays the kinetic energy flow rate through the throat as a function of time and Figure 20 presents the value of the convergence criterion as a function of time.

Table 13. Mesh convergence study flow region parameters for the biggest cell size allowed in the flow region.

	Case 17	Case 18	Case 19	Case 20
Base Grid (m)	2x2x2	2.3x2.3x2.3	2.5x2.5x2.5	3x3x3

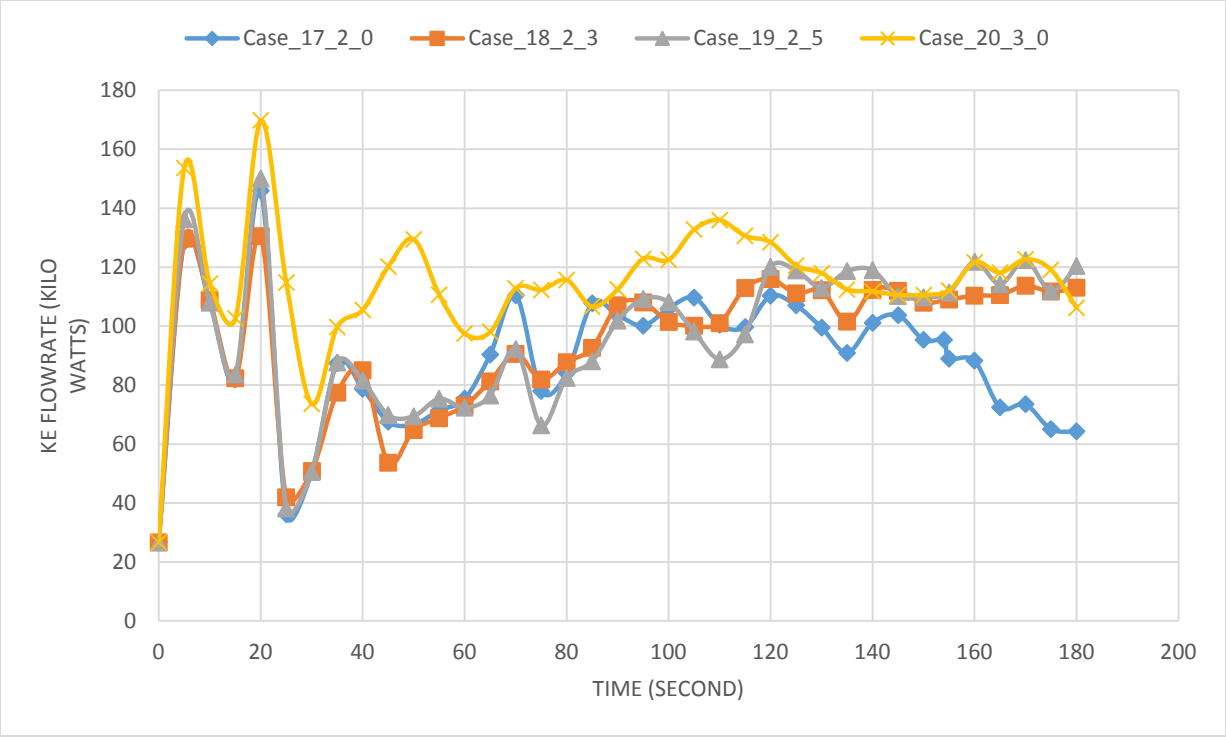

Figure 19. Kinetic energy flow rate in kilowatts vs time base grid mesh independent study.

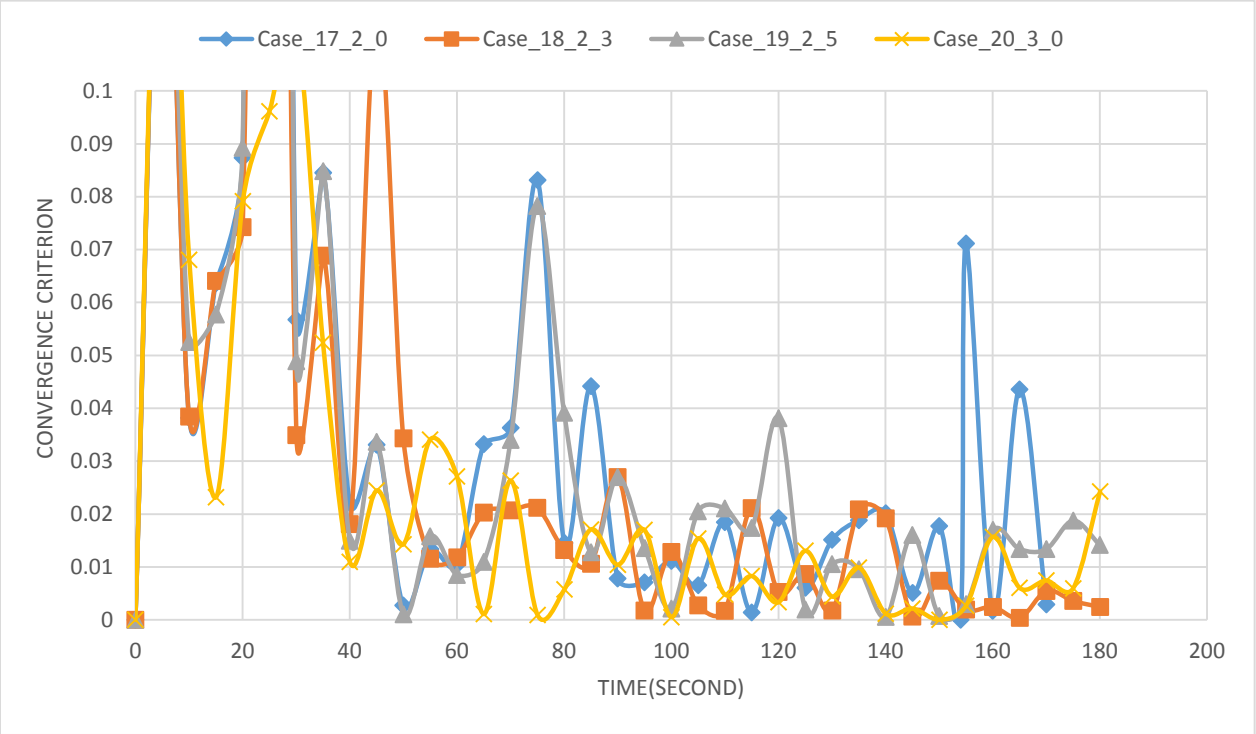

Figure 20. Convergence criterion vs time for base grid size mesh independent study.

After the completion of simulations, the values of the kinetic energy flow rate at the evaluation plane are: [case 17, 159 kW], [case 18, 94 kW], [case 19, 112 kW], [case 20, 118 kW]. It is at first surprising that the performance predicted by three of the meshes (case 18, 19, 20) is in very good agreement but the simulation using the mesh with the smallest base grid size (17) seems to diverge from the others after 140 s of simulation time. After much searching for an explanation, the explanation was found in differences in the time-history of the free surface of the cases. The flow visualization software permits capture of an "isosurface" for which the value of a specified variable is constant. Specifying that variable to be the one used by the VOF-model to track a two-fluid interface results in a surface that closely approximates the free surface. Figure 21 shows the predicted surface at 125 s and 180 s for the 2.0x2.0x2.0 and the 2.3x2.3x2.3 base grids. At the earlier time, it can be seen that there is significant agitation in the free surface near the outflow boundary for both meshes. As the 2.3-base-grid simulation continues, the surface agitation retreats toward the outflow boundary. In contrast, in the 2.0-base-grid simulation the agitation sweeps toward the inflow boundary with the consequence that by 180 s it has completely enveloped the flow channel and extends upstream of it. This simulation is unique in this regard as surface agitation does not extend to near the flow channel for either the 2.5-base-grid or the 3.0-base-grid simulation.

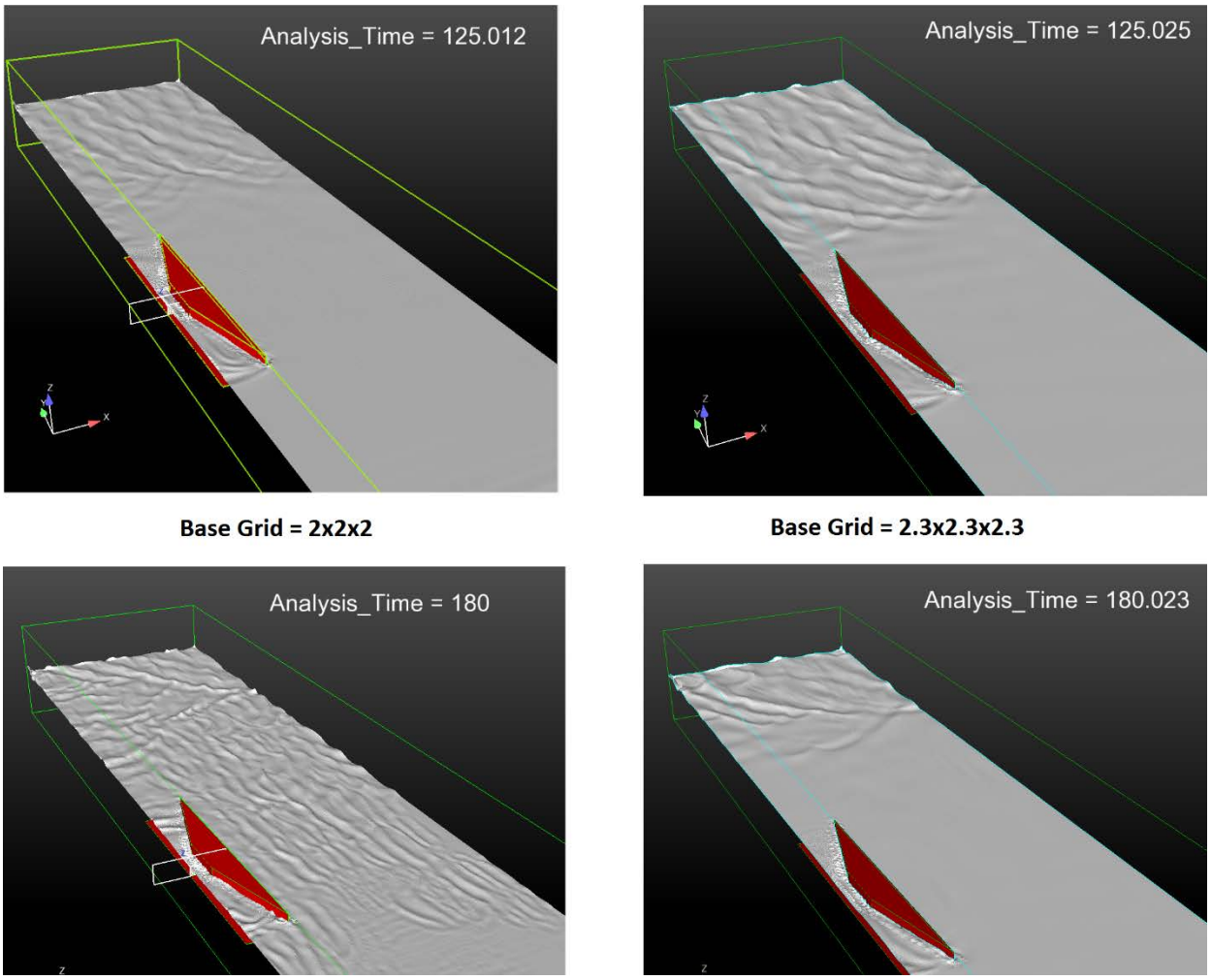

Figure 21. The predicted surface at 125 s and 180 s for the 2.0 and the 2.3 base grids

The reason for surface agitation near the outflow boundary is unknown. Review of all previous simulations, (and all subsequent simulations), shows that all exhibit some surface agitation near the outflow boundary. However, this particular 2.0-base-grid case is the only one in which the agitation extends upstream as far as the flow channel. It is speculated that the agitation is due to the imposition of a Dirichlet-velocity boundary condition at the outflow plane, (required to eliminate the monotonic rise/fall of the entire free surface problem), an inaccuracy in some other element of that boundary's model, or in some resonance unique to this flow simulation. Although

it is not possible with the tools available to the investigator to determine if any of these speculations is correct, it is reasonable to draw a conclusion with respect determination of a base grid size that ensures a mesh independent simulation.

The time-history of the kinetic energy flow rate for the 2.3- and 2.5-base-grid simulations are in excellent agreement throughout the simulation. Although the time-history for the 3.0-base-grid is a little different, it closely matches the other two beyond 130 s and predicts almost the same value as those at the time of simulation termination. It is therefore concluded that a 2.3x2.3x2.3 base grid size should ensure a mesh result for the remainder of the simulations performed in conduct of the present research.

The final parameter examined in the mesh convergence study was the value of the convergence tolerance for the k-ε turbulence model. This study was motivated when several simulations seemed to stall due to excessive iterations within a time step due to failure of the turbulence model to converge. Turbulence is not expected to have a significant influence on the flow being studied so it seemed reasonable to try to ease the default convergence criteria, developed for simulation of combustion in an internal combustion engine. Table 14 presents the values used for this investigation. Figure 22 displays the kinetic energy flow rate through the throat as a function of time and Figure 23 presents the value of the convergence criterion as a function of time. It is possible to conclude that the solution is not sensitive to the TKE convergence tolerance for the range of values studied. A k-ε convergence tolerance value of 0.1 was used for the remainder of the simulation.

Table 14. Parameters and cases for the convergence criterion study.

	Case 22	Case 23	Case 24
TKE Convergence tolerance	0.05	0.005	0.01

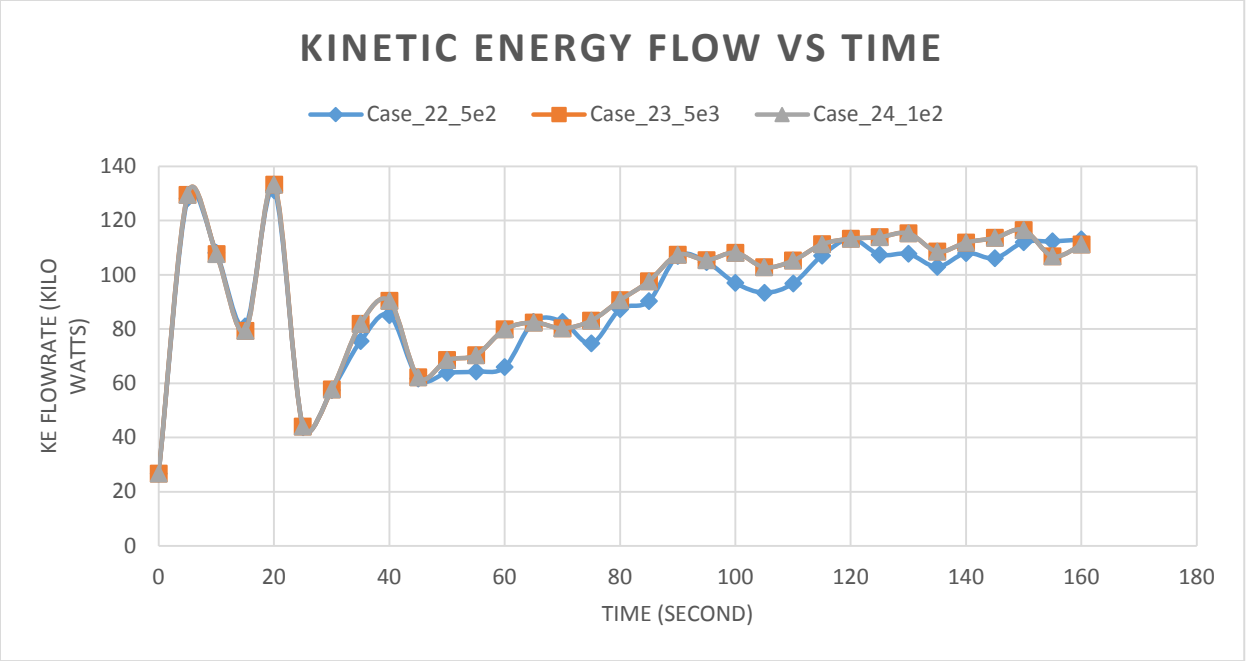

Figure 22. Kinetic energy flow rate vs time for the effect of turbulence criterion on results.

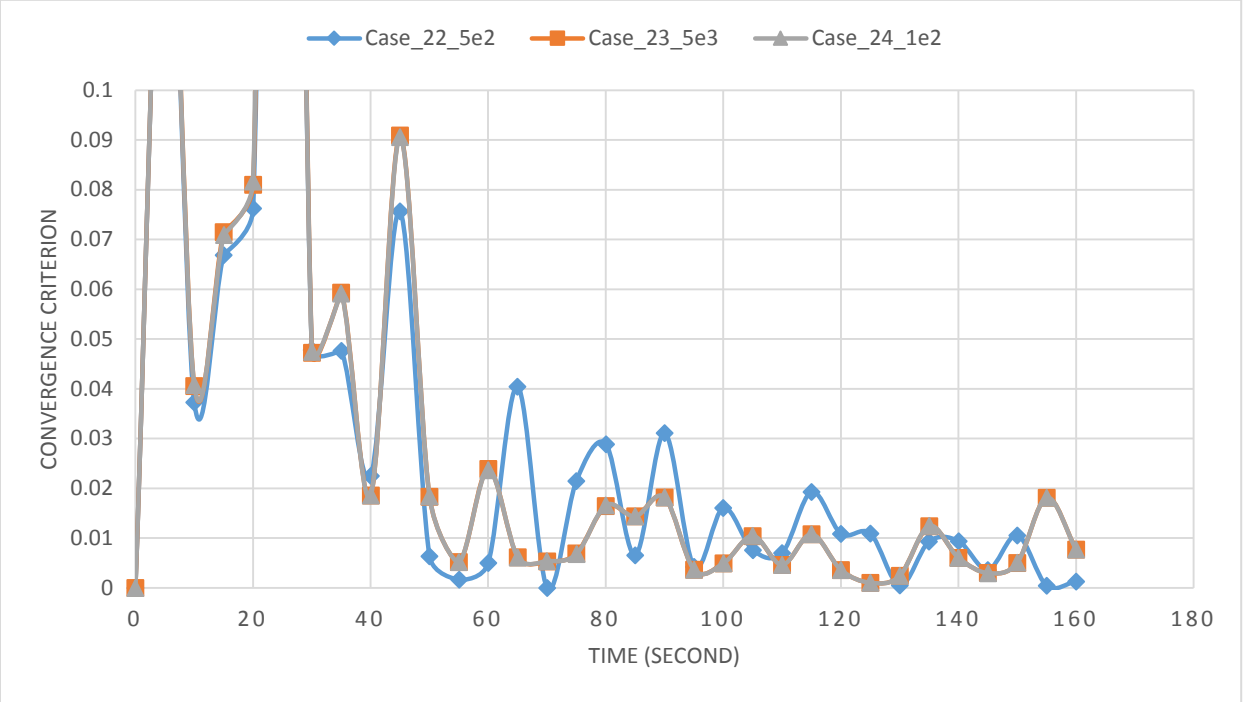

Figure 23. Convergence criterion vs time to verify the effect of turbulence criterion on results.

Table 15 summarizes the parameter values identified by the mesh convergence study as being adequate to ensure mesh independent simulation results for the purposes of the present research.

Table 15. Summary of mesh convergence studies and result for mesh independent solutions.

Mesh Convergence Study	Value	Machine Length
Distance between machine and outlet BC	120 m	2
Distance between machine and inlet BC	70 m	1.17
Distance between machine and side BC	51 m	0.85
Distance between machine and bottom BC	12.6 m	0.21
Fixed embedding layers	5	NA
Base grid	2.3m x 2.3m x 2.3m	NA
TKE Convergence Tol.	0.01	NA

III. Simulation Results and Conclusion

A. Simulation Results and Comparison

In order to understand the flow of interest inside the channel, and how the velocity changes in the flow started in the inlet section and through the discharge section, EnSight was used to display the flow velocity through clip planes inside the machine in Figure 24 (15 degree inlet model with AR=0.4). Figure 25 presents flow velocity on clip planes throughout the machine for the 60 feet channel model with 60% AR. EnSight was also used to display the free surface of the flow using the isosurface feature. Figure 26 provides an isoview near the power section of the machine plotted with flow velocity on the free surface. Figure 27 shows the free surface of the entire flow field to provide a general idea of the size of the machine when compared to the entire flow field.

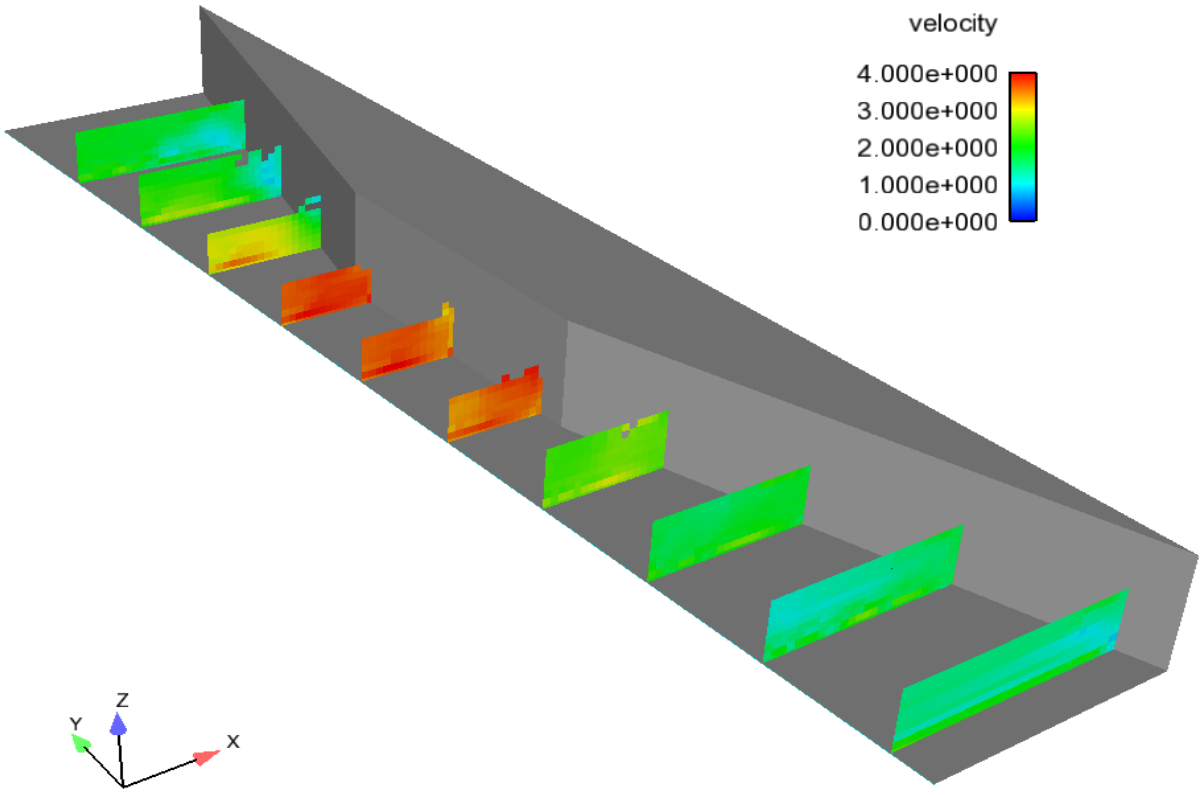

Figure 24. Velocity profiles of the flow inside the channel [15 deg., AR=0.4].

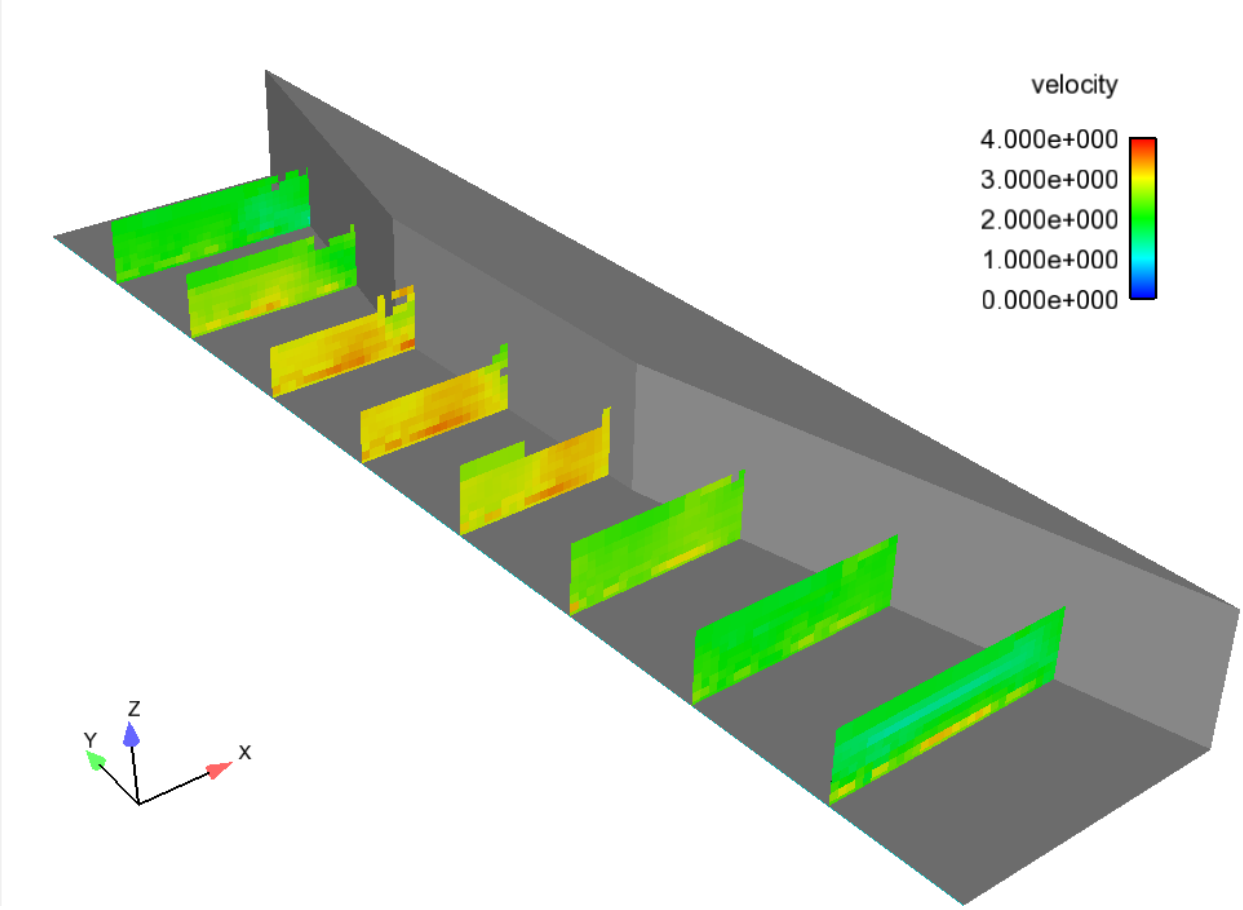

Figure 25. Velocity profiles of the flow inside the channel with [60 ft. AR=0.6].

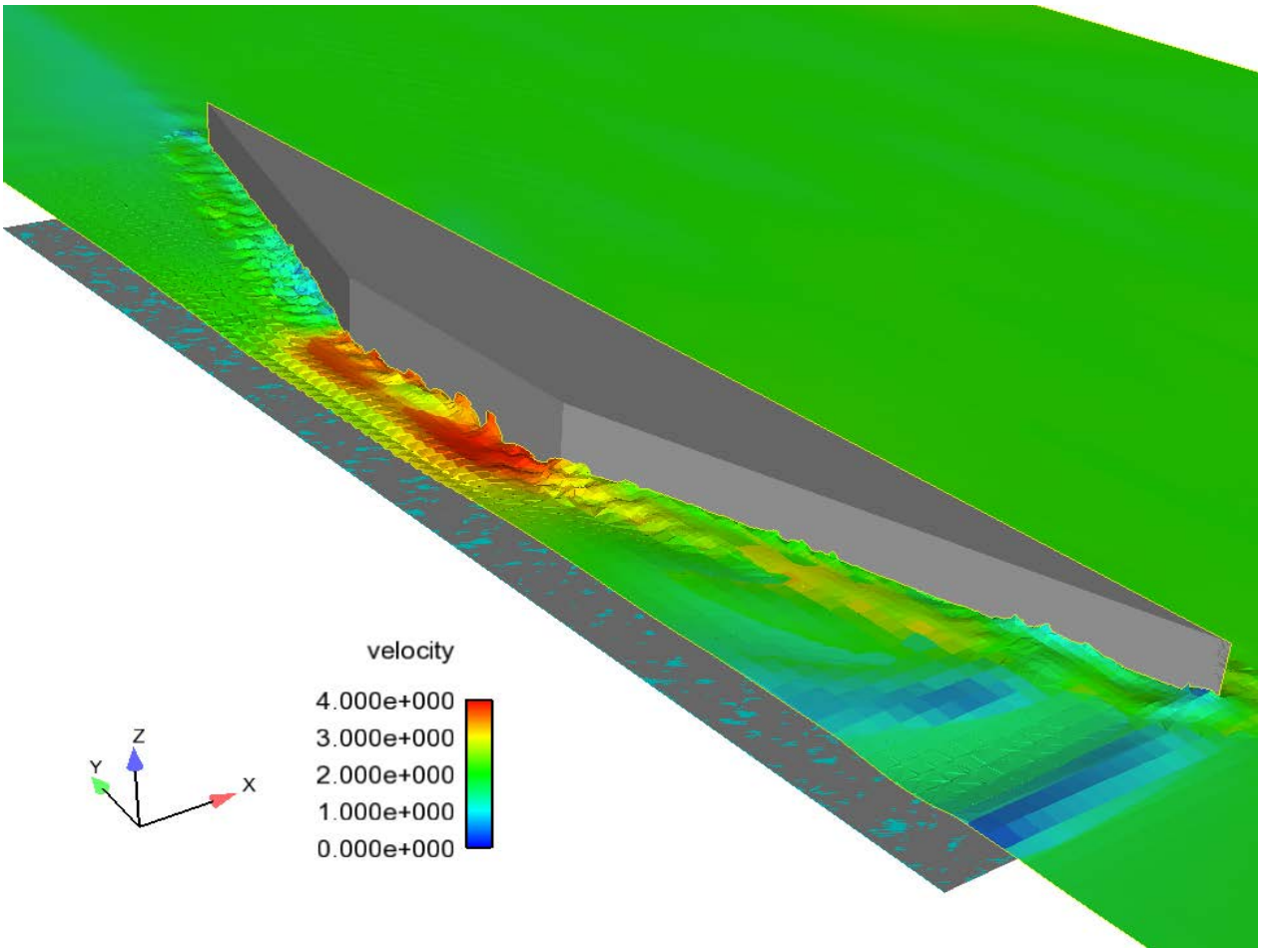

Figure 26. Close up picture of the flow inside the channel model with [15deg. AR=0.4].

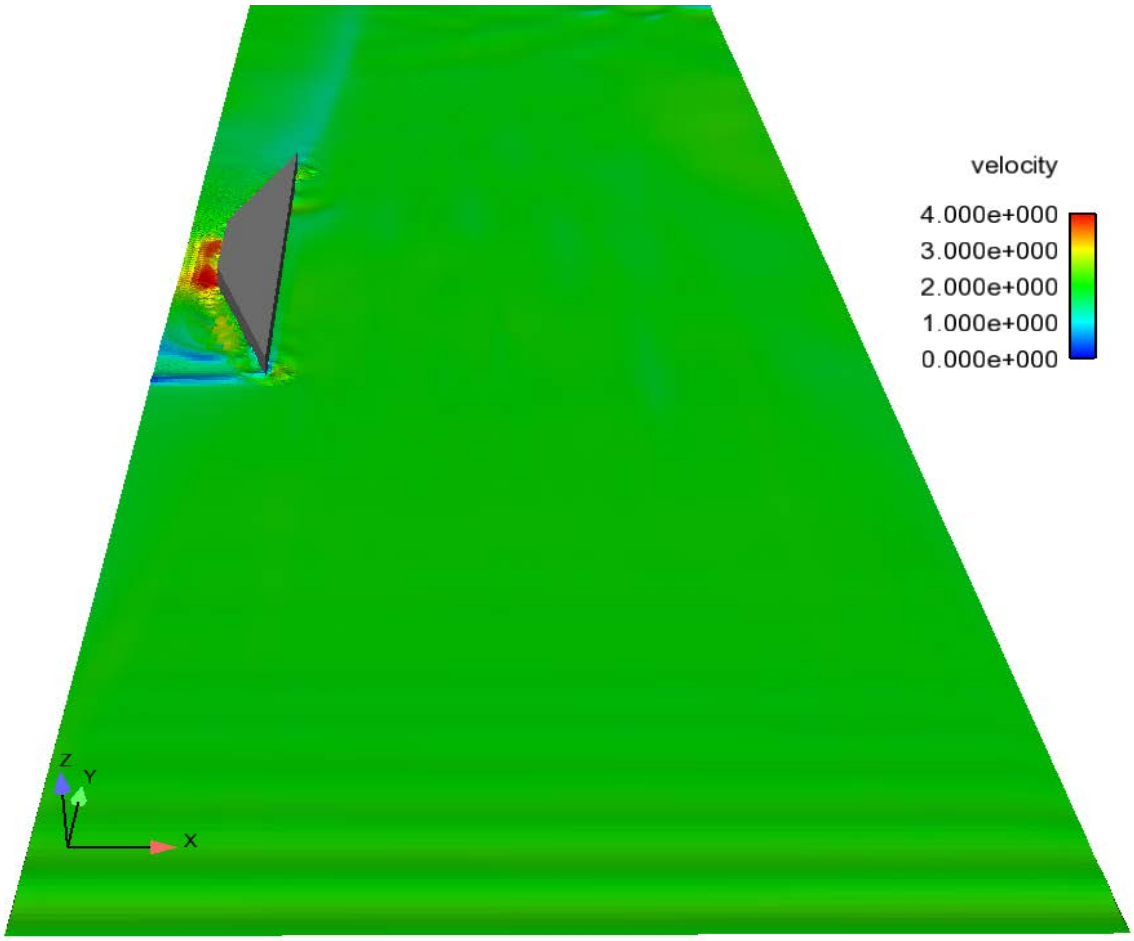

Figure 27. An overall view of the flow region and the machine.

The simulations with 15 degree inlet angle models were the first study to be simulated. The kinetic energy flow rate for each simulation was averaged from 120 seconds to 180 seconds, and those values are plotted as a function of AR in Figure 28. For this family of geometries, the KE flow rate seems to be almost insensitive to the changes in the value of AR between 0.4 and 0.7. The values are essentially the same for the AR=0.4 and 0.5 pair, and again for the AR= 0.6 & 0.7 pair. The maximum difference between all four cases is only 7%.

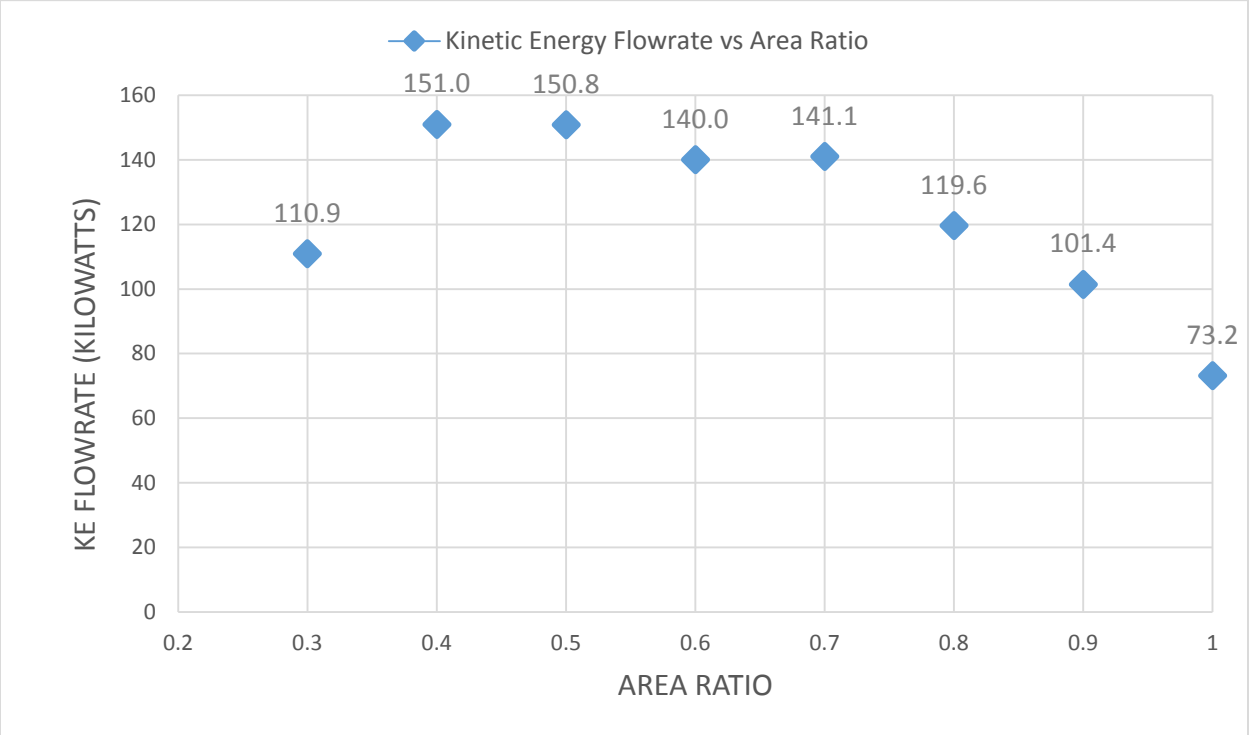

Figure 28. Kinetic energy flow rate as a function of Area Ratio for 15 deg.inlet angle models.

The 30 degree inlet angle models were the second study to be simulated. The kinetic energy flow rate from each simulation was averaged from 120 seconds to 180 seconds, and then those values are displayed as a function of AR in Figure 29. The highest kinetic energy flow rate for the 30 degree inlet angle study is the AR=0.6 case. Unlike the 15 degree inlet study, these simulations show a smooth curve for KE flow rate as a function of AR with a clear maximum value in the neighborhood of AR=0.6.

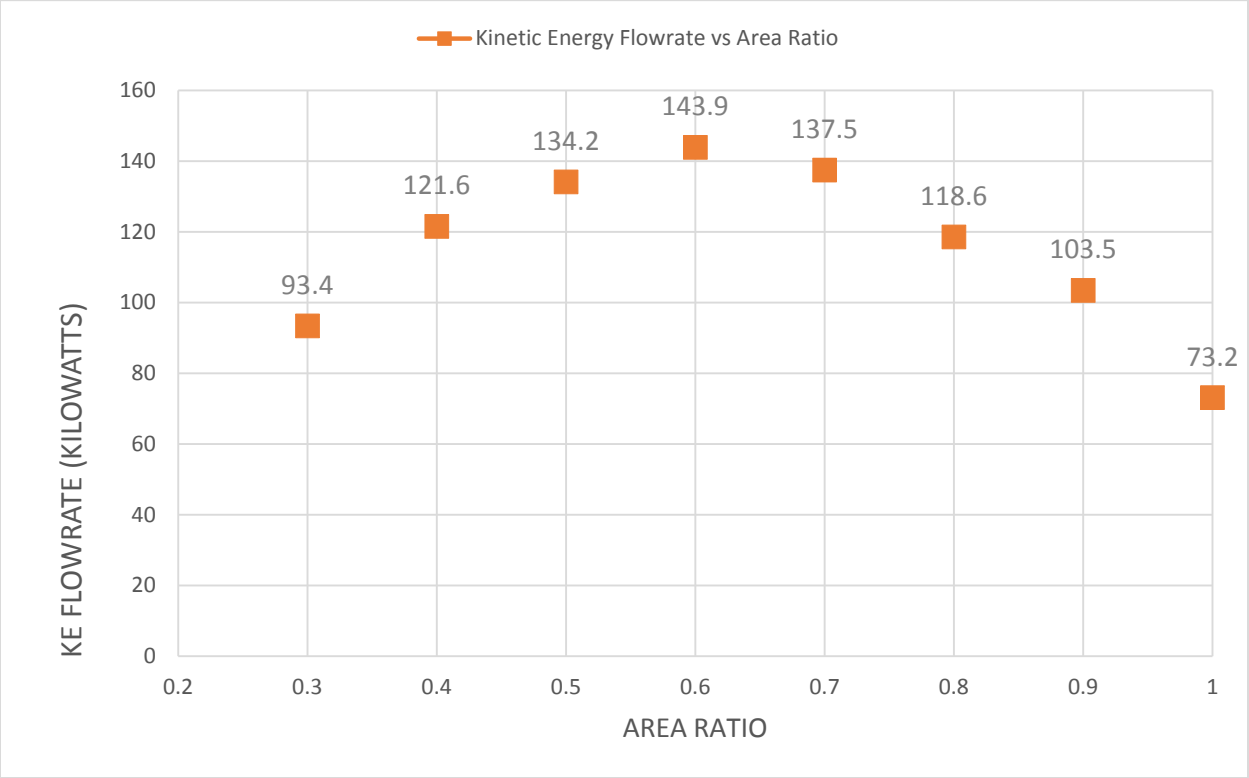

Figure 29. Kinetic energy flow rate as a function of Area Ratio for 30 deg. inlet angle models.

The 30 ft. inlet length study was the third set of cases to be simulated. The kinetic energy flow rate through the evaluation plane from each simulation was averaged from 120 seconds to 180 seconds, and those values are displayed as a function of AR in Figure 30. The values produce a smooth curve with a maximum of 145.4 kW in the neighborhood of AR = 0.6.

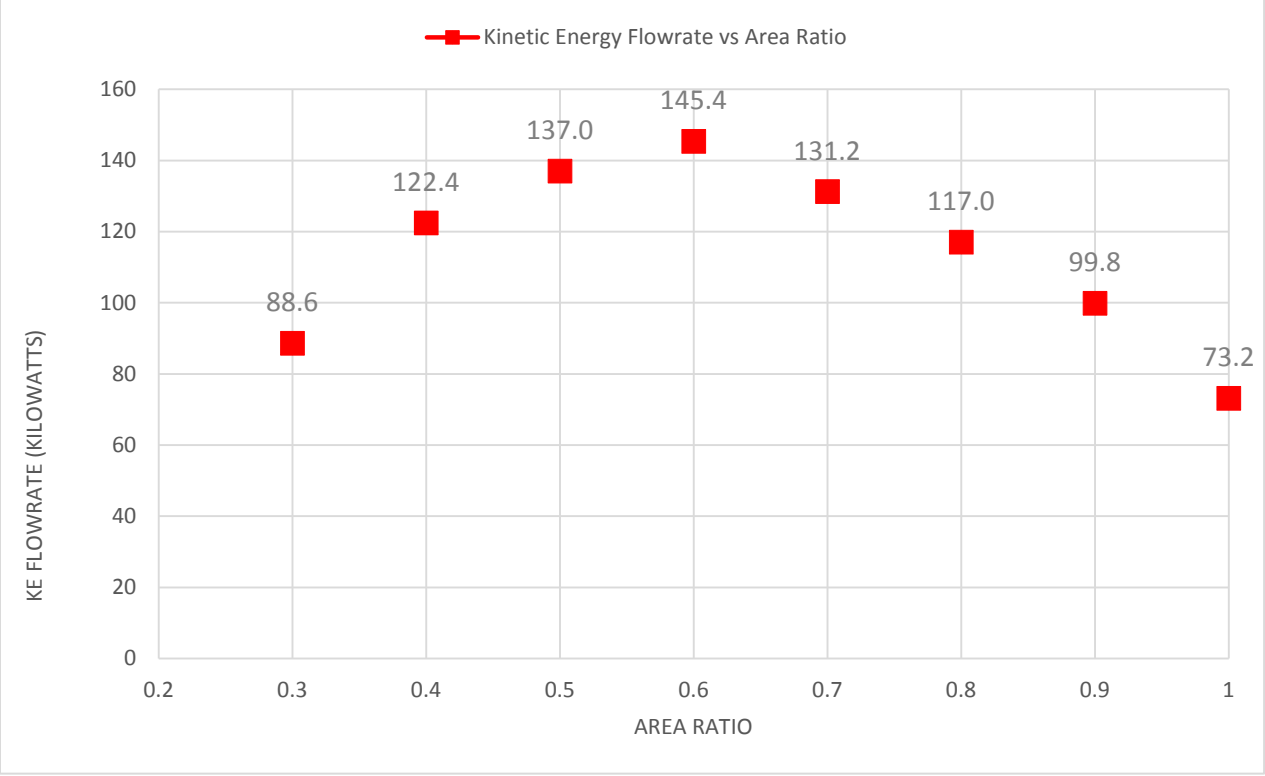

Figure 30. Kinetic energy flow rate as a function of Area Ratio for 30 ft. inlet length models.

The 60 ft. inlet length study was the last case to be simulated. The kinetic energy flow rate for each case is displayed as a function of AR in Figure 31. There again seems to be a plateau in KE flow rate for AR=0.4, 0.5, and 0.7, similar to that exhibited for the 15 degree inlet study. Although the maximum value is predicted for AR=0.6, the value for AR=0.4 is only 3% less than the maximum.

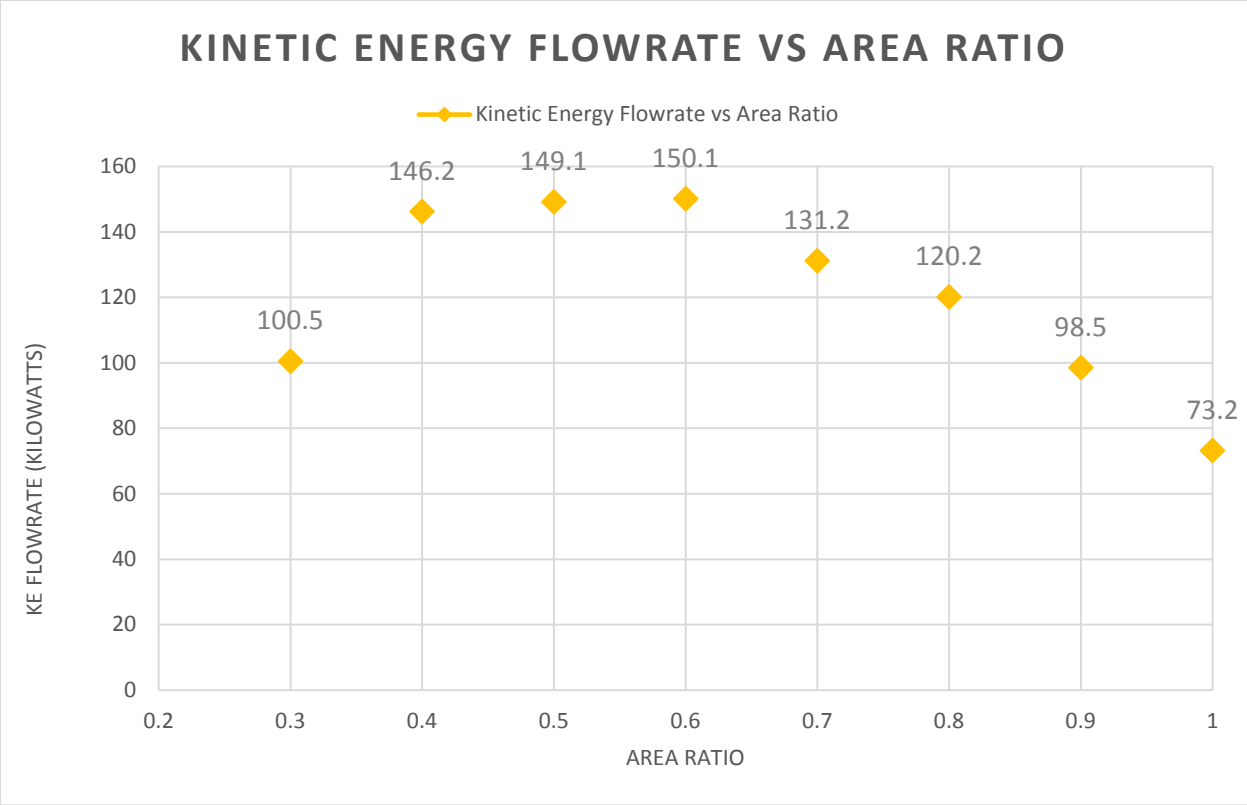

Figure 31. Kinetic energy flow rate as a function of Area Ratio for 60 ft. inlet length models.

B. Conclusions

For the purposes of this discussion, "performance" is judged as a function of kinetic energy flow rate with a larger rate equating to better performance. All conclusions are limited to the range of inlet angles and inlet lengths studied.

To provide insight into how inlet angle and inlet length influence channel performance, Figure 32 displays in a single plot the kinetic energy flow rate through the evaluation plane predicted for every case simulated. It reveals some very interesting characteristics of the channel flow.

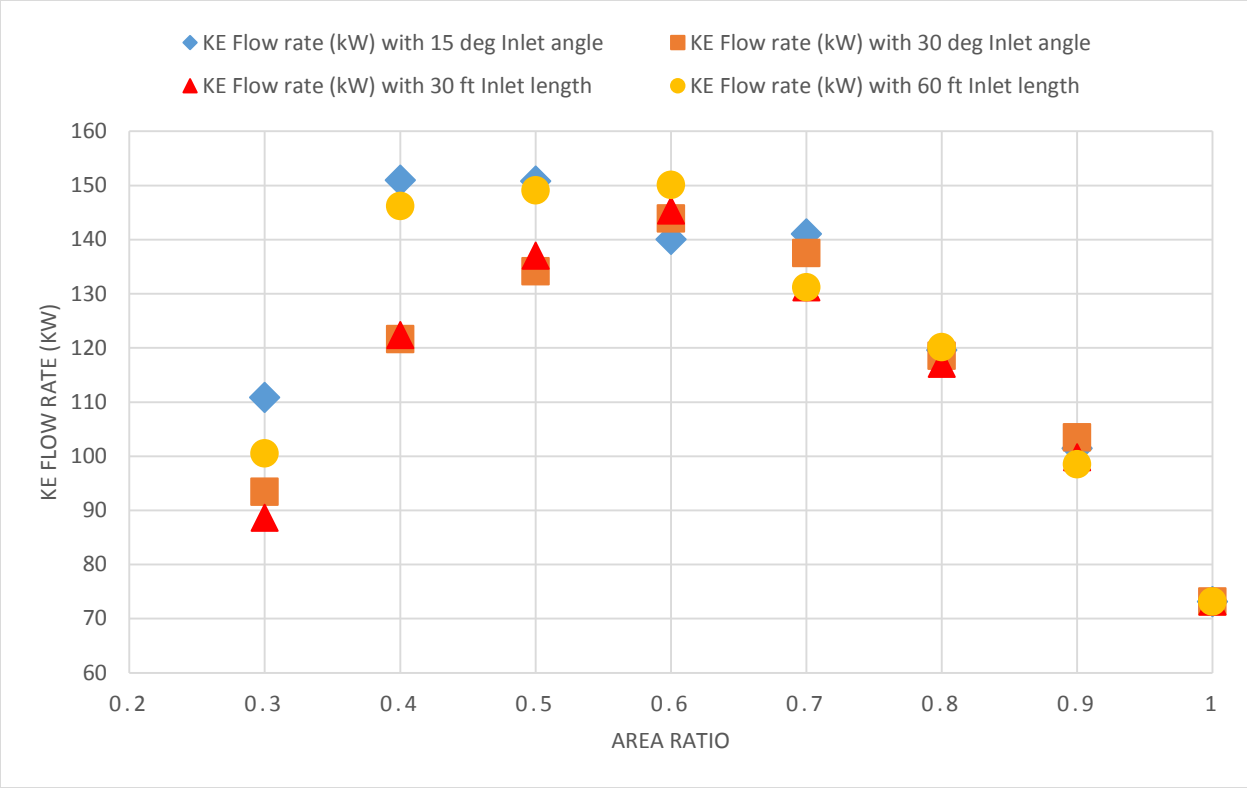

Figure 32. All of the kinetic energy flow rate from each models as a function of AR

- For values of AR> 0.6, the channel's performance seems to be insensitive to inlet angle or length.
- For values of 0.4< AR< 0.6, the inlets with a smaller half-angle, (the 15 degree family and the 60 ft. length family), significantly outperform the inlets with the steeper angles.
- Review of the geometry information collected into Table 16 reveals that all of the top performing channels have an inlet angle in the neighborhood of 15 degrees and that the level of performance for these cases seems to be insensitive to changes in the value of AR between 0.4 and 0.6.

- For all four cases with a value of AR= 0.3, the resistance to flow through the channel due to this amount of contraction has resulted in such an increase in bypass flow that the performance of these channels is only 50% of that predicted for the best performing channels.
- The lowest performing cases, the geometries of which are collected into Table 17, fall into two categories. The first, identified above, seem to be those with a low value of AR and therefore present a relatively large resistance to flow through the channel. The second are the cases with a very high value of AR. Although these outperform a channel with no contraction, they do not realize the benefit that can be obtained from a greater contraction of the flow channel. Table 17 clearly exposes two key features of low-performing channel geometries. The AR= 0.9 cases are low performing because the increase in throat section velocity is small in comparison to the other geometries. The AR=0.3 cases present so much resistance to flow that the increase in throat velocity is insufficient to overcome the effect of a decrease in mass flow rate through the channel.

Table 16. The top 5 performing channel models based on KE flow rate.

Area Ratio (%)	Inlet angle (deg.)	Inlet length (ft.)	Throat width (ft.)	KE flow rate (kW)
40%	15	67.18	24	151
50%	15	55.98	30	150.8
60%	11.31	60	36	150.1
50%	14.04	60	30	149.1
40%	16.7	60	24	146.2

Table 17.The bottom 5 preforming channel models based on KE flow rate.

Area Ratio (%)	Inlet angle (deg.)	Inlet length (ft.)	Throat width (ft.)	KE flow rate (kW)
30%	34.99	30	18	88.6
30%	30	36.37	18	93.4
90%	2.86	60	54	98.5
90%	5.71	30	54	99.8
30%	19.29	60	18	100.5

In summary, it is appropriate to draw two overarching conclusions:

1. A converging-diverging channel can significantly increase the performance of a machine designed to capture kinetic energy from a naturally occurring flow such as a river.
2. A 2D inlet with plane surfaces that provides a 2:1 contraction ratio and has a half-angle of approximately 15 degrees seems to maximize performance.

C. Future Work

Although the present research makes a significant contribution in that it supports the assertion that a properly designed channel can significantly improve the performance of the type of machine being studied, it only begins to explore the design space of the machine and does contribute to design of the turbomachinery. There is still work required to investigate the design space of a 2D inlet with plane walls. Determining the optimal shape for a 2Dcurved-wall inlet is yet to be studied. Will a 3D inlet outperform a 2D inlet? The influence of diffuser geometry on machine performance has yet to be determined. An optimal length for the power section is unknown as is the optimal location of the turbine within the power section. No work

has been done that explores interactions between the turbomachinery and the channel geometry that influence overall machine performance. No work has examined the performance of the turbomachinery. Is it better to use a horizontal-axis turbine or a vertical axis turbine. Can a horizontal-axis fully submerged turbine with helical blades outperform a partially-submerged paddlewheel-like turbine? For all of these, and related questions without answers, research can and should be conducted using computational simulations and physical experiments. Experiments will make an invaluable contribution to validating the computational simulations. Both experiments and computational simulations can play a valuable role in developing reliable dimensionless modeling tools. In short, the present work is just a very early step in a journey that can take many paths toward achieving the same goal: efficient production of power from the capture of the kinetic energy in a naturally occurring flow.

References

[1] M. Khan, M. Iqbal and J. Quaicoe, "River current energy conversion systems: Progress, prospects and challenges," *Renewable & sustainable energy reviews,* no. 12, pp. 2177-2193, 2008.

[2] F. Ponta and P. Jacovkis, "Marine-current power generation by diffuser-augmented floating hydro-turbines," *Renewable Energy,* no. 33, pp. 665-673, 2008.

[3] H. Willingham, "Power Generating Floating Vessel". United state Patent 8,772,957 B2, 8 July 2014.

[4] "Mississippi River Facts - Mississippi National River & Recreation Area (U.S. National Park Service)," Nps.gov, 2016. [Online]. Available: https://www.nps.gov/miss/riverfacts.htm. [Accessed 23 June 2016].

[5] F. Ponta and G. S. Dutt, "An improved vertical-axis water-current turbine incorporating a channelling device," *Renewable Energy,* no. 20, pp. 223-241, 2000.

[6] K. J. Richards, P. K. Senecal and E. Pomraning, *CONVERGE (v2.3),* Madison, WI: Convergent Science, (2016).

[7] P. M. Gerhart, A. L. Gerhart and J. I. Hochstein, Fundamentals of Fluid Mechanics, 8th ed., Hoboken, NJ: John Wiley & Sons, 2016.

[8] B. Cushman-Roisin and J.-M. Becker, Introduction to Geophysical Fluid Dynamics, Physical and Numerical Aspects, Waltham: Academic Press, 2011.

[9] D. L. Gaden and E. L. Bibeau, "A numerical investigation into the effect of diffusers on the performance of hydro kinetic turbine using a validated momentum sourse turbine model," *Renewable Energy,* no. 12, pp. 1152-1158, 2010.

Appendix A. Turbulence Setup for Boundary Conditions and for the Initial Condition

For most flows of interest, fluctuations in velocity due to turbulence occur over a much shorter time scale than changes in velocity due to changes in boundary conditions. Therefore, many turbulent flow models define the velocity as the sum of two contributions: one in which the velocity has been averaged over an elapsed time sufficient to "average out" fluctuations due to turbulence and a second that for any instant in time is added to the averaged value to produce the instantaneous velocity. Equation A.1 is a mathematical expression of this model in which is the averaged component and u' is the instantaneous fluctuation due to turbulence.

$$u = \overline{u} + u' \tag{A.1}$$

The k-ϵ model of turbulent flow has been used for the simulations performed in support of the research reported in this document. "k" is the turbulence kinetic energy (per unit mass) and is defined in terms of the turbulence component of the velocity: $k = \frac{1}{2}\left[(u_1')^2 + (u_2')^2 + (u_3')^2 \right]$. "ϵ", (epsilon), is the turbulence energy dissipation rate which is the rate at which the action of viscosity converts the turbulence kinetic energy into heat. The k-ϵ model solves a transport equation for each quantity and uses the local values to compute an "effective viscosity." Implementation of this model for turbulent flow requires specification of boundary conditions for the two quantities.

Converge provides two options for specification of a boundary condition for k: 1) a value for k, or 2) a value for the turbulence intensity, $I = \frac{1}{\overline{u}}\left[\frac{1}{3}\left((u_1')^2 + (u_2')^2 + (u_3')^2 \right) \right]^{1/2}$. The second option is offered because it is more common to have a reasonable estimate for I than for k, and one can be computed directly from the other.

$$k = \frac{3}{2} u_i^2 I^2 = \frac{3}{2}\left(u_1^2 + u_2^2 + u_3^2\right) I^2 \tag{A.2}$$

Typical values for turbulence intensity for well-designed wind tunnels are between 0.0002 and 0.01. [7] A value in the neighborhood of 0.1 is expected for atmospheric flows and lows in rivers. [7]

An appropriate boundary value for ϵ can be estimated using equation A.3. [7]

$$\varepsilon \sim \frac{u^3}{L} \tag{A.3}$$

Where L is an is the length scale of the energy containing eddies. For the present research the depth of the flow was used as the length scale.

Instead of using turbulence intensity, one can also input the turbulent kinetic energy, or k in the boundary condition setup using equation A.3.

To determine the sensitivity of the simulations to value specified as initial conditions or boundary conditions for the k-ϵ turbulence model, sensitivity study was conducted but after several simulations using different values on the two parameters, it was shown that the simulation results are not sensitive to turbulent kinetic energy and turbulent dissipation with different values.

Appendix B. How to prepare channel STL file in Converge Studio

In order to import a CAD model into Converge Studio, one must use a CAD software that will allow the user to export their model into STL (STereoLithography) format. Once the CAD model in STL format is ready, the user will also need to work on the model inside Converge Studio. The following steps will be required to setup our channeling device.

1. From the top left corner, select File, then in the drop-down menu, select Import, then Import STL.
2. Once Import STL is selected, a new window called “STL file(s) importing” will be opened, choose the STL model file on the left side.

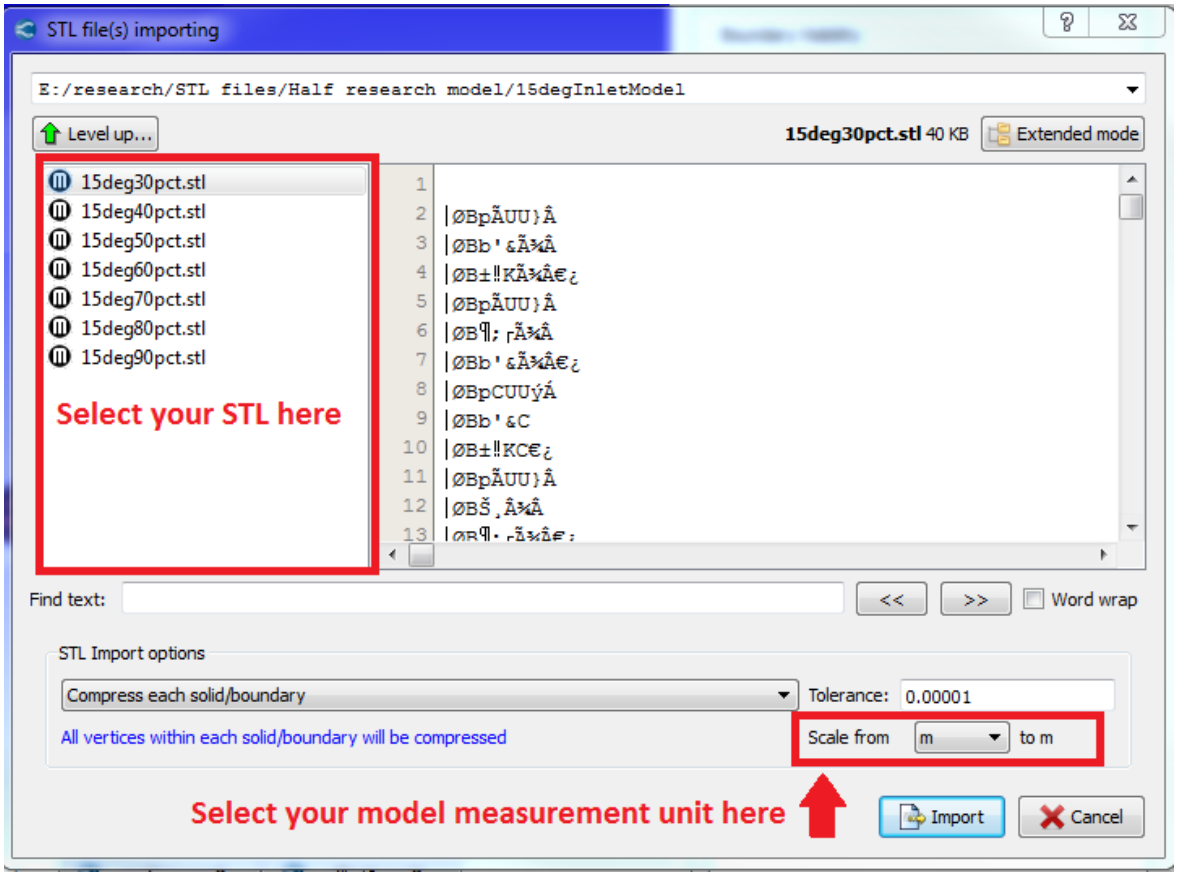

Figure 33. STL file(s) importing window and layout.

3. When the correct STL file is selected, make sure in the STL Import options, “Compress each solid/boundary” is selected.
4. Since Converge Studio requires users to use SI units for measurements, if the original CAD model was created with length measurement units other than SI (meter), one must specify the original length unit in the “Scale from” drop-down menu to convert your STL model length unit to meter.
5. Double check the correct unit is selected in the “Scale from” menu, then select “Import” button. The machine should become visible in the center window. You should be looking at the top-view of the air-box (for the “Thesis Example”). In the lower-right corner of the window is a list of the named boundaries. The left edge of the list is populated with check boxes, and each should selected as signified by the check in the box. The first line in the list is the “Not Assigned” assigned boundary. Although the list of boundaries was created in an earlier step, none have been assigned to the geometry. Therefore, the top of the air box is still green signifying the boundary has yet to be assigned a name. Click on the check-box in the first line of the list to remove all “Not Assigned” boundaries … which are all of those not defined in the CAD model. You should see a small black rectangle at the origin of the coordinate system. Use the mouse scroll-wheel to enlarge. The surfaces of the CAD model have are all brown because they have been assigned to the “Air inflow” boundary.
6. To begin the process of reassigning the CAD model surfaces to the correct boundary names, select the “Triangle” icon located in the ribbon near the top of the window.

7. Adjacent to the triangle icon is a drop-list of “Filter” options, defaulted to “Any”. From the drop-list, select “By Angle”.
8. Select the Boundary-button in the top left corner and then select the Flag-tab to reveal a list of named boundaries. (e.g., Water channel interior). In the center window, rotate the CAD model until you can see the interior surfaces. If necessary, hold down the Ctrl-key and the mouse scroll-wheel to “pan” using the mouse.
9. Select the interior surfaces of the machine, by (one-by-one) placing the mouse cursor over the surface and left-click: the surface(s) should turn red. Select “Water channel interior” from the list of named boundaries by clicking on that row of the list. Click the Apply-button. The surface(s) should change from red to the color assigned to the named boundary.

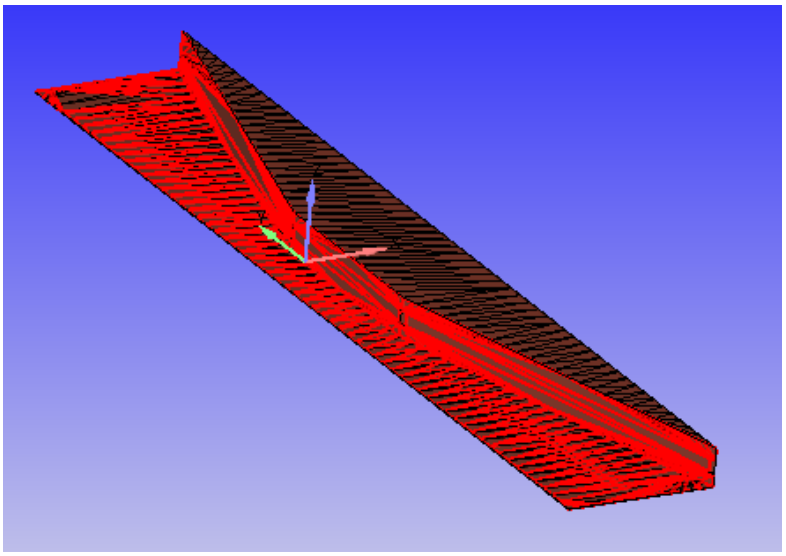

Figure 34. The selected interior surfaces of the machine highlighted in red during step 9.

10. Zoom-in to the leading edge of the channel as shown in the figure below. Although at first it may be difficult to see, there is a thickness to the bottom-plate of the channel. You want to select only this edge and assign it to a name. If any items appear in the list under

"Triangles" in the left pane, click on the "Clear All"-button to empty the list. If you click on just the thin edge, only it should be highlighted in red and only "Selection Set 0 – 20 entries" should appear in the list under Triangles in the left-pane. "Water channel interior" should still be selected in the named boundary list: click the Apply-button to assign the leading edge of the bottom-plate to this boundary name. The "Sum" associated with this boundary name should increase from 279 to 299.

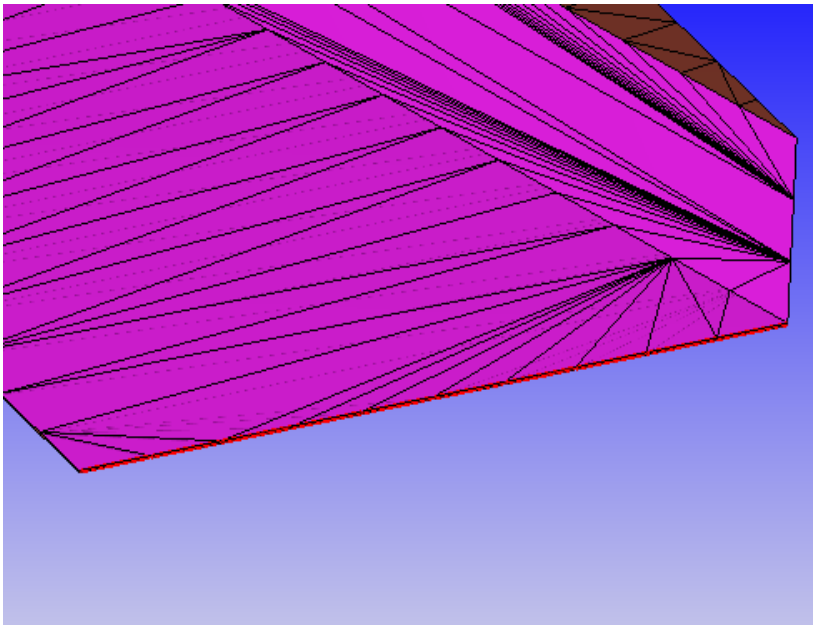

Figure 35. Assigning B.C. to the very thin surface of the machine facing the negative y-direction.

11. At the other end of the channel, follow the same procedure to assign the trialing-edge of the bottom-plate the "Water channel interior boundary". On the other end of the machine, apply the water channel interior boundary to the very thin surface of the machine facing the positive y-direction. If this is done correctly, the "Sum" for "Water channel interior" should now be 319.

12. After the interior of the machine has been properly labeled, select the improperly labeled outside surface and the bottom of the machine, and assign the water channel exterior boundary to the surfaces. (Sum= 264)
13. For the simulation to work properly, the top of the machine must extend into the air region. Select the Create-button in the top left corner of the window, and then select the Copy-tab" below.
14. In order to increase the height of the machine, one must specify a new height by making a copy of the top surface from the channeling device. Select "Copy Type" as "Triangle".
15. To select the top surface of the machine, select the "Triangle" icon located in the ribbon near the top left corner.
16. Then select the "Filter" drop-down menu (should be currently set to "Any"), and select "By Angle" as filter. This is the visual of the drop-down menu:

17. Position the mouse cursor on the top surface of the machine to select it: the edges of the triangles forming the surface should be highlighted in red.

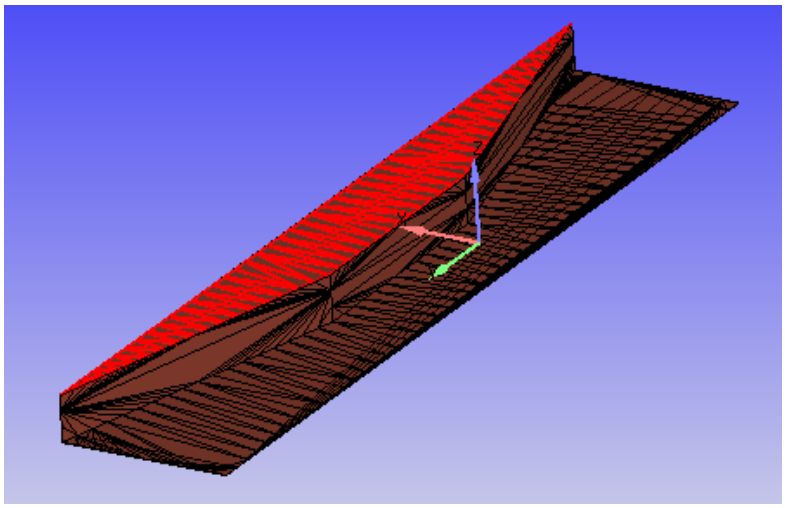

Figure 36. Highlighted top surface to be selected in step 10.

18. Back to the “Copy” menu, look for the “Offset (x,y,z)” in the interface, and specify the height you want to offset the top surface, which should be the height you would like the channeling device to be above the water surface in meters. 2 meters was used in the example simulation. To reproduce this increase in height, enter “2” in the z-coordinate field of the Offset(x,y,z) group.
19. Select “Apply”. Now there should be a new top surface created 2 meters above the original top surface. The new surface has not yet been assigned a name, so it should be green. Its outline is orange because all of its edges are “open.”
20. Assign the new top surface to the “Air channel” boundary: Boundary-button, Flag-tab, click on the line for “Air Channel” in the list, click on the top surface in the graphics field, click Apply-button.
21. To delete the previous top surface of the channel: Repair-button, Delete-tab, triangle-option, triangle icon and “By Angle” option in the top-ribbon, click on the previous top surface in graphics field, select Apply-button. In the graphics field, there is now an

opening where the previous top surface existed and the new top surface is hovering over that opening.

22. There are now two sets of open edges (colored in orange on the model): one around the new top and the other around the opening formed by removal of the previous top. To start the process of joining the new top to the rest of the model: select the Create-button in top-left of window, select the Triangle-tab, and the "Loft edges" option.
23. Click the check box next to the "Select first set of edges". From the ribbon near to the top of the window, from the "Filter" drop-list select "By Open Edge".
24. Left click one of the open-edge sets highlighted in orange: the edges in that set should have become red. That edge-set should now appear in the "Selected Entity" list .
25. Click the check box next to the "Select second set of edges" and click on the other open-edge set. That outline should turn red and that edge-set should appear in this list.
26. Make sure the "Auto match edge chains" box (immediately below the two lists), is checked.
27. In the "Placed in boundary" drop down menu, select the boundary condition that was created for the Channel Device exposed in the air ("air channel" was used in simulations).
28. Select "Apply". Now the newly created top surface should be connected to the rest of the channeling device, with the appropriate color signifying the correct boundary.
29. The example simulation takes advantage of a plane of symmetry to reduce the size of the computational domain to half of the entire flow field. To enforce this symmetry condition, the edge-surface of the bottom-plate cut by this plane of symmetry must be

removed. To start the surface deletion process, from the ribbon near the top of the window, select the “Triangle” icon and the “By Angle” option from the “Filter” drop-list.

30. Select the Repair-button, the Delete-tab, and then choose the “Triangle” option.
31. As was done for the thin surfaces at the leading- and trailing-edges of the channel, rotate and zoom the image in the graphics field until you can click on the surface of interest and only it becomes outlined in red. This surface should still have the color associated with the “Water channel exterior”, and only one “selection” should appear in the “Selected Entity” list.
32. Select “Apply” to confirm the deletion, and now there will be an open edge where the surface was removed, signified by the orange outline.
33. There are now two open-edge sets in the model: the one just created by removal of the edge-surface of the bottom plate, and the other created when the entire side of the water box coinciding with the symmetry plane was removed. To create a completely bounded computational domain, these edge-sets must be joined. The following figure depicting these edge sets is not to scale.

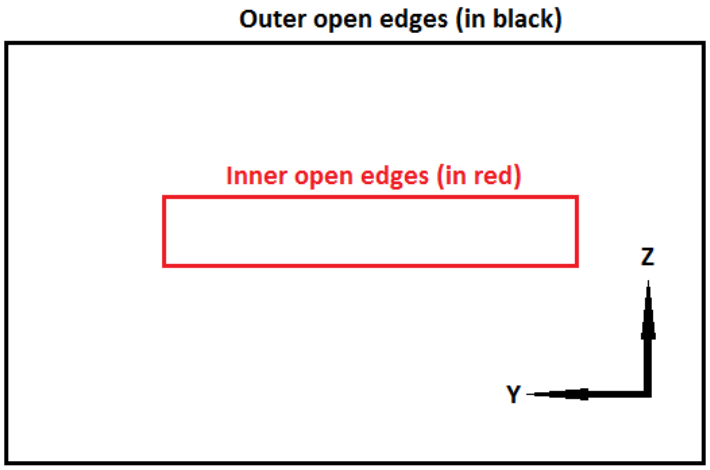

Figure 37. Demonstration of the two open edges in step 29.

To see the two open-edge sets in the graphics field, you must zoom-out to the size of the flow field boundaries, and turn back on the “Not Assigned” boundary.

To help establish a clear mental image of the computational domain to be created, consider a torus (e.g., a doughnut, a bagel) cut into halves along a plane of symmetry such that each half forms a circular trough. From a perspective above and normal to the cutting plane, each trough looks like two concentric circles. A “lid” could be formed for each trough by a plane, limited in size to the extent of the large circle, from which the smaller circle is cut. Attaching the lid to the trough defines a completely bounded domain within. The difference between the domain of the lidded half-torus and the domain of interest is that the bounding surfaces of the domain of interest are planes so the plane of symmetry looks like the figure above and instead of two concentric circles.

At present, the computational domain has no “lid” joining the two open-edge sets. To start the joining process: select the Create-button, the Triangle-tab, and select the “From three Vertices” option.

34. There are many options for making different choices, (e.g., which vertex to pick), in the following few steps that can achieve equally effective results. The following instructions match the figures presented. Click on the  icon to produce a view in graphics field that is normal to the cutting-plane. Zoom-in until you can select just the two vertices at the right-edge of the bottom plate. Select first the upper vertex and then the lower. Each time you select a vertex, it in enclosed by a red circle. You may wish to slightly rotate the image in the graphics field to ensure that the vertices you have picked are at the intersection of the bottom-plate and symmetry-plane. Both vertices should now appear in

the “Selected Entity” list. Immediately below the list, make sure that the check box next to “Seed selection with previous 2 vertices” is checked. Zoom-out and select the vertex at the top-right outer boundary as depicted in the figure below. Select the appropriate boundary name, “Symmetry water”, in the drop down menu in “Placed in boundary”. Select “Apply” to create a triangle defined by the three selected vertices. The figure greatly exaggerates the width of the triangle.

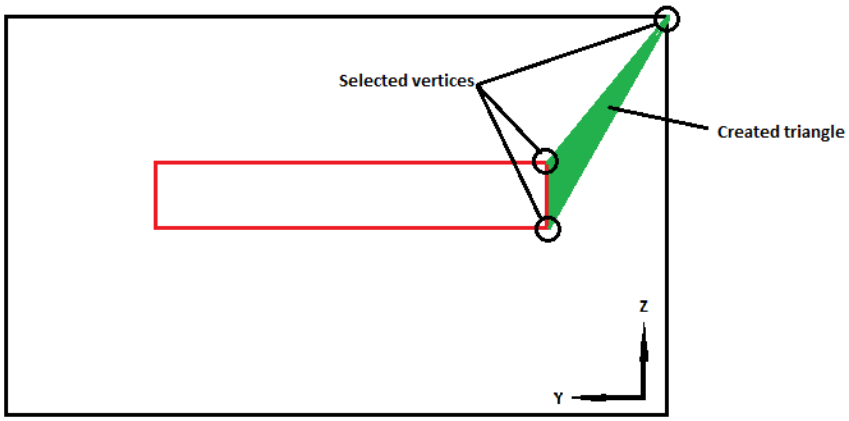

Figure 38. Demonstration of the two open edges and the first created triangle.

35. Although the first vertex selected in the previous step has been dropped from the “Selected Entity” list, the second and third have been retained. Selecting the vertex at the bottom-right edge of the outer-boundary adds it to the list. Make sure the appropriate boundary name is selected from the “Placed in boundary:” list. Click the Apply-button to create a second triangle as shown in the following figure.

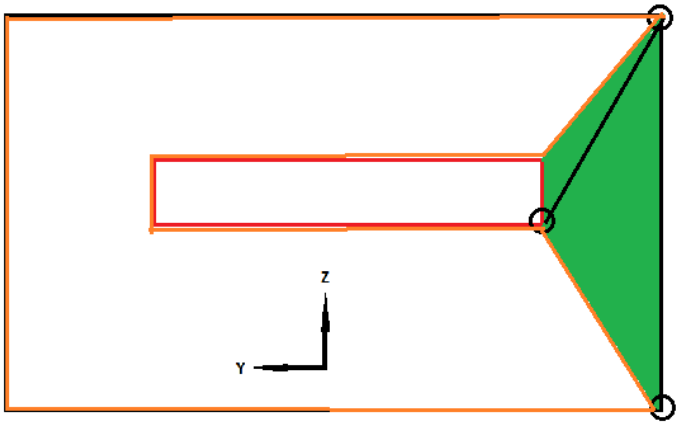

Figure 39. Demonstration of the two open edges and second created triangle.

As highlighted by an orange outline in the figure above, there is now only one set of open edges.

36. With only one open-edge set, the final part of the lid can be quickly formed. Click the Repair-button, select the Patch-tab, and select the "Free edge loop" option. You should be able to pick the entire open-edge set by clicking on any edge in the set. At present, there is a bug in the software. Instead of clicking on an edge, you must enclose it with the enclosure too, the dashed-rectangle in the ribbon, 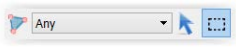

. Before using the tool, make sure that "Any" is selected from the Filter-list. Pick an edge from the open-edge set with the enclosure tool. The easiest to pick is probably the edge at the left-side of the domain. Once selected, that edge should turn red. Click the Apply-button to tessellate the entire surface enclosed by the open-edge set with triangles. There should now be no open edges in the model. The entire "lid" is formed by triangles. Depending on the details of the imported CAD model, these triangles may be very thin and may appear to be badly distributed on the surface. Neither aspect ratio nor distribution will

impact the quality of the computational mesh. Of crucial importance is that the surface is complete.

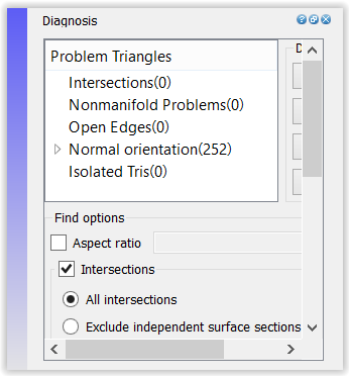

This is a good time to use the "Diagnosis" tools in a small window docked at the right-side of the CONVERGE Studio window. You may need to "undock" it by clicking on the middle of three icons in the upper-right of the Diagnosis-window. You can then enlarge it by dragging a corner. Select the Find-button. A list of potential problems with the geometry will appear in the window. At this point of development, the only item of interest is "Intersections". If the number of Intersections is other than zero, an error has been made and steps retraced to rectify it. The number of steps to be retraced is likely few. It is suggested to frequently check the diagnosis tool to detect when a problem is introduced. If no Intersections are identified, proceed.

37. The surface normal for each boundary must be pointed toward the fluid. To ensure this is the case, or to help make it so, use the tool invoked by clicking the "Normal toggle" icon positioned at the left-edge of the CONVERGE Studio window,  . Clicking this icon displays the currently defined normal to each triangle that forms a surface in the model.
38. Click the Transform-button, select the Normal-tab, and choose one triangle on any surface by clicking on it in the graphics field. That outline of that triangle turns red. Click the Apply-button. All normal should be pointed toward the fluid domain. To ensure this is true, use the Find-tool in the Diagnosis-window. The "Normal orientation" item should identify zero problems with this item.

To continue project initialization, return to Step 25 of Appendix C.

Appendix C. Instructions for Converge Studio Case Setup

This appendix presents a sequence of steps that will produce an input data set that defines a computational simulation to be performed by Converge. Although an expert user can directly edit input data files to accomplish this task, it is much easier for most users to define the simulation using the CONVERGE Studio graphical user interface. The following steps walk the user through the a process that defines the outer-bounds of the computational domain, imports a standard stl-file to define the geometric details of the machinery to be placed in the flow field, and specifies all of the physical parameters of the model such as material properties, boundary conditions, and initial conditions.

1. Assuming that CONVERGE Studio is installed on the computer, start this software, typically with a click on the appropriate icon. This will open the basic Converge Studio window containing several standard tools, similar to the image following this paragraph. The window is usefully described as having a left-pane, a center-pane, a right-pane, and tools organized in rows across the top of the window. The center-pane includes a graphics field in which model geometry is displayed in a fashion similar to most modern CAD programs. A row of text items along the top of the window leads to a drop-menu when any item is selected. Immediately below is a ribbon holding several icons and a few drop lists that facilitate model definition. In the left-pane, along the left-edge, are icons that facilitate actions to occur in the graphics field. The remainder of the left-pane,

and the right-pane, contain groups of tools that facilitate model definition. In the center-pane, select 

, to start specification of a new set of input data files.

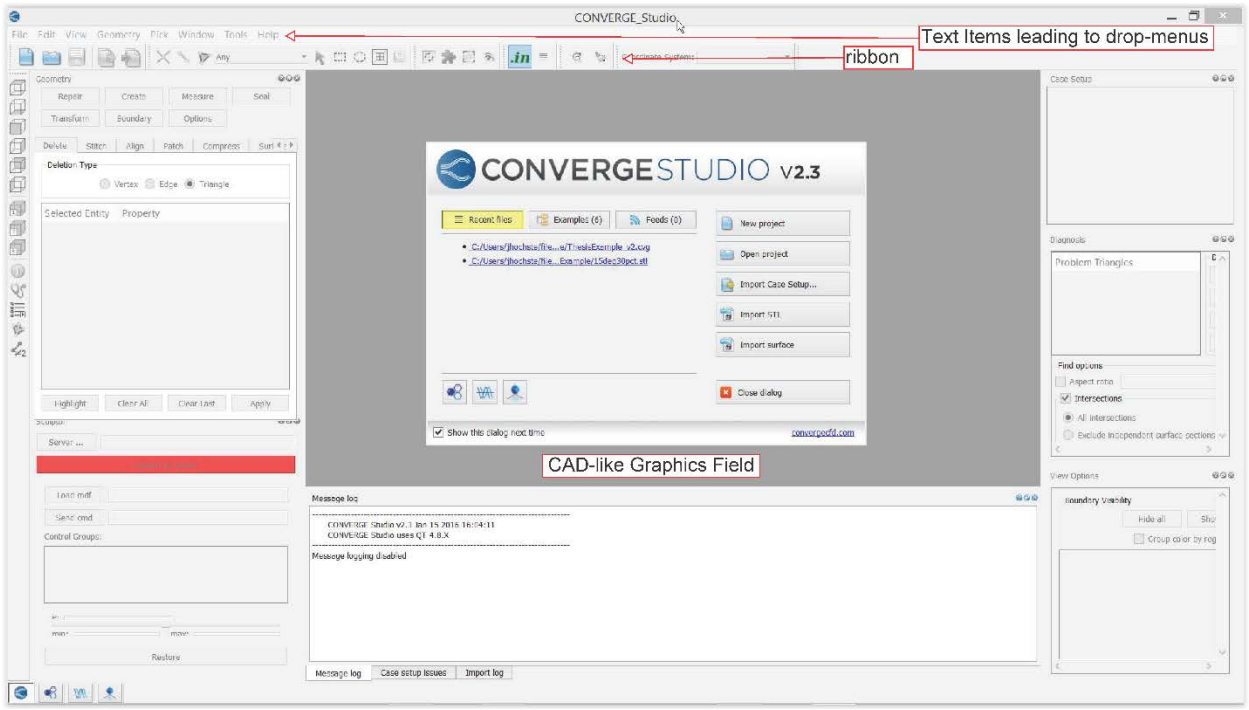

2. Before the physical description of the model can be specified, (e.g., material properties, boundary conditions), the geometry of the computational domain must be defined. To being the process, select the Create-button located in the top-left of the CONVERGE Studio window.
3. After clicking Create, select Shape tab, and select Box.
4. In order to create the flow region that describes the simulation, we need to determine where the free surface is in the coordinate system. In all the simulations, we decided that free surface is at z=0, which means air region and water region will be connected at z=0. Then, since we are using symmetry, we decided that the symmetry boundary wall will be located at x=0. Using the parameters from Table 5 and Table 15, we can determine the sizes of the

air and water region. To create the water box first: under Center, each box represents the coordinate of the center of the box being created, type in [30, 0, -7.5] into the corresponding boxes.

5. Under Size in meters (dx, dy, dz), type in [60, 250, 15] in the corresponding boxes. Click on the “Create”-button, and a green box should appear in the center window. If you have made an error in defining the water box, at the upper-left of the CONVERGE Studio window, click on “Edit” and click on the undo feature. You should be looking at the top of the water.

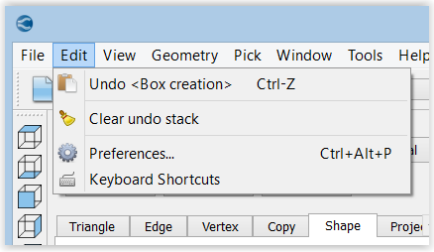

6. The top of the water-box must be “removed” because it must mate with the bottom of the air-box (to be created). To remove the top of the water-box, select Repair, then select the Delete-tab. Under Deletion Type, select the Triangle option. Move the cursor into each of the triangles on the top of the water-box in the center window, one at a time, and click on each, so that both are selected as indicated by a red outline. Click on the Apply button. To rotate the view of the water-box, much like most CAD programs, place the mouse cursor anywhere in the graphics field, hold-down the Ctrl-key, and move the mouse,. The box that represents the water region should look like the figure below.

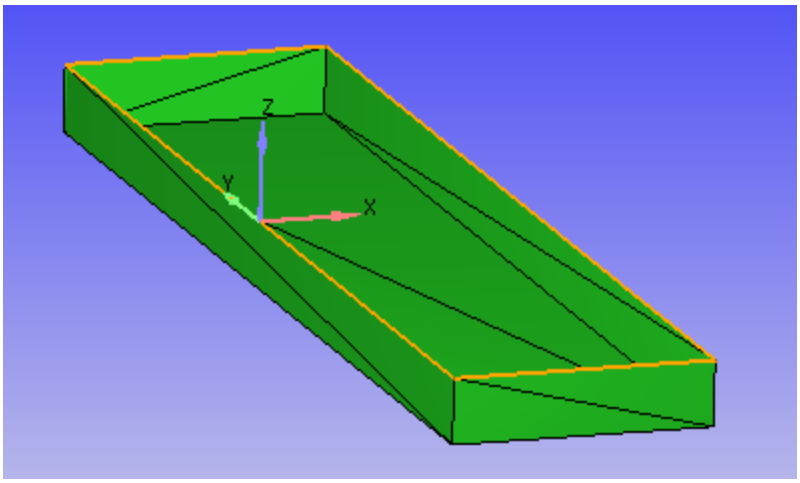

Figure 40. Box that represents the water region in step 7.

7. Once the box that represents the water region is created, we will create the box that represent air region by using the Mirror function in Converge Studio. On the top left corner, select the Transform-button, then select the Mirror-tab.
8. Under the Mirror Type, select Entire Surface.
9. Under the Mirror options, select About the X-Y plane (z*-1).
10. Check the box for Create a copy of mirrored cells.
11. Under the Boundary offset, input 0, then click Apply at the bottom. The box should now look like the picture below. Use the scroll button on the mouse to make the image larger or smaller within the graphics field.

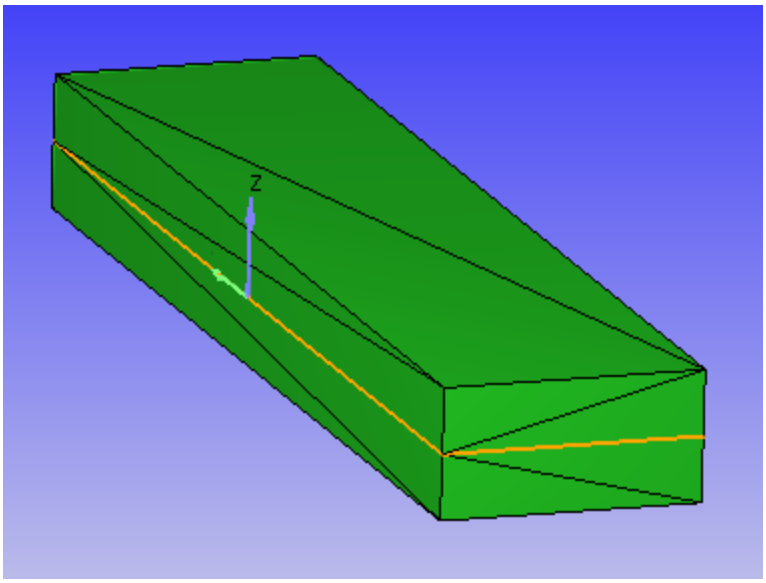

Figure 41. Boundary boxes created in step 12.

12. Now that the boxes that represent air and water regions have been created, we can see the orange outline appeared near the interface of the 2 regions. This indicates that there is an open edge at the interface of the two regions. In order to eliminate the open edge, select the Repair-button from the top left corner, and then select the Compress-tab.
13. Under the Compress Options, select All vertices.
14. For the Tolerance, input 1e-5, and then click Apply. The outline should change from orange to black to show a boundary edge, but not an open edge.
15. Once the flow region has been created, boundaries must be named so that boundary conditions can be specified. Select the Boundary-button from the top left corner, and then select the Flag-tab.
16. Click the Create a new boundary button  , a new window called Boundary definition will open.
17. Check the box for Create multiple boundaries, then input 1 as the Starting boundary ID.

18. Input 13 as the Number of boundaries to create, then click OK. The newly created boundaries should show up in a list on the left side under the Flag-tab.
19. To rename each boundary, right click the name of the boundary under the boundary list, and type in the new name for that specific boundary. The following list consist of all the boundaries used in the example simulation. At your discretion, you can have spaces between multiple words in a boundary name.

Table 18. List of boundary conditions require renaming in step 20.

Boundary 1	Air inflow
Boundary 2	Air outflow
Boundary 3	Air side
Boundary 4	Air top
Boundary 5	Air channel
Boundary 6	Water inflow
Boundary 7	Water outflow
Boundary 8	Water side
Boundary 9	Water bottom
Boundary 10	Water channel exterior
Boundary 11	Water channel interior
Boundary 12	Symmetry Water
Boundary 13	Symmetry Air

20. To prepare for importing the CAD geometry, select the Repair-button, select the Delete-tab, and for Deletion Type, select Triangle.

21. In order to prepare for importing the channel model, select the Left Side View icon  on the left side of the Converge Studio window. In the graphics field, you should be looking directly at the left-face of the boxes and you should see the z-coord.-arrow pointing up and the y-coord.-arrow pointing to the left.

22. Select the bottom 2 triangles, (the left-face of the water box): place cursor on each triangle and click to activate indicated by red outline of each. Click the Apply-button. The area with the deleted triangles should now have an orange outline that represents an open edge. You are now looking through an open-face. The diagonal line you see is actually the boundary between the two triangles on the far-face of the box.

23. Follow the directions in Appendix B to import the appropriate channel model. To help ensure that your work to this point is not lost, save the project file by selecting the File menu from the top-left of the window, select “Save” from the drop-menu, and use the dialog-window that opens to name the project and save the ____.cvg file to the desired directory.

24. The geometry of the computational field has been fully defined. To begin specification of the physical description of the flow field, (e.g., material properties,), in the left-pane, click on the Boundary-button and select the Flag-tab.

25. To assign inflow boundary conditions, us the Front View icon,  , orient the image in the graphics filed so that the view is normal to the inflow boundary.

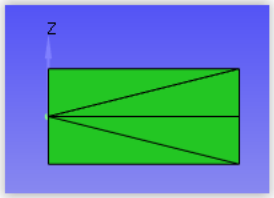

26. To define the surface on with “Air inflow” boundary conditions, (BCs), are to be imposed, select the top two triangles, select the appropriate row from the list in the left-pane, and click the Apply-button. The two triangles should take-on the color associated with the Air inflow boundary.
27. Assign the bottom two triangles to the Water inflow boundary following a similar process.
28. Assign named boundaries for outflow from the computational domain by flipping the image using the Back View icon,  , and repeating the name assignment process for both the air and water regions.
29. Assign named boundaries for the side of the computational domain, using the Right Side View icon,  , to facilitate repetition of the boundary name assignment process.
30. Assign named boundaries for the top and bottom of the computational domain using the process of the previous steps.
31. Assignment of boundary names for surfaces in the symmetry plane is a bit different from the process used for the other domain boundaries. Use the Left Side View icon,  , to orient the image in the graphics field so that the symmetry plane lies in the view-plane. From the ribbon at the top of the window, select “By Angle” from the Filter-list, select any triangle on the surface of the water box, select the appropriate line from the named boundary list, and click the Apply-button. This should have assigned a name to only the water box surface and you would repeat the process for the surface of the air box. However, at the time these instructions were prepared, there is a software bug that results in name assignment to the entire domain surface coincident with the symmetry plane.

This mis-assignment is easily corrected by selecting “Any” from the Filter-list, selecting the two tringles that tessellate the entire portion of the surface to be associated with the air region, selecting “Symmetry Air” from the named boundary list, and clicking the Apply-button. All surfaces bounding the computational domain should now be associated with a boundary name.

32. Once all the surfaces have been labeled with proper boundary conditions, at the bottom right corner, select Case Setup, then click Begin Case Setup. A new window will open.
33. In the Begin Case Setup window, without selecting either IC engine or General flow, click Done.
34. Select Materials under Case Setup, a new window called Case Setup with open, tick both boxes for Gas simulation and Liquid simulation, and un-tick all other boxes, click Done.
35. Select Gas simulation under Case Setup, a new window will open, next to Equation of state, select Ideal gas from the drop-down menu, then select Gas thermodynamic data, a new window will open, select N2, click OK. And click OK again to close the Gas simulation window.
36. Select Liquid simulation under Case Setup, a new window will open, select Predefined liquids, another window called Liquid database will open, select H2O_WATER from the Predefined list, and then click Add selected.
37. In order to simplify the simulation, using constant liquid properties are preferred. Converge Studio provides liquid property table ranging from 0 K to 650 K. Since the simulation is assumed to be at 300 K, all other liquid property data needs to be removed. In the liquid property table, select all the liquid properties that is not at 300 K, and select  on the top right corner of the table to remove them from the liquid property table.

38. Once all the other liquid properties are removed, the simulation can be further simplified by changing the surface tension value to 0.
39. After changing the surface tension, tick the box next to Constant liquid properties, and click OK.
40. Select Global transport parameters under Case Setup, a new window will open, and the default value will be used by clicking OK for the Prandtl number and Schmidt number.
41. Select Species under Case Setup, a new window will open. Under the Gas tab, select  , and a new item will appear under Gas species. Type N2 to use nitrogen as the gas species for the air region.
42. Under the Liquid tab, select  , and a new item will appear under Liquid species. Type H2O_WATER to use water as the liquid species for the water region. Click OK.
43. Select Simulation Parameters under Case Setup, a new window will open, tick the box next to Body forces, and click done.
44. Select Run parameters under Case Setup, a new window will open. Under Run Mode, New run should be selected, and under Solver tab, Solver should be Transient, and Simulation mode should be Full hydrodynamic. Gas flow solver and Liquid flow solver should be changed to Incompressible to simplify the simulation.
45. Select Misc tab on the same window, select Concise as the Screen print level. Untick anything other than Solve momentum and Reread Inputs,in each time-step, then click OK.
46. Select Simulation time parameters under Case Setup, a new window will open. Under General tab, start time should be set at 0 s, end time should be set at 180 s, Time-step

selection should be Use variable time-step algorithm. Initial time-step should be 1e-5 s, Minimum time-step should be 1e-5 s, and Maximum time-step should be 0.05 s.

47. Once all the time-step sizes are set, click OK.
48. Select Body forces under Case Setup, a new window will open. Under Gravity, change the gravity in z direction to -9.81 m/s^2 to apply gravity to the simulation. Click OK.
49. Select Solver parameters under Case Setup, a new window will open. Under PISO tab, Minimum number of PISO iterations should be 10, and Maximum number of PISO iteration should be 21. These values are provided by Converge Science Support.
50. Under Convective flux scheme for Solver parameters, Flux blending fraction for FV scheme should be 1 for Momentum tab, Species/Energy/Density/Passive tab, and Turbulence tab.
51. Under Misc. tab for Solver parameters, Fraction of the momentum portion in conservative form should be 0.
52. Under Equations for Solver parameters, Table 19 is provided below for each equations.

Table 19. Different parameter used for equation solvers.

Equation	Solver type	Convergence tolerance	Min iteration	Max iteration	SOR relaxation
Momentum	SOR	1e-06	0	300	1.0
Pressure	BiCGSTAB	1e-06	2	800	N/A
Density	SOR	1e-04	0	2	1
Energy	SOR	1e-05	0	2	1
Species	SOR	1e-05	0	2	1
Passive	SOR	1e-05	0	30	1
TKE	SOR	1e-02	2	3000	0.7
Epsilon	SOR	1e-02	2	3000	0.7
Omega	SOR	1e-02	2	3000	0.7
Radiation	SOR	1e-08	0	2500	1

53. Select Post variable selection under Case setup, a new window will open. Under Cells tab, the following parameters should be selected: Density, Velocity, Void Fraction, and Region ID. Click OK.
54. Select Output files under Case setup, a new window will open. For Inter-region flow rate output, it should be selected as “Do not generate output”.
55. Time interval for writing 3D output data files controls how often 3D output files are generated for post processing, 5 seconds per output files were used for this research.
56. Time interval for writing text output controls how often Converge records data into output files. 1e-05 seconds was used for this research.
57. Time interval for writing restarting controls how often Converge creates restart files in case of unexpected interruptions. 1 second was used for this research.
58. Select Regions and initialization under Case Setup, a new window will open. Click Add, and a new region is created. For the research, there are two regions: air region and water region. Double click the name of the region recently created, and rename it as Air region.
59. Once the region has been named, on the right side, input [0, 2, 0] m/s as Velocity.
60. Under Species, click  on the right side, a new specie <NONE> is created under Species. Double click the name of the specie, and select N2 from the drop down menu. Then input 1 as the Mass Fraction.
61. In the same Regions and initialization window, Click Add and renamed the newly created boundary as Water region.
62. Once the region has been named, on the right side, input [0, 2, 0] m/s as Velocity.
63. Under Turbulence initialization, enter 0.0024 as the Turbulent Kinetic Energy, and 0.1 as the Turbulent Dissipation.

64. Under Species, click  on the right side, a new specie <NONE> is created under Species. Double click the name of the specie, and select H2O_WATER from the drop down menu. Then input 1 as the Mass Fraction.
65. Click OK.
66. Select Boundary under Case Setup, a new window will open. On the left side of the new window contains all the boundaries created earlier in the case setup with its region undefined. Double click Region Undefined next to the air inflow, and select Air region.
67. Repeat step 70 for each boundary condition to assign the appropriate region (i.e. air top should be in air region, and water bottom should be in water region.)
68. Once all the boundary conditions have been assigned to its appropriate region, use the following tables to configure each boundary.

Table 20. Boundary condition setup for step 72.

Boundary Name	Boundary Type	Pressure Boundary Condition	Velocity Boundary Condition	TKE Boundary Condition	Eps Boundary Condition
air inflow	INFLOW	NE	DI=[0,2,0]	Intensity =0.02	Length scale =0.003
air outflow	OUTFLOW	NE	DI=[0,2,0]	NA	NA
air side	OUTFLOW	NE	DI=[0,2,0]	NA	NA
air top	INFLOW	DI=100000 Pa (Total pressure)	NE	Intensity =0.02	Length scale =0.003
air channel	WALL	NA, roughness= 0.5	Wall motion type= Stationary, Law of wall.	NE	Wall model
water inflow	INFLOW	NE	DI=[0,2,0]	Intensity =0.1	DI=0.5
water outflow	OUTFLOW	NE	DI=[0,2,0]	NA	NA
water side	OUTFLOW	NE	DI=[0,2,0]	NA	NA
water bottom	OUTFLOW	NE	DI=[0,2,0]	NA	NA
Water channel exterior	WALL	NA, roughness= 0.5	Wall motion type= Stationary, Law of wall.	NE	Wall model
Water channel interior	WALL	NA, roughness= 0.5	Wall motion type= Stationary, Law of wall.	NE	Wall model
Symmetry Water	SYMMETRY	NA	NA	NA	NA
Symmetry Air	SYMMETRY	NA	NA	NA	NA

69. Select Boundary under Case Setup, a new window will open. Tick the box next to Events, then click Done.
70. Select Events under Case Setup, a new window will open. Tick the box next to PERMANENT tab, and click  to add a new row to the table.
71. Under Region 1, double click Region Undefined, and select Air region from the drop-down menu.
72. Under Region 2, double click Region Undefined, and select Water region from the drop-down menu. Event should be OPEN. Click OK.
73. Select Physical Model under Case Setup, a new window will open. Tick the boxes next to Turbulence modeling and Volume of Fluid (VOF) modeling. Click Done.
74. Select Turbulence Modeling under Case Setup, a new window will open. Select Standard k-ε from the drop-down menu next to Turbulence model, then click Set recommended model values button near the bottom of the window. Then under RANS Constants, $C_{\varepsilon 2}$ is set incorrectly due to bugs, change the value of $C_{\varepsilon 2}$ to 1.92, and click OK.
75. Select Volume of Fluid (VOF) modeling under Case Setup, a new window will open. Select 2: PLIC from the drop-down menu next to VOF model, and click OK.
76. Select Grid Control under Case Setup, a new window will open. Tick the boxes next to Adaptive mesh refinement, and Fixed embedding, click Done.
77. Select Base grid under Case Setup, a new window will open. Under Base grid size, you can customize the how each cell is sized in dx, dy, and dz. Beware that base grid is the biggest cell allowed in the simulation without refinement. A base grid size of [2.3, 2.3, 2.3] was used in the research after mesh convergence study.

78. Select Adaptive mesh refinement under Case Setup, a new window will open. Users can set a limit to the number of cells generated by input a value on Maximum cells. In the research, 3e+08 was use for Maximum cells since we did not require a limit on cell counts.
79. Under AMR Groups tab, select Air region and Water region under Available Regions, and click  to activate these regions for the AMR group.
80. Tick the box next to the Void fraction tab. Then under Void fraction tab after selecting it, set the Max. embedding level to 2, and the Sub-grid criterion to 0.01. Click OK.
81. Select Adaptive mesh refinement under Case Setup, a new window will open. Click Add 3 times to create 3 Fix embedding, then use the table below to configure each Embedding. The reason behind Embedding 3 is to create very fine mesh near the free surface so that Converge will be able to generate the free surface accurately at the very beginning.

Table 21. Types of Fixed embedding added to the simulation for step 85.

Name	Entity type	Mode	Scale	Embedding specific
Embedding 1	Region (Region ID = water region)	PERMANENT	1	NA
Embedding 2	Boundary (Boundary ID = water channel interior)	PERMANENT	3	Embed layers = 5
Embedding 3	BOX	SEQUENTIAL Start time =0 End time = 1e-05	4	Center of a box = [30, 25, 0] Half length of each direction = [30, 125, 1]

82. Once all the lists under Case Setup have a green check mark ✅ next to them, now it is possible to export the input files for Converge simulation. Select File from the top left corner, select Export, then select Export Input Files to the desired location for simulation.

Appendix D. Instructions for Performing Simulations on the HPC and Raptor

Once the input files created, the case will be ready to simulate. The Converge CFD simulation can be run on a high performance workstation(Raptor) at the Flow Research Center, or it can also be sent to the HPC. The following provides step by step instructions on how to run simulations on both HPC and Raptor.

I. Running Converge on Raptor

1. Once the input files are generated in a properly named folder (For the purpose of demonstration, we will call the folder Case1A). Click Start Menu, then select Computer, then open Local Disk (C:).
2. Once inside the Local Disk (C:), open Program Files folder, and then open CONVERGE folder.
3. Converge folder contains many different execute files for different processing such as serial and parallel processing. Raptor is capable of parallel processing using maximum of 20 CPU on the workstation, so parallel processing is preferred for the task. Right click converge-2.2.0-mpich2-windows-64-082114.exe, and select Copy.
4. Once the execute file for Converge parallel processing is copied, paste it inside the Case1A folder.
5. Rename converge-2.2.0-mpich2-windows-64-082114.exe to mpich2.exe so that it is easier to type the command in Command Prompt.
6. Now it is ready to start the Converge simulation, it is possible to run Converge with 1 CPU by simply double click mpich2.exe inside the folder, but in order to take advantage of the processing power of Raptor, it is required to use command prompt to run Converge. Click

Start Menu, and in the search window, type in cmd.exe and hit enter. The command prompt window should open with the directory of E:\Users\[your UUID]> on the window.

7. Navigate the directory to the Case1A folder location, there are several commands that you can use to navigate: [cd..] will bring your directory to its parent directory. [cd (folder name)] will bring your folder to a sub folder. [C:] will bring your directory to the C drive.
8. Once you navigated your directory to Case1A folder, type in mpiexec –n 20 mpich2.exe. Number 20 represents the CPU used for the simulation, and it can be changed to a lower CPU count.
9. Once the simulation is complete, refer to Appendix E for post-processing the output files from the simulation.

II. Running Converge on HPC

1. Once the input files are generated in a properly named folder (For the purpose of demonstration, we will call the folder Case1A). In order to run Converge CFD on HPC, the user must request HPC user access from HPC department.
2. Once access has been granted to the user, 2 softwares must be downloaded: MobaXterm is a free software that allows user to connect to HPC server and input user commands; And WINSCP is a free software that allows user to access HPC server to transfer documents.
3. In order to transfer Case1A to the HPC server, open WINSCP.exe  from your desktop, and a Login window will open.
4. Under Session, SCP should be selected on the drop-down menu for File protocol.
5. Input penguin1.memphis.edu as the Host name.
6. Input 22 as the Port number.

7. Input your UUID as the user name, and your UUID login password as the login password.
8. Once the user informations have been filled in, click the Save button, and a new window will open.
9. In the Save session as site window, input HPC under Site name, and tick the box next to Create desktop shortcut and Password. Click OK to close the window.
10. Click the Login button 

near the bottom. The user should now be able access the user folder in HPC. The left window shows the directory in the user's hard drive, and the right window shows the directory in the assigned folder for user, which the directory should be /home/(UUID).
11. Navigate the directory on the left window to locate the Case1A, and select the upload button 

near the top left corner to upload the simulation case inputs to HPC.
12. In order to submit the Case1A simulation job to HPC to run CFD simulation, a submit.sh file must be created inside the Case1A folder. Select Files from the top left corner, and select New, then select File. A new window called Edit file is opened.
13. Input submit.sh as the file name under Enter file name, and click OK.
14. Copy the following commands and paste it in the newly created file, and click save  .

```
#!/bin/sh
#PBS -l nodes=3:thin:ppn=24
#PBS -l walltime=720:00:00
#PBS -A MECH
#PBS -N [Enter job name here]

# source the module command
source /etc/profile.d/modules.sh
# load some modules
module load nwchem
export RLM_LICENSE=53327@itls4

export PATH=$PATH:/public/apps/converge/2.3.5/l_x86_64/bin

cd $PBS_O_WORKDIR

mpirun -np $PBS_NP -machinefile $PBS_NODEFILE converge-2.3.5-openmpi super
```

Inside the script above, thin represents the node being used for computing, while the number of nodes being used can be changed as well (currently 3 nodes in the script). Ppn represents the number of processors being used per node.

15. In order to submit the script file submit.sh to the HPC job queue to start the computing, MobaXterm must be utilized to submit the job. Open MobaXterm  from the desktop.
16. Once MobaXterm is open, click Session button 

from the top left corner, a new window called Session settings will open.
17. Click 

button, then under Basic SSH setting, type in [yourUUID]@penguin1.memphis.edu, and click the OK button. A new session tab named Default Setting will be created.
18. Under the new session tab, the command window will prompt the user for the password, input the UUID password and hit enter, and the uder will be logged into the HPC system.
19. Input cd Case1A on the command window to navigate to the Case1A folder on the HPC.
20. Input qsub submit.sh to submit a job queue to the HPC. The user can check the run duration of the simulation by input qsub –u [your UUID] in the command window.
21. Another way to run simulation is to submit jobs interactively, so that the user can hold on to the computing nodes as long as possible to run jobs sequentially without waiting in queue for every case. In the MobaXterm command window after logging in,
    input: qsub -I -l nodes=3:thin:ppn=24 -l walltime=3000:00:00 -N Converge
    Once the job is ready to be interacted, the following command must be typed into the command window:

```
source /etc/profile.d/modules.sh
module load nwchem
export RLM_LICENSE=53327@itls4
export PATH=$PATH:/public/apps/converge/2.3.5/l_x86_64/bin
```

22. Once the above command is typed into the command window, navigate the directory to Case1A folder. Then input the following command:

    ```
    mpirun -np $PBS_NP -machinefile $PBS_NODEFILE converge-2.3.5-openmpi super
    ```

    The user should now be able to see the Converge CFD simulation running on the command window. If the user wish to stop the simulation, use Ctrl+c to interrupt the job.

23. Once the simulation is completed, refer to Appendix E to post-process the 3D output files from the output folder inside the Case1A folder.

Users can also utilize the command called pbsnodes to view the availability of the HPC nodes, and the command qstat –a can also be used to view all the jobs being queued on the HPC.

Appendix E. Post-processing 3D output files Using EnSight

Governing Equations:

Volumetric Flow Rate

$$Q = \frac{Volume}{Time} = \int \vec{V} \cdot \hat{n}\, dA \qquad \text{(Equation 1)}$$

Mass Flow Rate

$$\dot{m} = \frac{Mass}{Time} = \int \rho \vec{V} \cdot \hat{n}\, dA \qquad \text{(Equation 2)}$$

Momentum Flow Rate

$$\dot{m}\, \vec{V} = \frac{Momentum}{Time} = \int \vec{V} \rho \vec{V} \cdot \hat{n}\, dA \qquad \text{(Equation 3)}$$

Kinetic Energy Flow Rate

$$\frac{KE}{Time} = \frac{Momentum}{Time} \cdot \frac{KE}{Mass} = \dot{m}\, \left(\frac{1}{2} V^2\right) = \int \left(\frac{1}{2} V^2\right) \rho \vec{V} \cdot \hat{n}\, dA \qquad \text{(Equation 4)}$$

Operating Procedures:

In order to use EnSight, one must have the output files from Converge solver, then use post_convert_64.exe to create the necessary EnSight case file named in the post_convert executable.

1. Uncheck the Boundary on the Part window on the left side of your EnSight window in order to see the fluid body.

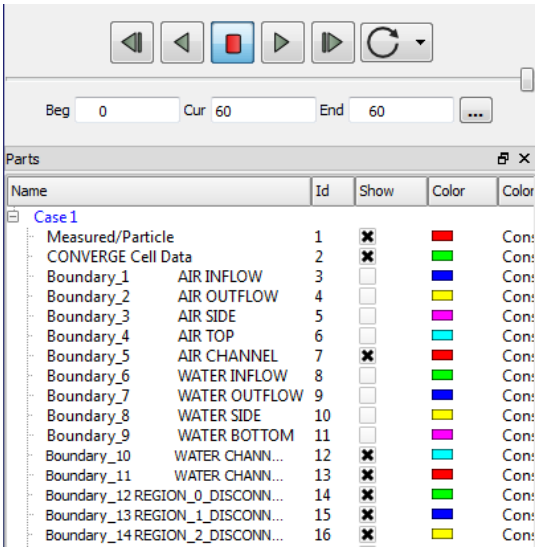

2. Once the Boundaries have been unchecked, create a Isosurface on the fluid surface, click the outer boundary box on your model, then on the top left corner of your screen, click **Create**, then click **Isosurface**. On the Variable dropdown menu, select **(E) alpha**, then under Creation, choose **Isosurface**, and value at **MID-RANGE**, and # of Surface to be **1**, and click **Create with select parts**.

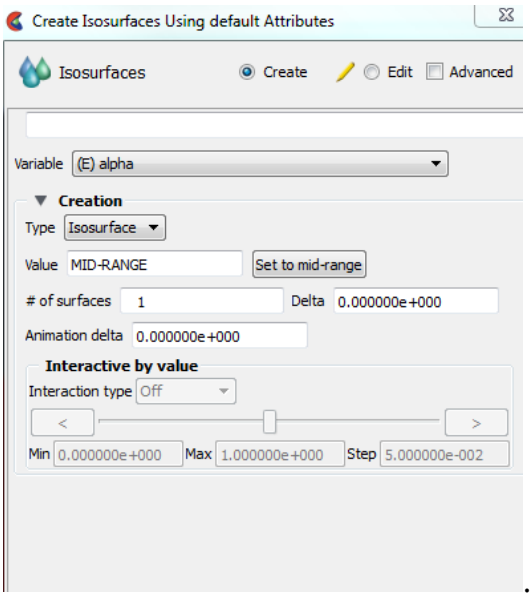

3. Once the Isosurface is created, one will be able to visualize the fluid surface velocity by dragging the velocity variable under the Variable Window (located under the boundary list on the left), to the Isosurface.

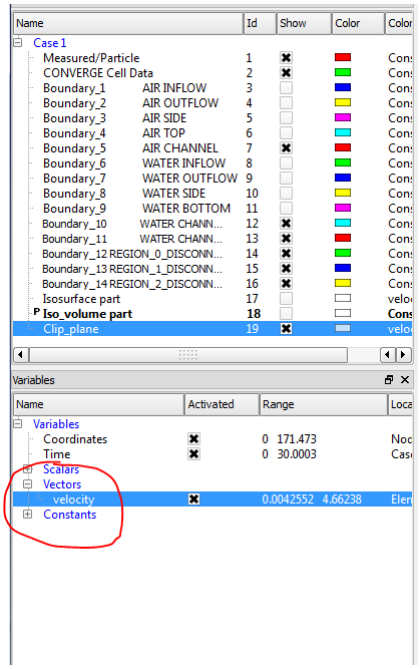

4. One can also create a Clip plane to view the velocity profile on planes normal to the xyz axis by selecting the boundary box, Select Create, Clip, then in the Clip menu, select XYZ on Tool dropdown menu, and choose your desired plane from Mesh slice, and Value(your clip location), and # of slices. Delta is your distance between your clip planes if you are creating multiple ones.

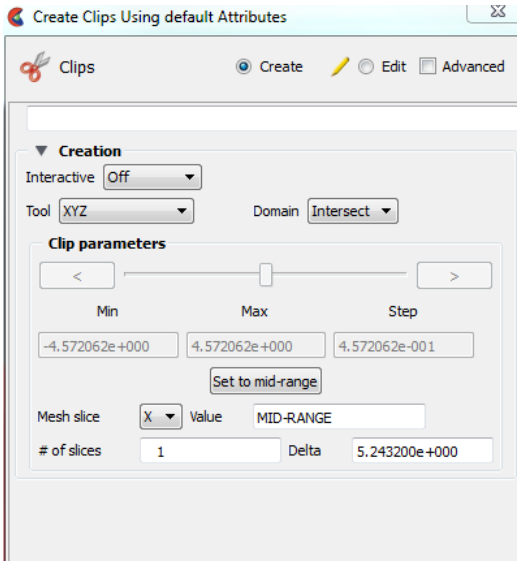

5. In order to create a clip plane that would only include the flow within the channel, one must create a Isovolume in the fluid model, by selecting **Create, Isosurface**, and under **Type** dropdown menu, select **Isovolume,** and change the **Isovolume range min to 0, max to 0.5**, then select **Create with select parts.**

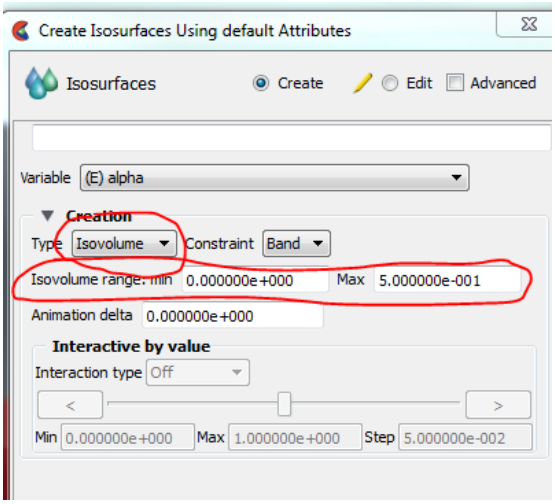

6. With the creation of Isovolume, one should temporarily hide the Isovolume part by unchecking it on the Boundary List on the left. And then select **Tools**, and select **Plane**, then on the screen, move your mouse to the center of the Plane, and right click, and select Edit. Now you can edit the Origin of the Plane, Normal of the Plane. In our Channel case, change the Normal to 0, 1, 0, (so it will be facing the Y direction) and hit enter. Origin stays the same.

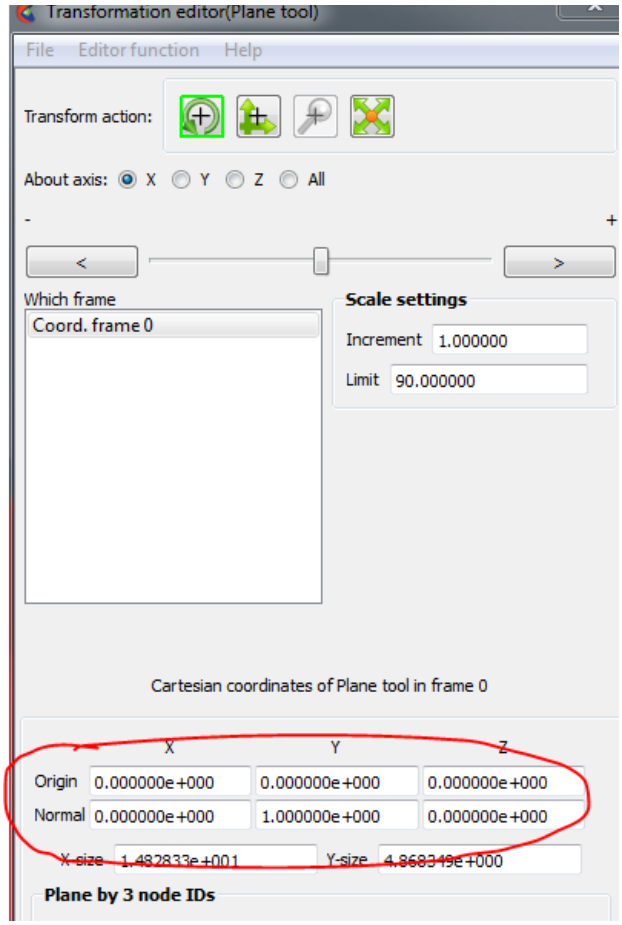

7. Close the Plane tool editor, and we need to resize the plane tool so it will include the portion we want to measure the flow rate by dragging the corner of the plane tool. Once completed, it should look similar to the picture below:

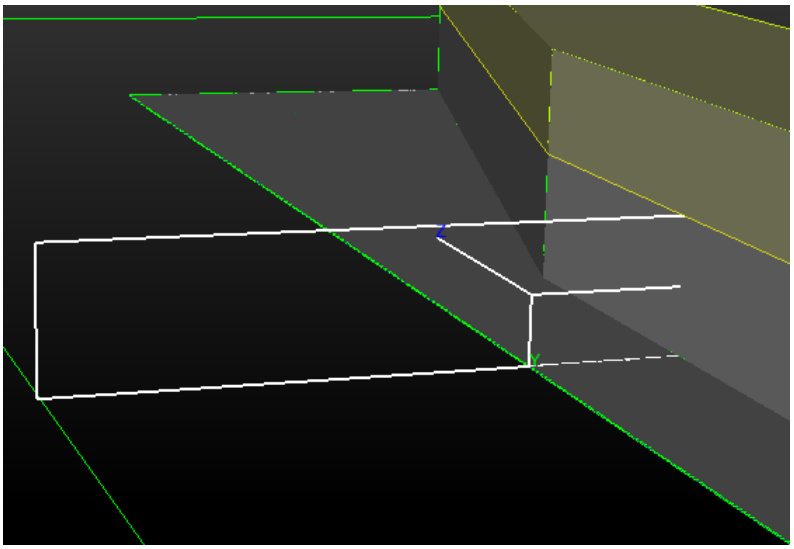

8. Now select the Iso_volume part on your boundary list, select Create, and Clip, from the newly opened window, open the Tool dropdown menu and select Plane, then on the Clip parameter, select Finite, then select Create with selected parts.

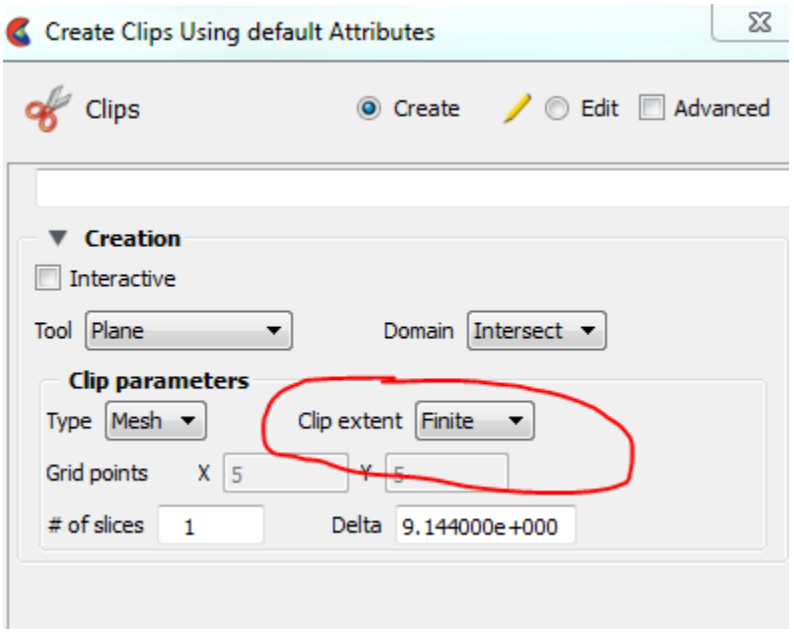

9. Once the clip part is created, you can then drag the velocity variable to the clip part, it should look like the picture below.

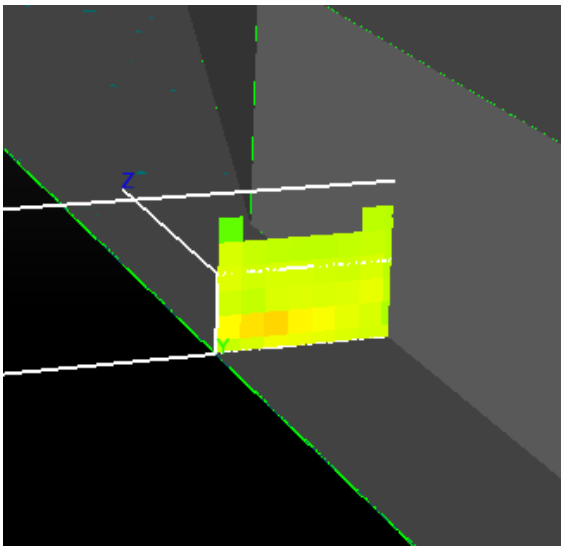

10. Now in order to calculate the flow rates, select the clip_plane on the boundary list, and select Calculator icon from the top left corner.

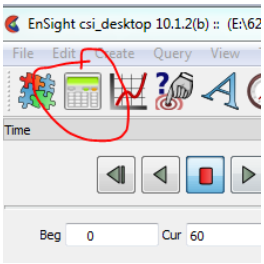

11. On the newly opened window, in the search box type in speed, and select Speed from the function below, and then rename the **Variable name as Myspeed**, then under **Predefined function parameters**, select **velocity** from the dropdown menu, then **select Evaluate for selected parts.**

12. Use Calculator Tool again and select Build your own functions, create a variable named RhoV, and in the Expression box, create the equation **density*velocity** using the variables below expression, then **select Evaluate for selected parts.**

13. Now to create more variables, here's the list of variable needed to be created.

Name	Function Type	Equation	Expression/Parameters
Area	Predefined (area)	$\mathbf{dA}$	NA
KEvariable	Build your own	$\left(\frac{1}{2}V^2\right)\rho\vec{V}$	½ *Myspeed^2*density*velocity
Momentumvar	Build your own	$\vec{V}\rho\vec{V}$	velocity*density*velocity
KEFlowrate	Predefined (Flow)	$\int\left(\frac{1}{2}V^2\right)\rho\vec{V}\cdot\hat{n}\,dA$	Use KEvariable as velocity parameter
Massflowrate	Predefined (Flow)	$\int\rho\vec{V}\cdot\hat{n}\,dA$	Use RhoV as velocity parameter
Volumeflow	Predefined (Flow)	$\int\vec{V}\cdot\hat{n}\,dA$	Use velocity as velocity parameter
Momentumflow	Predefined (Flow)	$\int\vec{V}\rho\vec{V}\cdot\hat{n}\,dA$	Use Momentumvar as velocity parameter
MeanVeloMag	Predefined (SpaMean)	**NA**	Use velocity as variable
MeanVeloY	Predefined (SpaMean)	**NA**	Use velocity as variable, then choose [Y] as component.

14. Now you should see each flow rate in the variable window on the left.

Appendix F. Detailed Simulation data from Case Study 1 and Case Study 2.

This appendix includes the raw data generated by EnSight post-processing software. Each of the flow-rates from the table is calculated from the evaluation plane inside the straight channel of the machine. The column of data named AreaPlane represents the cross-sectional area of the evaluation plane.

Table 22. Detailed simulation data from [AR= 0.30 / θ= 15 deg] model.

Time (s)	AreaPlane (m^2)	MeanVeloMag (m/s)	MassFlow (kg/s)	KEFlow (J/s)	MomentumFlow ($kg*m/s^2$)
0.00	6.69	2.00	13332.57	26665.14	26665.14
5.01	6.85	3.40	22369.94	129636.88	74305.62
10.01	5.32	3.51	17571.31	108779.26	59888.52
15.04	4.86	3.30	15010.91	82263.98	47946.86
20.02	5.23	3.72	18792.42	130540.62	67876.30
25.01	7.98	2.16	15627.25	41921.86	33347.38
30.05	6.44	2.60	14969.58	50869.71	36706.36
35.03	4.82	3.23	14793.92	77407.27	46189.66
40.01	4.94	3.32	15398.75	85069.13	49424.18
45.03	6.90	2.56	15786.44	53703.70	38661.48
50.01	5.98	2.84	15822.38	64758.66	43442.19
55.02	6.27	2.89	16111.00	68735.60	44674.09
60.04	5.31	3.09	15197.80	73058.63	45204.13
65.03	5.11	3.24	15450.14	81280.14	48358.32
70.00	5.36	3.28	16643.97	90612.31	52991.39
75.01	5.48	3.16	16084.62	81930.98	49284.63
80.00	5.27	3.25	16265.43	87711.02	51884.40
85.02	5.28	3.33	16597.74	92633.17	53564.85
90.01	5.11	3.53	17171.42	107066.20	58564.60
95.00	5.15	3.54	17214.63	108005.81	58987.63
100.02	5.19	3.44	17008.16	101460.15	56917.28
105.03	5.15	3.43	16936.39	100087.98	56409.27
110.01	5.27	3.42	17087.61	100951.56	56798.00
115.02	5.23	3.55	17843.94	112931.71	61381.48
120.01	5.07	3.64	17488.92	115967.48	61641.72
125.02	5.19	3.55	17537.36	111129.58	60391.16
130.03	5.19	3.57	17614.41	112119.63	60741.34
135.03	5.11	3.46	16894.65	101538.81	56532.52
140.03	5.23	3.54	17838.60	112314.23	61381.25
145.01	5.23	3.55	17696.31	111972.27	60868.06
150.02	5.28	3.50	17549.71	107975.16	59461.85
155.03	5.36	3.49	17760.97	109026.59	60241.06
160.02	5.32	3.52	17661.67	110373.90	60330.98
165.03	5.23	3.53	17708.29	110579.57	60617.10
170.02	5.11	3.59	17544.99	113676.40	61069.67
175.01	5.19	3.56	17501.79	111688.41	60428.80
180.02	5.23	3.55	17867.78	113062.45	61560.17

Table 23. Detailed simulation data from [AR= 0.40 / θ= 15 deg] model.

Time (s)	AreaPlane (m^2)	MeanVeloMag (m/s)	MassFlow (kg/s)	KEFlow (J/s)	MomentumFlow ($kg*m/s^2$)
0.00	8.83	2.00	17588.76	35177.52	35177.52
5.01	9.30	3.12	27637.30	134335.38	83991.83
10.04	6.58	3.41	21341.18	123998.02	70293.62
15.02	6.74	3.60	22635.36	146664.34	78815.23
20.04	6.85	3.72	24222.90	167926.86	87106.95
25.03	9.71	2.40	21326.49	64474.29	48805.25
30.04	7.27	3.26	22533.26	120056.59	71002.89
35.01	6.80	3.43	22456.22	131909.41	74818.78
40.01	6.77	3.36	21386.19	120873.02	69547.20
45.02	7.19	3.25	22190.05	119723.96	70323.26
50.04	8.35	2.85	21595.65	88934.89	59189.68
55.02	7.19	3.23	21990.40	114868.83	68610.09
60.02	6.83	3.38	21948.63	126215.88	71928.77
65.02	6.88	3.38	22061.06	125988.45	71941.45
70.00	7.10	3.25	22125.98	118085.59	69837.58
75.02	7.88	3.11	22208.80	109832.52	67168.37
80.02	7.02	3.36	22125.10	125811.85	72134.74
85.01	6.88	3.55	23408.87	147574.58	80474.49
90.01	6.77	3.62	23291.18	153051.19	81782.90
95.02	6.91	3.65	24022.55	160268.38	85163.86
100.04	6.94	3.48	23045.08	140766.77	77755.42
105.01	7.08	3.41	22836.18	135433.86	76006.77
110.02	7.02	3.47	23203.31	141011.14	78280.81
115.02	6.80	3.59	23382.13	151470.91	81461.98
120.00	6.94	3.59	23618.68	152342.06	82361.47
125.00	6.99	3.63	24353.47	160771.22	85579.14
130.03	6.80	3.54	23031.26	144738.30	78830.68
135.01	7.10	3.48	23660.77	144558.19	80111.15
140.01	6.94	3.58	23838.37	153764.25	82755.27
145.00	6.77	3.67	23567.06	159475.17	84041.70
150.03	6.91	3.61	23806.42	156092.41	83499.56
155.03	6.94	3.54	23392.39	147828.94	80315.65
160.00	6.80	3.59	23339.21	150752.66	81014.66
165.01	6.94	3.57	23688.51	151808.98	82059.79
170.03	7.02	3.48	23447.19	143088.11	79148.69
175.02	6.96	3.51	23155.67	143791.30	78707.29
180.01	6.94	3.59	23761.50	154010.34	82511.77

Table 24. Detailed simulation data from [AR= 0.50 / θ= 15 deg] model.

Time (s)	AreaPlane (m^2)	MeanVeloMag (m/s)	MassFlow (kg/s)	KEFlow (J/s)	MomentumFlow ($kg*m/s^2$)
0.00	11.03	2.00	21987.77	43975.53	43975.53
5.01	10.94	2.89	30547.50	127626.27	86292.05
10.02	8.39	3.29	26587.82	144140.06	84850.41
15.01	8.55	3.43	28241.36	166547.09	94377.73
20.04	11.27	2.91	30155.14	131540.36	85706.20
25.03	11.03	2.80	29576.22	116585.40	80400.09
30.01	9.30	3.21	28215.47	145974.38	88214.18
35.01	8.34	3.45	28077.74	167856.17	95154.08
40.01	8.56	3.47	28713.13	173605.72	97443.34
45.00	10.87	2.99	29199.24	134339.95	85292.61
50.01	10.23	2.98	27250.65	122552.09	79449.70
55.01	8.79	3.38	28562.73	164248.06	94488.20
60.02	8.57	3.30	27207.99	148507.13	87352.95
65.02	8.64	3.23	26723.04	139865.52	83800.42
70.04	9.28	3.12	27154.04	134763.34	83107.89
75.03	9.19	3.21	27816.71	145180.64	87300.66
80.04	8.71	3.24	26949.91	142432.22	85174.95
85.01	8.54	3.41	27867.63	162873.59	93037.94
90.02	8.63	3.38	27817.28	161003.38	91758.84
95.02	9.05	3.13	27006.69	135619.03	82776.64
100.01	8.71	3.22	27061.88	141610.30	85624.33
105.01	8.48	3.42	27662.81	162331.89	92342.50
110.01	8.48	3.30	26889.71	147561.81	86565.63
115.01	8.73	3.35	28074.83	159218.53	91926.72
120.02	8.80	3.24	27134.40	144810.95	85919.05
125.03	8.95	3.13	26909.60	134562.84	82359.96
130.02	8.55	3.34	27589.45	155388.28	90450.13
135.00	8.48	3.36	27639.00	156598.11	90715.05
140.01	9.04	3.27	28104.26	153629.05	90325.04
145.02	8.63	3.34	27723.98	155932.22	90477.90
150.02	8.73	3.27	27358.24	148738.59	87528.69
155.02	8.42	3.22	26114.40	136791.22	82129.81
160.02	8.34	3.44	27515.70	164278.77	92784.80
165.01	8.56	3.33	27559.78	154418.88	89779.22
170.00	8.64	3.21	26741.90	140005.39	84249.86
175.01	8.56	3.35	27591.38	155902.58	90394.03
180.04	8.56	3.38	27789.70	159644.80	91924.13

Table 25. Detailed simulation data from [AR= 0.60 / θ= 15 deg] model.

Time (s)	AreaPlane (m^2)	MeanVeloMag (m/s)	MassFlow (kg/s)	KEFlow (J/s)	MomentumFlow ($kg*m/s^2$)
0.00	13.24	2.00	26386.77	52773.54	52773.54
5.02	12.82	2.69	33171.58	120500.63	87037.02
10.02	10.16	3.05	29804.37	139255.58	88177.66
15.02	13.07	2.80	33352.53	133581.59	90857.80
20.04	13.07	2.91	35171.37	150858.20	99770.11
25.04	13.07	2.72	32821.20	122584.73	86197.07
30.01	10.74	3.20	32632.45	167646.17	101669.97
35.03	10.24	3.09	30422.41	146239.05	91661.80
40.02	12.15	2.96	33414.02	147893.92	97051.92
45.03	12.74	2.99	33952.55	153351.38	99665.75
50.02	10.32	2.97	29444.14	131637.58	85636.97
55.03	10.16	3.12	30634.21	151198.59	93960.10
60.02	11.49	2.93	31086.20	136341.48	89431.66
65.00	12.24	2.92	32163.51	140362.80	92331.95
70.01	10.24	3.11	30765.10	149173.42	93280.70
75.01	12.07	3.01	32854.75	152079.20	97005.89
80.02	10.57	3.03	30643.07	142131.66	90970.23
85.01	10.16	3.14	30731.88	152676.94	94271.99
90.04	10.49	2.95	29667.42	130939.28	85269.41
95.00	10.07	3.08	29684.65	141642.22	88917.79
100.02	10.33	3.05	30078.31	141622.05	89492.15
105.01	11.49	2.91	30736.65	133819.97	88023.54
110.03	11.58	2.91	31066.02	134391.41	88446.72
115.03	10.41	3.03	30188.63	141127.73	89708.47
120.00	10.99	2.93	30455.58	133204.72	87462.81
125.03	10.49	3.03	30462.41	141055.22	90122.99
130.02	12.07	2.92	31715.28	139725.80	91237.56
135.01	11.99	2.95	32210.26	144373.27	93580.82
140.02	11.07	2.99	31160.39	142291.72	91231.98
145.00	10.41	3.05	30533.22	143621.75	91094.00
150.03	12.24	2.90	31692.64	137122.22	90583.34
155.00	10.33	3.04	30174.18	140881.39	89673.24
160.01	11.83	2.95	31854.14	143163.86	92882.98
165.01	10.41	3.01	30143.70	138653.30	89152.15
170.00	10.57	2.97	29997.85	134229.31	87274.93
175.02	11.49	2.98	31750.04	143912.59	92962.88
180.01	10.49	3.01	30188.30	138150.88	88919.34

Table 26. Detailed simulation data from [AR= 0.70 / θ= 15 deg] model.

Time (s)	AreaPlane (m^2)	MeanVeloMag (m/s)	MassFlow (kg/s)	KEFlow (J/s)	MomentumFlow ($kg*m/s^2$)
0.00	15.44	2.00	30781.85	61563.70	61563.70
5.03	15.16	2.53	36355.83	116888.02	89273.77
10.03	14.85	2.62	34696.33	120813.16	88088.48
15.00	15.54	2.63	37960.80	133351.73	97201.34
20.01	15.44	2.59	37182.71	124801.66	92846.60
25.01	14.93	2.75	37562.03	142901.31	99975.14
30.02	15.10	2.74	37237.66	140736.56	98895.91
35.02	14.91	2.77	37710.05	145930.59	101350.00
40.03	15.46	2.72	37978.14	141889.22	100285.23
45.03	15.16	2.72	37778.70	140311.45	100786.05
50.00	15.18	2.71	37602.37	139254.45	100322.09
55.00	14.68	2.55	35243.66	115269.41	88478.70
60.03	14.51	2.47	33073.61	101865.01	79607.09
65.03	14.60	2.53	34109.95	110593.43	83678.89
70.01	15.43	2.52	34531.13	112040.80	84510.02
75.04	14.66	2.59	34212.10	116747.05	85943.15
80.02	15.01	2.61	34801.17	119814.41	87495.71
85.01	15.28	2.73	37232.91	141311.91	98624.27
90.01	15.00	2.66	35509.69	127618.49	91600.84
95.03	14.11	2.78	35080.50	137418.53	94584.23
100.01	14.66	2.68	35172.46	128004.25	91754.54
105.02	14.65	2.73	35549.48	135446.86	94669.40
110.03	15.20	2.67	36009.46	131738.05	93806.35
115.02	14.25	2.74	34663.00	133390.89	92855.69
120.03	14.95	2.70	36241.34	134816.08	95059.35
125.03	14.50	2.79	36386.01	144881.94	99521.53
130.01	14.66	2.76	35840.71	139961.33	96347.98
135.02	14.79	2.81	36796.11	147963.61	100888.37
140.02	14.53	2.73	35500.18	135902.83	94733.38
145.01	14.95	2.75	36756.63	142044.30	98909.66
150.02	14.90	2.78	36640.65	143681.59	98948.58
155.03	14.76	2.75	35913.70	138197.94	96276.52
160.04	14.82	2.78	36462.46	143742.72	98558.26
165.00	15.03	2.80	37510.46	148819.75	102148.09
170.00	14.53	2.76	35672.16	138149.53	96253.13
175.01	14.57	2.75	35778.86	138439.19	96375.09
180.02	15.03	2.72	36425.28	137186.80	96273.48

Table 27. Detailed simulation data from [AR= 0.80 / θ= 15 deg] model.

Time (s)	AreaPlane (m^2)	MeanVeloMag (m/s)	MassFlow (kg/s)	KEFlow (J/s)	MomentumFlow ($kg*m/s^2$)
0.00	17.65	2.00	35180.86	70361.71	70361.71
5.02	17.59	2.38	38894.69	110749.30	89127.64
10.02	17.54	2.35	38815.62	108705.04	87945.73
15.03	17.57	2.50	41282.68	130469.10	100166.70
20.04	17.65	2.41	39872.52	116314.10	92779.59
25.01	17.43	2.49	40131.28	125239.02	96119.93
30.01	17.65	2.54	41386.08	134079.88	101392.68
35.05	17.49	2.52	40710.68	130206.42	99677.08
40.04	17.37	2.49	40031.91	125244.15	97044.53
45.01	17.43	2.45	38446.93	116752.63	91195.91
50.01	17.43	2.43	38483.78	115167.50	90186.62
55.01	17.38	2.47	38988.34	120400.56	93221.23
60.00	17.43	2.33	37641.12	102960.16	85619.97
65.03	17.59	2.41	37742.57	110649.30	86832.20
70.04	17.80	2.36	37800.86	107819.12	86555.25
75.00	17.37	2.45	39005.36	119576.42	92274.69
80.04	17.60	2.47	38672.50	119761.77	92350.95
85.03	17.51	2.42	38384.07	113929.73	89535.01
90.00	17.57	2.47	38911.88	120360.94	93196.66
95.01	17.49	2.49	38683.82	121644.59	93694.55
100.04	17.21	2.45	38118.68	115886.68	90393.88
105.03	17.32	2.48	38645.19	120558.41	92996.81
110.03	17.34	2.43	38055.34	114199.91	89444.96
115.02	17.28	2.48	39152.92	121608.80	94914.32
120.03	17.43	2.46	38460.56	116904.68	89876.77
125.01	17.18	2.49	38197.52	120032.80	91984.11
130.04	17.45	2.45	38659.23	117974.29	91812.35
135.02	17.56	2.45	39381.16	119851.40	93164.15
140.02	17.62	2.47	38917.18	120080.93	93121.43
145.02	17.18	2.44	38022.88	114846.27	89722.82
150.02	17.52	2.46	39161.51	119891.45	93064.26
155.01	17.65	2.49	39892.52	125574.19	96074.53
160.02	17.29	2.48	38883.34	121428.51	94118.25
165.02	17.26	2.48	39002.61	122283.81	94244.00
170.00	17.48	2.42	38978.25	115376.73	92442.66
175.00	17.34	2.46	38604.85	117395.05	91145.30
180.01	17.57	2.49	39511.93	123398.23	95146.18

Table 28. Detailed simulation data from [AR= 0.90 / θ= 15 deg] model.

Time (s)	AreaPlane (m^2)	MeanVeloMag (m/s)	MassFlow (kg/s)	KEFlow (J/s)	MomentumFlow ($kg*m/s^2$)
0.00	19.86	2.00	39575.93	79151.87	79151.87
5.02	19.86	2.28	41386.71	110529.36	88022.92
10.02	19.86	2.25	42105.54	107591.50	90503.50
15.01	19.90	2.25	42294.61	107707.95	91503.85
20.03	19.81	2.27	42505.84	110625.48	92519.65
25.02	19.73	2.33	42985.61	117747.01	95984.38
30.02	19.81	2.31	42676.75	114055.37	94635.09
35.04	19.86	2.33	42648.98	116551.58	95340.59
40.01	19.86	2.27	41386.52	108157.17	89857.64
45.02	20.03	2.25	40620.44	104614.89	87284.98
50.03	19.70	2.21	39691.49	98246.51	83725.23
55.00	19.60	2.17	39544.61	95522.11	82944.52
60.01	19.28	2.15	38085.20	90969.35	78895.76
65.03	19.48	2.15	38493.74	91797.67	78959.73
70.03	19.98	2.15	39662.62	93254.00	81594.26
75.00	19.57	2.21	39389.09	97294.52	83221.38
80.02	19.82	2.23	40278.16	101239.45	86014.81
85.02	19.90	2.15	39719.10	93349.34	82320.91
90.02	19.52	2.24	39352.45	100372.15	83955.67
95.03	19.90	2.22	40401.38	100722.00	85224.23
100.00	19.82	2.26	40535.80	104531.41	87870.05
105.00	19.69	2.19	39420.94	95984.85	82463.60
110.03	19.73	2.22	39719.06	99223.80	84245.33
115.03	19.90	2.20	39728.04	97213.27	83290.34
120.01	19.73	2.22	39884.07	100064.57	84620.06
125.00	19.69	2.22	39927.68	99505.88	84866.88
130.00	19.65	2.22	39784.32	98951.77	84232.95
135.00	19.81	2.20	39680.73	97362.45	83277.48
140.02	19.69	2.24	40209.57	102351.27	85954.61
145.02	19.90	2.23	40615.04	101945.01	86272.43
150.01	19.69	2.24	40439.42	102666.23	86799.41
155.02	19.90	2.21	40268.76	99984.52	85086.51
160.02	19.69	2.24	40566.77	103067.84	86940.95
165.02	19.69	2.28	40948.04	107677.76	89383.77
170.02	19.77	2.22	40389.88	100484.53	85619.85
175.03	19.65	2.25	40611.43	103849.67	87600.17
180.03	19.86	2.21	40619.50	100792.26	86113.45

Table 29. Detailed simulation data from [AR= 0.30 / θ= 30 deg] model.

Time (s)	AreaPlane (m^2)	MeanVeloMag (m/s)	MassFlow (kg/s)	KEFlow (J/s)	MomentumFlow ($kg*m/s^2$)
0.00	6.62	2.00	13195.08	26390.16	26390.16
5.01	6.67	2.92	18413.90	79471.20	52484.29
10.00	4.95	3.37	15620.02	88680.90	50854.20
15.02	5.16	3.90	19375.33	147833.53	73680.53
20.03	6.58	2.65	15997.07	63418.22	42543.25
25.01	6.45	2.72	16505.88	61568.93	43330.60
30.05	5.21	2.94	14662.65	63747.51	41953.63
35.03	5.20	3.35	16679.17	94228.06	54495.95
40.00	5.50	3.11	16432.70	82165.53	50564.66
45.03	6.37	2.85	16254.86	67888.55	45235.60
50.01	5.58	3.06	15915.52	74905.44	46874.74
55.04	5.20	3.12	15449.97	75914.09	46744.12
60.01	5.25	3.32	16585.56	92301.75	53608.61
65.04	5.54	3.03	15865.26	75310.69	46873.06
70.01	5.50	3.01	15651.29	72116.30	45660.97
75.02	5.37	3.21	16163.74	84540.91	50522.74
80.01	5.21	3.20	15988.03	82843.74	49863.70
85.04	5.33	3.28	16628.29	90936.97	53247.11
90.04	5.21	3.26	16397.21	88336.57	52238.64
95.01	5.41	3.22	16519.85	87475.73	51726.45
100.03	5.21	3.32	16580.34	92235.16	53257.45
105.03	5.46	3.26	16706.38	90880.66	53193.05
110.00	5.08	3.37	16457.97	94000.84	53741.23
115.03	5.33	3.40	17221.46	102057.28	57246.21
120.02	5.29	3.34	16999.49	96730.27	55690.41
125.01	5.33	3.28	16724.32	92120.74	53578.63
130.01	5.29	3.30	16673.02	92718.16	53637.30
135.01	5.33	3.32	16923.57	95512.48	54706.91
140.02	5.16	3.33	16430.02	92540.58	53057.17
145.00	5.25	3.35	16833.60	96417.90	54942.88
150.02	5.33	3.32	16802.81	95581.15	54563.32
155.00	5.33	3.32	16906.67	95221.72	54560.63
160.01	5.25	3.32	16722.61	94842.13	54492.21
165.02	5.33	3.27	16673.76	91739.39	53472.64
170.00	5.33	3.29	16693.67	92116.86	53542.76
175.01	5.50	3.23	16682.96	89088.98	52449.28
180.01	5.33	3.26	16599.00	89979.08	53068.39

Table 30. Detailed simulation data from [AR= 0.40 / θ= 30 deg] model.

Time (s)	AreaPlane (m^2)	MeanVeloMag (m/s)	MassFlow (kg/s)	KEFlow (J/s)	MomentumFlow ($kg*m/s^2$)
0.00	8.82	2.00	17587.36	35174.73	35174.73
5.02	8.46	2.73	21603.66	80901.42	56881.80
10.03	6.66	3.49	22309.29	135841.20	75632.82
15.00	6.85	3.76	24883.88	176513.33	91473.35
20.01	8.99	2.71	22270.90	87442.26	59226.13
25.00	8.49	2.86	23173.59	95713.93	64619.92
30.02	6.80	3.27	21510.30	115417.84	68712.45
35.01	6.96	3.24	21694.41	115429.84	68800.82
40.02	7.08	3.29	22518.58	124082.29	72639.79
45.01	7.41	3.16	22249.50	113748.13	68636.41
50.02	8.44	3.06	23245.38	110846.44	69124.50
55.03	7.08	3.18	21517.59	109538.94	66351.61
60.04	6.80	3.27	21319.75	114821.22	67952.95
65.04	7.10	3.24	22007.88	116853.13	69557.17
70.01	7.69	3.03	21723.07	101903.66	64203.27
75.03	7.96	3.08	22175.67	107143.17	66355.98
80.01	6.94	3.26	21553.02	115352.91	68415.07
85.01	6.94	3.48	23264.33	142087.16	79121.73
90.02	7.10	3.22	21944.49	116431.59	69227.26
95.02	7.27	3.19	21859.98	113767.35	67864.92
100.01	7.10	3.37	22903.25	131780.81	75471.99
105.05	6.85	3.39	22358.61	129344.76	73547.11
110.03	7.10	3.29	22285.28	123553.13	71781.94
115.04	7.35	3.27	22525.22	122917.39	71525.94
120.03	6.99	3.32	22359.76	125330.45	72602.61
125.02	7.19	3.28	22349.14	122602.63	71620.52
130.01	7.27	3.29	22688.40	125364.60	73102.80
135.02	7.27	3.27	22440.93	122839.36	71880.62
140.00	7.19	3.25	22111.67	119028.17	70116.59
145.02	7.02	3.28	22168.06	121436.76	71199.37
150.03	7.27	3.23	22325.26	118380.91	70219.38
155.00	7.35	3.14	21768.19	108722.46	66368.06
160.01	7.05	3.33	22329.49	125030.65	72401.26
165.02	6.94	3.35	22342.54	126594.10	73048.98
170.02	7.19	3.33	22754.86	129151.05	74232.70
175.00	7.19	3.23	22144.79	118247.22	69943.77
180.00	7.13	3.25	22003.73	118029.57	69720.86

Table 31. Detailed simulation data from [AR= 0.50 / θ= 30 deg] model.

Time (s)	AreaPlane (m^2)	MeanVeloMag (m/s)	MassFlow (kg/s)	KEFlow (J/s)	MomentumFlow ($kg*m/s^2$)
0.00	11.03	2.00	21988.11	43976.23	43976.23
5.02	10.63	2.62	26179.71	90491.67	66674.70
10.00	8.55	3.47	28651.72	172911.98	96958.03
15.03	10.70	3.11	29789.36	149447.02	91232.14
20.02	11.03	2.68	28437.77	103733.54	74298.27
25.04	10.88	3.07	29849.87	141866.95	89486.37
30.02	8.79	3.18	26712.40	136164.80	83224.19
35.02	8.79	3.28	27759.83	151471.06	89286.88
40.04	10.03	3.07	28388.60	136693.61	84900.73
45.01	10.45	3.05	28823.79	136653.83	86195.76
50.03	9.04	3.26	27955.86	151070.05	89179.52
55.02	8.77	3.21	27153.80	142759.36	85436.48
60.02	8.79	3.10	26241.12	128683.16	80204.27
65.04	9.64	3.10	27571.88	134737.30	83326.39
70.00	9.88	3.01	27253.88	125585.97	80647.16
75.03	8.96	3.12	26622.46	130981.42	80958.23
80.02	8.81	3.17	26472.23	135276.28	81544.24
85.03	8.80	3.21	26965.17	140565.70	84420.48
90.00	8.89	3.14	26446.27	132611.23	80698.91
95.00	8.87	3.13	26433.33	131749.45	80689.16
100.02	8.63	3.21	26540.93	138391.11	83097.59
105.01	8.88	3.17	26800.95	136516.22	82532.88
110.03	8.73	3.13	26113.13	129822.40	79838.37
115.04	8.64	3.19	26426.33	135594.33	82036.55
120.05	8.80	3.23	27173.25	143648.08	85649.63
125.02	8.80	3.14	26520.23	133031.14	81373.92
130.03	8.88	3.14	26440.60	132600.77	80923.34
135.02	8.80	3.17	26411.48	134225.41	81612.14
140.01	8.64	3.18	26175.18	133178.38	80919.52
145.01	8.63	3.25	26969.22	143702.30	85854.95
150.02	8.80	3.13	26399.32	131135.05	80680.62
155.01	9.73	3.04	27251.68	128271.38	81353.91
160.02	9.11	3.15	27117.72	136448.11	83250.55
165.01	8.80	3.17	26820.65	137749.55	83447.98
170.02	8.80	3.11	26272.35	128104.61	80078.53
175.00	8.72	3.18	26562.94	135266.58	82344.77
180.01	8.88	3.08	26318.96	126598.66	79654.61

Table 32. Detailed simulation data from [AR= 0.60 / θ= 30 deg] model.

Time (s)	AreaPlane (m^2)	MeanVeloMag (m/s)	MassFlow (kg/s)	KEFlow (J/s)	MomentumFlow ($kg*m/s^2$)
0.00	13.24	2.00	26388.86	52777.73	52777.73
5.02	12.49	2.53	29569.39	95757.84	72611.16
10.05	10.41	3.10	31052.71	150426.19	94066.33
15.00	13.24	2.68	33686.71	123584.50	88037.52
20.04	12.99	2.82	33718.19	135961.53	92983.87
25.02	12.82	2.84	33035.57	135160.19	91673.15
30.03	11.82	3.05	33498.63	158002.25	100229.49
35.04	12.16	2.97	33296.42	148189.63	96129.48
40.04	12.16	2.99	33213.07	150708.77	97316.84
45.03	11.24	2.99	31832.39	144247.92	93311.09
50.00	11.49	2.95	31549.89	140577.06	91566.88
55.02	12.07	2.90	31813.87	137538.14	90462.69
60.04	11.16	2.93	30329.11	133668.63	86959.34
65.02	12.32	2.83	31528.11	129194.33	87159.02
70.02	11.99	2.83	31155.21	127445.48	86151.05
75.00	10.83	2.94	29864.82	132133.73	85950.52
80.01	11.99	2.90	31424.49	136338.11	89243.64
85.01	10.66	3.02	30555.96	142051.83	90703.08
90.03	12.41	2.91	32158.19	139926.16	91534.82
95.02	10.24	3.02	29711.24	136524.02	87321.78
100.04	11.00	2.95	30374.07	135790.27	87846.89
105.02	11.24	2.94	30527.05	135042.11	88456.68
110.03	10.49	2.98	29831.11	134632.33	86816.39
115.00	12.24	2.93	32542.76	143353.59	94082.30
120.03	11.24	2.99	30828.41	140771.44	90480.65
125.01	12.32	2.89	31805.81	137429.39	90489.92
130.03	10.24	3.04	29824.38	140074.34	88868.87
135.03	12.24	2.92	31948.15	141015.11	92092.17
140.03	12.41	2.86	31953.72	134549.61	89725.76
145.01	11.24	2.99	30586.85	140762.56	89921.63
150.03	11.07	2.99	30989.01	140894.66	90793.56
155.02	11.57	3.03	31971.23	150313.69	95243.96
160.01	12.65	2.95	33482.21	149432.33	96606.51
165.02	10.66	3.06	31268.39	148947.77	93453.16
170.00	10.07	3.08	30019.75	144761.31	91129.05
175.02	12.66	2.96	33485.43	151689.97	97515.26
180.03	12.91	3.04	34777.79	165598.27	103505.05

Table 33. Detailed simulation data from [AR= 0.70 / θ= 30 deg] model.

Time (s)	AreaPlane (m^2)	MeanVeloMag (m/s)	MassFlow (kg/s)	KEFlow (J/s)	MomentumFlow ($kg*m/s^2$)
0.00	15.44	2.00	30781.15	61562.30	61562.30
5.01	15.01	2.47	33906.20	104707.98	80113.49
10.01	15.10	2.61	36094.82	125182.32	91113.44
15.01	15.44	2.62	38000.43	132432.27	97068.80
20.05	15.36	2.55	35971.90	118024.48	88639.13
25.03	14.95	2.78	37993.67	148911.41	102862.73
30.01	15.18	2.62	36454.58	126220.37	92400.74
35.03	14.68	2.84	38165.54	155842.97	105352.89
40.02	14.45	2.70	36115.24	132680.58	94248.98
45.02	14.53	2.73	36271.71	136118.83	96278.96
50.05	14.79	2.62	35068.95	122591.68	89609.29
55.03	14.18	2.74	35553.63	135565.83	95099.10
60.01	15.01	2.60	35349.17	122333.05	89497.12
65.02	14.61	2.64	35300.44	125638.95	91002.96
70.02	14.93	2.63	35008.17	123056.84	88593.90
75.03	14.90	2.64	35074.68	123790.72	89474.91
80.01	15.01	2.66	35682.71	128440.84	91942.02
85.03	14.90	2.61	34844.31	120387.80	88028.70
90.00	14.85	2.68	35244.79	128527.78	91584.94
95.01	15.18	2.67	35956.46	131082.28	93501.51
100.00	15.25	2.69	36757.67	135420.80	96113.70
105.04	14.73	2.75	35831.46	137167.42	95403.35
110.04	14.73	2.74	35899.94	136752.17	95570.59
115.01	15.19	2.72	36711.59	137746.03	97113.08
120.02	14.85	2.76	36444.56	141642.27	98322.52
125.01	14.58	2.77	36007.91	140826.64	97295.00
130.03	15.36	2.74	37564.32	143673.28	100166.95
135.02	14.85	2.73	36146.90	137667.31	96192.78
140.01	14.75	2.77	36377.97	142040.11	98503.25
145.03	14.85	2.74	36190.07	138327.28	96770.14
150.01	15.26	2.74	37198.18	141748.06	98572.22
155.01	15.19	2.70	36383.83	134868.97	95614.05
160.01	15.29	2.72	37048.12	140352.41	98382.42
165.04	15.11	2.68	36198.85	132592.72	94502.91
170.01	15.36	2.68	36810.73	135144.95	96224.48
175.01	14.95	2.63	35455.44	125601.43	90543.84
180.01	15.28	2.68	36511.55	133292.03	95019.79

Table 34. Detailed simulation data from [AR= 0.80 / θ= 30 deg] model.

Time (s)	AreaPlane (m^2)	MeanVeloMag (m/s)	MassFlow (kg/s)	KEFlow (J/s)	MomentumFlow ($kg*m/s^2$)
0.00	17.65	2.00	35181.90	70363.80	70363.80
5.00	17.57	2.43	38056.68	114992.39	86646.19
10.00	17.54	2.35	38614.72	108140.89	86701.88
15.00	17.49	2.53	41004.91	132226.83	100352.36
20.00	17.46	2.42	40236.49	119165.52	94825.09
25.03	17.65	2.48	40835.56	126893.96	97919.10
30.00	17.65	2.53	41100.16	133746.22	101027.95
35.05	17.43	2.55	41098.78	134450.73	101206.24
40.01	17.62	2.45	39770.04	120458.93	95076.82
45.01	17.62	2.53	40280.30	131116.47	98717.72
50.01	17.37	2.43	38879.86	117309.94	91334.34
55.02	16.37	2.47	37611.19	115411.50	89666.24
60.01	17.12	2.38	37174.47	108263.85	86254.83
65.02	17.68	2.38	38561.19	110644.40	88327.70
70.01	17.37	2.47	38538.28	119591.56	90944.49
75.02	17.43	2.44	39005.49	117332.30	92488.41
80.00	17.57	2.49	39268.44	123182.17	94558.45
85.03	17.43	2.44	38594.81	115683.58	90840.97
90.02	17.54	2.48	39343.85	122047.80	94095.87
95.05	17.34	2.46	38146.53	117102.52	90571.96
100.04	17.23	2.47	38308.97	118128.48	91243.02
105.01	17.60	2.47	38853.03	119538.41	92075.86
110.03	17.15	2.46	37887.88	115626.05	89894.54
115.02	17.23	2.43	37751.96	113118.17	88832.70
120.01	17.31	2.51	38412.00	122517.87	92940.99
125.03	17.24	2.43	37720.98	112684.06	88127.62
130.00	17.37	2.48	38651.97	120756.61	93266.96
135.02	17.59	2.42	38568.46	114037.76	89916.29
140.02	17.49	2.48	38726.82	120312.88	91892.67
145.03	17.27	2.47	38289.26	117366.36	90778.91
150.02	17.52	2.48	38785.57	120016.61	92134.62
155.00	17.46	2.47	38739.61	118832.92	91312.54
160.00	17.51	2.42	38394.25	113341.80	89366.45
165.02	17.21	2.47	38298.34	119002.72	91351.28
170.03	17.52	2.42	38638.13	114485.66	90503.58
175.02	17.51	2.50	39354.75	124419.76	94299.48
180.03	17.43	2.49	39595.11	123396.63	94709.43

Table 35. Detailed simulation data from [AR= 0.90 / θ= 30 deg] model.

Time (s)	AreaPlane (m^2)	MeanVeloMag (m/s)	MassFlow (kg/s)	KEFlow (J/s)	MomentumFlow ($kg*m/s^2$)
0.00	19.86	2.00	39574.19	79148.38	79148.38
5.04	19.86	2.34	41280.84	116969.95	87867.70
10.02	19.86	2.25	41766.64	107757.94	88906.30
15.00	19.90	2.24	41801.18	106030.16	89509.82
20.02	19.86	2.30	42440.59	113597.89	93406.14
25.01	19.65	2.34	42948.55	118843.19	96209.67
30.00	19.61	2.29	41529.64	109928.90	90839.05
35.01	19.52	2.31	41677.77	112502.52	92175.07
40.05	19.90	2.30	41420.23	111756.22	90737.93
45.03	19.52	2.26	40771.43	105847.46	88621.99
50.04	19.44	2.30	40486.18	108367.21	88522.34
55.03	19.48	2.20	39794.67	97601.27	84090.26
60.04	19.86	2.20	39076.73	96615.97	81028.52
65.01	19.65	2.18	38108.31	93406.14	78854.00
70.01	18.81	2.18	38090.73	92802.81	79390.29
75.03	19.86	2.11	38558.27	86950.72	77556.98
80.00	19.90	2.22	39760.07	99515.55	83770.48
85.04	19.82	2.21	39717.76	97690.68	83588.76
90.02	19.65	2.23	39345.87	99356.02	83381.92
95.01	19.61	2.22	39799.16	99015.27	84249.41
100.04	19.48	2.28	40453.55	105969.54	88108.78
105.03	19.73	2.29	41036.86	108426.08	89229.12
110.00	19.61	2.30	40544.00	108957.54	88362.78
115.02	19.73	2.27	40519.89	105734.13	87357.71
120.04	19.65	2.32	40758.97	110785.62	89090.24
125.01	19.65	2.30	40626.45	108202.45	88230.64
130.03	19.65	2.32	40666.39	110675.31	88624.85
135.03	19.69	2.24	39917.00	100758.95	84898.32
140.01	19.44	2.26	39498.57	101672.95	84959.59
145.04	19.69	2.25	40538.30	103222.42	86797.22
150.01	19.73	2.24	39800.82	101243.23	84218.40
155.03	19.73	2.27	40114.48	103961.60	86124.16
160.02	19.86	2.25	40538.24	103380.61	86010.57
165.00	19.57	2.30	40126.33	106956.81	86216.54
170.03	19.82	2.25	39743.10	101442.63	83739.69
175.01	19.65	2.18	39468.48	94462.84	82435.22
180.03	19.86	2.21	40060.78	98340.07	83775.29

Table 36. Detailed simulation data from [AR= 0.30 / Inlet Length= 30 ft] model.

Time (s)	AreaPlane (m^2)	MeanVeloMag (m/s)	MassFlow (kg/s)	KEFlow (J/s)	MomentumFlow ($kg*m/s^2$)
0.00	6.62	2.00	13194.79	26389.58	26389.58
5.02	6.62	2.80	16881.43	67077.75	45792.27
10.00	4.91	3.54	16588.95	104361.01	57186.70
15.03	5.12	3.76	18624.46	132402.17	68454.04
20.01	6.79	2.48	15726.51	51774.86	38000.64
25.03	6.45	2.83	16771.36	67763.69	46059.97
30.02	5.29	2.84	14229.10	57601.00	39109.75
35.04	5.45	3.34	17256.37	97236.84	56378.03
40.01	5.45	3.04	15700.57	74280.42	46357.51
45.00	6.29	2.90	16576.25	70726.91	46508.19
50.04	5.20	3.08	15212.60	72803.34	45413.41
55.03	5.37	3.29	16606.36	90548.50	53077.17
60.03	5.29	3.14	15854.67	79807.74	48640.98
65.01	5.46	3.03	15678.00	73247.05	46261.57
70.02	5.62	3.03	15888.94	74081.55	46794.37
75.01	5.12	3.11	15233.28	74063.25	45939.34
80.03	5.29	3.26	16325.67	87696.21	51881.87
85.03	5.33	3.28	16695.59	91763.99	53619.09
90.03	5.41	3.14	16170.90	82413.59	49725.19
95.00	5.37	3.13	15791.53	79263.36	47943.13
100.00	5.33	3.34	16977.68	96524.88	55268.25
105.00	5.25	3.28	16438.80	90096.65	52596.49
110.03	5.21	3.38	16947.01	98199.72	55948.08
115.04	5.41	3.21	16486.22	87808.55	51763.56
120.01	5.37	3.25	16526.05	89682.34	52441.24
125.03	5.12	3.30	16147.06	88583.23	51584.04
130.01	5.20	3.32	16536.09	92281.22	53304.57
135.00	5.29	3.20	16170.93	84347.95	50327.30
140.01	5.29	3.21	16010.68	83612.08	49738.58
145.02	5.25	3.22	16147.57	84919.38	50590.43
150.02	5.16	3.30	16439.11	90347.74	52824.38
155.02	5.25	3.32	16794.73	94139.87	54625.28
160.00	5.33	3.21	16412.73	86926.09	51743.69
165.00	5.29	3.23	16256.19	86185.58	51067.57
170.00	5.33	3.34	16964.00	96430.47	55361.71
175.03	5.33	3.21	16407.81	87352.13	51773.24
180.02	5.41	3.22	16452.80	87381.17	51734.48

Table 37. Detailed simulation data from [AR= 0.40 / Inlet Length= 30 ft] model.

Time (s)	AreaPlane (m^2)	MeanVeloMag (m/s)	MassFlow (kg/s)	KEFlow (J/s)	MomentumFlow ($kg*m/s^2$)
0.00	8.83	2.00	17593.90	35187.80	35187.80
5.02	8.72	2.75	22111.06	83533.63	58318.99
10.00	6.66	3.49	22352.29	135986.63	75821.08
15.00	6.86	3.73	24713.65	172946.47	90246.91
20.05	8.91	2.73	22401.68	89294.88	60109.91
25.04	8.63	2.85	23055.49	94720.68	63771.39
30.03	7.13	3.31	22488.21	123136.35	72377.99
35.04	6.94	3.23	21598.24	114186.67	68272.17
40.01	7.14	3.30	22751.14	126442.69	73783.90
45.01	7.30	3.13	21846.75	109335.30	67179.39
50.00	7.38	3.11	21596.68	106505.56	65526.71
55.02	6.91	3.23	21389.82	112929.27	67555.61
60.02	7.05	3.30	22204.02	121727.46	71386.47
65.02	7.11	3.12	21317.17	105568.32	65030.36
70.02	7.36	3.02	20925.49	96899.62	61388.32
75.02	8.02	3.11	22739.89	111700.89	68744.55
80.02	7.02	3.18	21384.15	109382.99	66141.66
85.02	6.86	3.37	22378.73	128169.02	73811.59
90.01	7.08	3.28	22262.63	122305.05	71457.06
95.03	7.19	3.22	21997.11	117402.51	69197.70
100.01	7.30	3.26	22507.67	122186.16	71913.52
105.05	7.02	3.28	22054.27	120935.35	70600.16
110.02	6.94	3.34	22251.26	125473.80	72424.52
115.00	7.02	3.22	21761.45	114581.85	68387.38
120.04	7.36	3.26	22497.59	121873.33	71452.24
125.00	7.02	3.33	22376.18	125882.50	72674.16
130.01	7.02	3.30	22326.13	123579.92	72035.48
135.02	7.02	3.35	22732.64	130969.88	74983.62
140.01	7.11	3.22	22006.55	117302.70	69698.11
145.01	7.44	3.23	22649.96	120565.96	71586.26
150.02	7.02	3.32	22214.30	123253.61	71475.94
155.00	6.94	3.39	22688.11	131716.13	74951.09
160.00	7.02	3.30	22252.24	123650.35	71890.80
165.02	7.02	3.21	21528.50	112897.62	67595.84
170.02	7.02	3.26	22038.45	118233.74	70054.87
175.00	7.11	3.25	22077.05	117920.99	69999.09
180.03	7.19	3.29	22466.97	123372.11	71989.84

Table 38. Detailed simulation data from [AR= 0.50 / Inlet Length= 30 ft] model.

Time (s)	AreaPlane (m^2)	MeanVeloMag (m/s)	MassFlow (kg/s)	KEFlow (J/s)	MomentumFlow ($kg*m/s^2$)
0.00	11.03	2.00	21982.72	43965.44	43965.44
5.03	10.72	2.65	26761.97	94293.10	68978.85
10.04	8.39	3.43	27756.69	163407.05	92723.41
15.01	9.21	3.22	27952.48	148538.86	88297.49
20.05	10.96	2.72	28573.61	106967.30	75395.67
25.05	10.11	2.99	28044.40	126437.83	81828.41
30.01	8.55	3.22	26522.63	138140.94	83471.52
35.01	8.95	3.35	28650.60	162792.64	93951.10
40.02	8.77	3.25	27659.82	148985.05	88643.19
45.04	10.45	3.04	28542.08	135223.23	84904.60
50.04	8.73	3.23	26925.30	141822.55	85210.97
55.01	8.48	3.24	26521.54	140612.42	84082.55
60.03	8.71	3.20	26883.15	139851.34	84191.09
65.01	9.86	3.09	28246.04	137910.97	85494.56
70.01	9.39	3.01	26114.61	120396.83	76746.82
75.02	8.57	3.23	26550.23	139291.81	83544.80
80.03	8.56	3.20	26311.49	135812.63	81859.26
85.01	8.80	3.19	26735.52	137301.06	82899.62
90.02	8.56	3.16	26170.54	131830.56	80697.95
95.01	8.81	3.17	26482.00	134653.38	81552.73
100.01	8.56	3.22	26589.30	139141.61	83505.23
105.04	8.56	3.16	26140.92	131387.28	80812.87
110.03	8.73	3.21	26854.96	139578.16	83975.94
115.02	8.73	3.17	26313.32	133629.80	81009.47
120.04	8.95	3.17	26737.54	136899.27	82928.26
125.01	8.73	3.14	26097.93	130461.10	80198.41
130.00	8.55	3.19	26282.39	134967.55	82005.77
135.03	8.80	3.20	26901.67	138551.09	83636.14
140.04	8.64	3.16	26210.17	132328.03	80973.59
145.01	8.81	3.17	26737.89	136139.38	82852.37
150.01	8.71	3.19	26696.35	137199.88	83333.48
155.03	8.80	3.16	26512.17	134339.36	81825.56
160.01	8.89	3.14	26751.28	133213.28	81972.07
165.02	8.81	3.20	26977.24	139309.14	84403.07
170.01	8.64	3.27	27204.60	146408.81	86840.76
175.02	8.63	3.24	26819.06	142357.64	84695.40
180.01	8.96	3.18	27078.36	138982.00	84098.60

Table 39. Detailed simulation data from [AR= 0.60 / Inlet Length= 30 ft] model.

Time (s)	AreaPlane (m^2)	MeanVeloMag (m/s)	MassFlow (kg/s)	KEFlow (J/s)	MomentumFlow ($kg*m/s^2$)
0.00	13.24	2.00	26386.22	52772.43	52772.43
5.03	12.90	2.60	31502.05	107033.75	79663.45
10.03	10.24	3.09	30488.93	146077.31	91692.53
15.02	13.24	2.72	33583.94	126841.55	89242.17
20.02	13.07	2.82	34107.05	136558.47	93568.27
25.00	13.07	2.79	33106.82	129812.13	90110.88
30.03	11.24	3.10	32899.09	159769.84	100128.04
35.03	12.57	2.97	33309.89	150078.20	97174.51
40.03	12.82	3.01	34716.85	159197.80	101851.52
45.04	11.66	3.01	32665.98	149976.25	96261.74
50.02	10.99	3.07	31504.88	150163.20	94321.24
55.03	10.66	3.05	31575.99	149803.52	95431.31
60.01	11.15	2.93	30658.57	133915.86	88227.82
65.02	11.57	2.98	32446.53	146618.02	95615.93
70.01	11.82	2.98	32148.03	145216.13	93459.02
75.01	10.57	3.08	31283.10	151013.52	94567.66
80.01	10.24	3.04	29975.17	139891.50	89178.09
85.01	12.07	3.03	33037.82	156141.39	98988.98
90.02	11.24	3.00	31346.98	143928.02	92237.73
95.03	10.49	3.03	30445.51	142400.52	90710.39
100.04	10.74	3.04	31242.18	147747.33	93374.61
105.03	10.41	3.02	30151.30	139771.67	89137.67
110.03	10.16	3.06	30081.72	142945.34	90532.59
115.04	10.41	3.08	30878.79	148971.09	93294.91
120.02	10.32	3.00	29997.33	137438.39	88907.99
125.01	10.74	3.07	31587.28	150800.72	94909.26
130.04	10.41	3.08	30915.41	148104.63	93404.17
135.02	10.49	2.99	30144.34	137548.31	88688.42
140.03	10.41	3.09	30649.83	149132.09	93024.62
145.00	10.24	3.08	30477.25	146536.64	91971.52
150.04	10.49	3.03	30313.26	142097.13	90128.99
155.00	10.41	3.07	30472.47	146361.80	91569.68
160.02	10.16	3.10	30243.26	147198.73	91959.17
165.03	10.41	3.09	30826.17	149886.08	93324.70
170.00	10.24	3.05	30341.55	142478.63	91146.60
175.00	10.24	3.06	30532.74	144685.58	92568.91
180.01	10.66	3.06	31114.82	147595.45	92668.79

Table 40. Detailed simulation data from [AR= 0.70 / Inlet Length= 30 ft] model.

Time (s)	AreaPlane (m^2)	MeanVeloMag (m/s)	MassFlow (kg/s)	KEFlow (J/s)	MomentumFlow ($kg*m/s^2$)
0.00	15.44	2.00	30781.83	61563.65	61563.65
5.01	15.18	2.52	36029.08	114575.50	87930.17
10.01	14.83	2.63	34993.64	122450.67	88799.73
15.01	15.44	2.64	37925.32	133723.06	97133.10
20.04	15.44	2.57	37065.63	122856.52	92117.02
25.02	15.18	2.78	37983.53	147936.66	102332.64
30.01	15.26	2.71	37301.95	138191.11	98256.11
35.01	14.70	2.76	37420.46	144503.89	100498.06
40.01	15.08	2.71	37338.31	138538.47	98144.21
45.02	15.10	2.73	36930.14	139992.70	98096.55
50.00	14.66	2.71	35875.12	134201.02	95035.93
55.01	15.20	2.69	36539.01	133796.95	95908.23
60.04	14.90	2.59	34858.21	118795.41	87844.80
65.05	14.90	2.64	35309.88	125012.53	90735.23
70.01	14.75	2.63	34870.85	122541.41	88793.25
75.02	14.82	2.68	35389.28	128544.73	91416.50
80.03	15.04	2.66	35589.99	128044.15	91735.26
85.05	15.11	2.75	36508.88	141538.02	97837.22
90.05	15.11	2.72	36351.34	137486.19	96247.49
95.02	14.83	2.71	35441.02	131929.45	93282.55
100.00	14.93	2.70	35830.36	132456.00	93690.01
105.02	15.03	2.70	36201.81	134542.75	95085.41
110.01	14.76	2.72	35844.77	135442.73	94911.81
115.03	14.73	2.72	35718.23	134036.52	94510.64
120.01	14.86	2.74	36367.34	138708.84	96906.07
125.01	14.91	2.70	35774.06	132261.16	93625.97
130.01	14.75	2.66	34587.68	125250.05	89914.95
135.03	15.10	2.67	35794.17	129995.00	92606.39
140.00	15.03	2.67	35926.55	130479.53	93474.63
145.03	14.65	2.70	35317.78	131730.27	92673.95
150.02	14.73	2.67	35220.55	128110.42	91683.34
155.01	15.03	2.73	36586.37	139180.20	97533.41
160.01	15.28	2.56	35576.14	119069.16	88845.62
165.00	14.40	2.79	36158.71	143378.94	98928.98
170.01	15.10	2.57	35279.73	117398.12	88137.70
175.01	15.10	2.75	36887.20	141478.16	99044.66
180.01	15.36	2.63	36704.39	128737.63	93494.62

Table 41. Detailed simulation data from [AR= 0.80 / Inlet Length= 30 ft] model.

Time (s)	AreaPlane (m^2)	MeanVeloMag (m/s)	MassFlow (kg/s)	KEFlow (J/s)	MomentumFlow ($kg*m/s^2$)
0.00	17.65	2.00	35179.89	70359.79	70359.79
5.02	17.67	2.41	39745.30	115614.36	92196.94
10.02	17.60	2.34	38481.96	106378.52	86698.18
15.02	17.54	2.52	41415.02	132617.42	101044.84
20.01	17.62	2.41	40110.92	116989.80	93137.62
25.04	17.48	2.52	40529.12	129511.63	98462.33
30.02	17.60	2.56	41240.29	135531.39	101948.97
35.05	17.34	2.54	40462.08	130883.52	99364.78
40.00	17.59	2.51	40307.39	127847.02	97665.59
45.00	16.59	2.48	38149.11	117949.11	91184.34
50.04	17.54	2.38	37719.01	108658.01	86742.86
55.02	17.18	2.37	36936.01	104805.90	84576.51
60.03	17.12	2.31	36225.41	98709.52	81042.07
65.04	17.46	2.36	37523.08	105951.01	85150.77
70.01	17.54	2.34	37507.59	104423.21	84962.23
75.01	17.52	2.43	38140.08	114617.16	89428.32
80.04	17.31	2.45	37622.07	114890.82	89096.42
85.01	17.46	2.40	38231.97	111987.87	88611.16
90.03	17.57	2.42	38534.14	114452.59	90302.80
95.03	17.09	2.43	37168.00	112014.53	87580.17
100.03	17.65	2.45	39064.79	118630.65	92996.29
105.02	17.49	2.44	38452.80	116423.70	90007.75
110.04	17.35	2.46	37626.23	116525.15	89169.02
115.02	17.85	2.40	38428.66	113195.02	89082.23
120.03	17.24	2.44	38056.25	115545.52	89676.41
125.02	17.40	2.45	38225.49	117533.63	90778.04
130.02	17.57	2.50	39529.30	126085.21	96044.02
135.01	17.45	2.44	38462.25	116117.88	90646.39
140.02	17.27	2.47	38507.61	118470.87	92780.38
145.05	17.31	2.45	37977.14	115521.68	89665.64
150.01	17.54	2.41	38696.26	114361.55	90423.91
155.03	17.48	2.48	39135.86	122106.82	94081.31
160.01	17.29	2.42	37914.09	113148.06	89167.42
165.01	17.62	2.43	39281.63	117607.41	91896.55
170.02	17.32	2.44	37644.56	114251.42	88582.77
175.02	17.31	2.46	38219.82	118127.37	91012.35
180.03	17.51	2.40	38493.66	112746.97	89440.13

Table 42. Detailed simulation data from [AR= 0.90 / Inlet Length= 30 ft] model.

Time (s)	AreaPlane (m^2)	MeanVeloMag (m/s)	MassFlow (kg/s)	KEFlow (J/s)	MomentumFlow ($kg*m/s^2$)
0.00	19.86	2.00	39577.90	79155.80	79155.80
5.03	19.86	2.23	42012.54	104867.19	90007.52
10.01	19.86	2.23	41787.56	105211.73	89272.23
15.04	19.90	2.24	41975.80	106067.13	89882.51
20.01	19.81	2.30	42821.75	114263.88	94491.61
25.01	19.86	2.29	42644.31	112852.10	94175.25
30.03	19.90	2.29	42702.59	112947.96	93843.65
35.04	19.73	2.27	41341.09	107605.62	89419.92
40.01	19.73	2.24	40864.85	103983.45	87013.34
45.03	19.78	2.23	40899.63	102952.83	87304.38
50.03	19.99	2.23	39677.41	100186.88	84480.98
55.02	19.40	2.19	38668.55	94024.13	80146.56
60.01	19.56	2.19	38924.92	93641.83	80916.77
65.04	19.81	2.20	38970.04	95923.78	81249.64
70.01	19.74	2.20	39525.31	97069.14	82368.61
75.02	19.69	2.20	39465.60	96882.91	82371.08
80.03	19.81	2.23	40020.69	101755.07	85147.21
85.02	19.86	2.22	40705.96	101389.91	86109.74
90.03	19.61	2.21	39720.09	98003.51	83842.84
95.00	19.64	2.24	39435.26	99960.95	84064.92
100.04	19.78	2.25	40511.59	104084.87	86825.95
105.00	19.73	2.23	40171.65	101305.28	85617.59
110.03	19.90	2.21	40007.04	99266.02	84464.88
115.02	19.78	2.24	39942.48	102042.88	85216.13
120.02	19.69	2.21	39756.44	98718.27	83978.48
125.03	19.77	2.27	40601.88	105280.80	87628.04
130.03	19.65	2.21	39850.41	98235.31	83891.87
135.03	19.78	2.29	40946.83	108857.97	89628.41
140.03	19.78	2.20	39470.14	97285.23	82529.51
145.01	19.65	2.24	39981.51	101925.73	85595.27
150.01	19.73	2.23	39972.87	100391.71	85265.92
155.02	19.74	2.22	39979.86	99449.53	84631.94
160.00	19.52	2.20	38987.00	95642.16	81938.17
165.02	19.35	2.20	38432.31	94369.23	80304.16
170.04	19.86	2.21	39768.45	98601.74	83607.78
175.02	19.90	2.20	40364.39	99632.77	84716.41
180.03	19.65	2.22	39753.90	99123.68	84632.35

Table 43. Detailed simulation data from [AR= 0.30 / Inlet Length= 60 ft] model.

Time (s)	AreaPlane (m^2)	MeanVeloMag (m/s)	MassFlow (kg/s)	KEFlow (J/s)	MomentumFlow ($kg*m/s^2$)
0.00	6.62	2.00	13192.56	26385.13	26385.13
5.03	7.04	3.27	21854.68	117619.85	69722.26
10.02	4.83	3.23	14753.00	77278.18	46016.20
15.03	5.04	3.58	17211.01	110645.18	59685.14
20.05	5.16	3.60	17734.62	115525.77	61659.68
25.02	6.79	2.28	14192.33	37431.96	30357.20
30.02	6.33	2.58	14718.18	49399.54	35867.56
35.03	5.04	3.24	15503.81	81700.43	48471.94
40.03	5.04	3.20	15509.68	79621.86	48034.48
45.03	6.79	2.65	16499.29	59321.57	41881.67
50.01	5.54	2.97	14903.63	66605.36	42573.56
55.02	5.83	2.89	15203.87	64838.47	42195.71
60.04	5.12	3.26	15727.08	84399.55	49551.11
65.03	5.16	3.34	16498.35	92516.95	53358.58
70.01	6.24	2.97	16590.15	76784.11	48041.56
75.02	5.16	3.18	15347.85	78390.88	47300.16
80.02	5.20	3.32	16405.13	91394.48	52828.23
85.01	5.20	3.43	17119.39	101191.86	57050.32
90.02	5.29	3.41	17072.90	99651.80	56300.88
95.03	5.16	3.46	17158.07	103092.09	57422.57
100.02	5.25	3.43	17135.14	101510.76	56973.62
105.02	5.25	3.40	17063.13	99653.66	56248.17
110.02	5.04	3.44	16476.11	97850.21	54856.57
115.02	4.95	3.55	16760.23	106675.26	57811.05
120.00	5.08	3.51	17099.41	105761.42	58084.16
125.01	5.25	3.46	17383.15	104455.06	58279.99
130.01	5.08	3.39	16232.31	94719.98	53436.91
135.03	5.12	3.40	16542.76	96296.19	54404.57
140.01	5.12	3.43	16644.34	98582.13	55210.53
145.00	5.37	3.37	17341.22	99897.41	56997.31
150.01	5.33	3.45	17375.01	105240.10	58352.43
155.04	5.29	3.40	17273.12	100689.37	56849.34
160.00	5.29	3.45	17313.69	104136.34	57838.70
165.03	5.20	3.43	16853.77	101002.13	56139.61
170.02	4.96	3.39	15967.03	92269.86	52501.60
175.02	5.29	3.41	17185.35	101328.75	56883.07
180.03	5.37	3.41	17317.85	102140.15	57280.29

Table 44. Detailed simulation data from [AR= 0.40 / Inlet Length= 60 ft] model.

Time (s)	AreaPlane (m^2)	MeanVeloMag (m/s)	MassFlow (kg/s)	KEFlow (J/s)	MomentumFlow ($kg*m/s^2$)
0.00	8.83	2.00	17588.71	35177.42	35177.42
5.04	9.10	3.08	27008.10	128520.59	81182.02
10.03	6.58	3.35	20832.87	116773.82	67378.23
15.03	6.85	3.72	23800.98	164611.48	85734.71
20.01	6.94	3.59	23787.04	154463.80	82528.75
25.04	9.24	2.43	20812.41	62703.37	47824.36
30.03	7.10	3.31	22404.19	123156.34	71953.58
35.00	6.94	3.40	22554.39	130600.69	74411.80
40.02	6.83	3.41	21955.44	128309.29	72532.13
45.02	7.30	3.25	22555.01	121556.66	71498.82
50.01	8.38	2.85	21092.15	87175.24	58105.15
55.00	6.80	3.32	21349.07	118195.20	68821.63
60.04	6.80	3.32	21496.63	118649.85	68805.70
65.02	6.83	3.37	21849.29	124180.27	71085.02
70.04	7.05	3.33	22401.65	125154.02	72323.65
75.02	7.02	3.15	20971.36	105358.36	64069.52
80.03	7.21	3.31	22584.18	125177.63	72648.77
85.02	6.83	3.55	23018.67	146018.23	79489.51
90.03	6.77	3.62	23427.64	153943.19	82573.72
95.01	6.91	3.60	23553.46	152731.72	82032.05
100.05	6.99	3.51	23527.31	146193.58	79993.71
105.03	6.91	3.46	22909.46	137945.22	76956.40
110.00	6.80	3.48	22603.83	137356.64	76240.14
115.04	6.85	3.59	23577.90	152259.41	82088.84
120.03	6.94	3.60	23788.82	154226.31	82918.14
125.01	6.99	3.63	24142.63	159463.42	84954.61
130.01	7.10	3.46	23409.32	141824.83	78591.52
135.01	7.07	3.41	22818.52	135458.92	75835.41
140.04	7.02	3.52	23520.39	147644.11	80399.13
145.01	6.72	3.62	23241.00	152348.64	81414.87
150.04	6.80	3.62	23377.49	153998.05	81811.29
155.02	6.88	3.52	23114.13	144357.80	78956.70
160.02	7.10	3.43	23337.49	139018.84	78029.55
165.01	6.85	3.47	22737.35	138137.13	76818.93
170.01	7.02	3.49	23449.27	143942.41	79582.52
175.03	6.74	3.54	22885.77	143707.25	78656.91
180.02	7.08	3.49	23751.99	146424.64	81020.23

Table 45. Detailed simulation data from [AR= 0.50 / Inlet Length= 60 ft] model.

Time (s)	AreaPlane (m^2)	MeanVeloMag (m/s)	MassFlow (kg/s)	KEFlow (J/s)	MomentumFlow ($kg*m/s^2$)
0.00	11.03	2.00	21981.34	43962.68	43962.68
5.05	11.03	2.91	30890.79	131047.41	88038.77
10.02	8.56	3.32	27280.88	150573.03	87987.06
15.03	8.48	3.43	28124.48	165967.56	94027.32
20.04	10.71	2.97	28845.52	130188.41	83320.28
25.02	11.03	2.80	29647.69	117143.15	80656.05
30.05	10.71	3.21	30883.17	159626.00	96280.78
35.01	8.39	3.45	27919.09	166308.81	93836.16
40.01	8.55	3.46	28561.59	171042.81	96469.43
45.00	10.93	2.97	28997.61	130906.44	83579.04
50.01	10.21	2.89	26921.13	113851.70	75824.74
55.04	8.73	3.32	27755.42	153628.05	89708.90
60.00	8.63	3.28	27231.93	146975.05	86966.63
65.03	8.57	3.21	26470.12	137235.16	83211.86
70.01	10.29	3.09	28546.75	138846.75	86531.13
75.04	9.36	3.19	27810.15	143685.50	87112.84
80.03	8.63	3.31	27374.84	151701.94	88154.16
85.02	8.55	3.43	27831.93	164273.27	92736.18
90.01	8.56	3.35	27587.88	156330.42	90015.44
95.01	9.10	3.19	27595.74	142686.09	85714.18
100.03	8.96	3.29	28099.51	154466.89	90410.06
105.01	8.53	3.37	27760.43	159666.09	91830.63
110.02	8.80	3.23	26920.40	142666.72	84802.66
115.04	8.55	3.31	27125.43	149459.77	87378.68
120.02	8.73	3.30	27431.21	151993.06	88690.41
125.01	8.46	3.26	26556.33	142204.36	83958.57
130.01	8.62	3.30	27073.62	148228.98	87128.64
135.03	8.71	3.31	27599.92	153265.50	89418.19
140.05	8.53	3.29	27004.60	147115.56	86270.51
145.03	8.80	3.25	27094.60	145010.83	86033.38
150.04	8.55	3.26	26846.93	143500.08	85154.60
155.01	8.71	3.22	26729.49	141576.72	84476.60
160.04	8.41	3.37	27277.94	156198.80	89826.24
165.02	8.87	3.33	28114.16	158851.70	91320.71
170.03	8.78	3.36	28269.46	161031.91	92447.06
175.00	8.55	3.31	27141.68	149924.52	87504.38
180.03	8.78	3.20	26821.74	139574.67	83764.55

Table 46. Detailed simulation data from [AR= 0.60 / Inlet Length= 60 ft] model.

Time (s)	AreaPlane (m^2)	MeanVeloMag (m/s)	MassFlow (kg/s)	KEFlow (J/s)	MomentumFlow ($kg*m/s^2$)
0.00	13.24	2.00	26384.86	52769.71	52769.71
5.01	13.07	2.75	34868.36	132328.06	93762.73
10.02	10.32	3.09	30622.63	146012.02	91930.96
15.02	12.90	2.82	32203.46	129779.07	88248.44
20.04	12.57	2.95	33499.84	148613.72	96924.39
25.04	13.24	2.71	33799.93	124558.67	88506.80
30.02	11.99	3.12	33826.04	165289.05	102846.14
35.02	10.75	3.13	32076.49	158973.72	97987.08
40.01	11.41	2.99	32041.32	144386.86	94360.82
45.02	13.07	2.89	33848.64	144576.55	96146.04
50.02	12.40	2.92	32305.03	140101.27	92558.30
55.02	10.24	3.17	31028.70	157227.97	96231.82
60.01	10.41	3.07	30613.86	145600.39	91838.49
65.04	11.99	2.93	32074.34	139213.27	91651.95
70.02	11.41	3.03	31898.54	149434.95	95010.57
75.00	12.66	2.97	33561.99	151890.34	97636.35
80.00	10.32	3.14	30947.78	154038.28	94970.34
85.01	10.49	3.11	31408.16	153093.78	95380.92
90.03	11.74	2.92	31435.95	137500.41	90194.23
95.02	11.57	3.04	32397.02	152401.47	96562.58
100.03	10.91	3.04	31288.36	147821.47	93051.61
105.02	10.32	3.01	29546.03	136132.00	86948.51
110.01	10.41	3.06	30259.17	143268.84	90365.41
115.01	10.24	3.10	30558.15	147482.69	92345.08
120.04	10.32	3.01	29530.44	135586.86	86773.44
125.02	11.07	3.06	31500.78	149309.19	94179.09
130.03	10.24	3.11	30447.89	148925.16	92563.86
135.02	10.49	3.06	30936.07	146101.30	92230.84
140.00	10.33	3.10	30876.60	148965.69	93253.27
145.02	12.65	2.98	33424.48	152748.34	97993.02
150.00	12.07	2.98	32603.07	149522.89	95847.61
155.04	10.07	3.15	30382.59	151750.53	93362.84
160.04	10.32	3.15	31206.27	156954.33	96115.14
165.02	12.16	2.97	32498.48	146106.39	94483.57
170.04	12.24	3.04	33434.55	158785.28	99989.53
175.02	12.91	3.00	34326.84	160398.19	101841.85
180.04	10.24	3.09	30358.98	146031.98	91548.72

Table 47. Detailed simulation data from [AR= 0.70 / Inlet Length= 60 ft] model.

Time (s)	AreaPlane (m^2)	MeanVeloMag (m/s)	MassFlow (kg/s)	KEFlow (J/s)	MomentumFlow ($kg*m/s^2$)
0.00	15.44	2.00	30781.83	61563.65	61563.65
5.01	15.18	2.52	36029.08	114575.50	87930.17
10.01	14.83	2.63	34993.64	122450.67	88799.73
15.01	15.44	2.64	37925.32	133723.06	97133.10
20.04	15.44	2.57	37065.63	122856.52	92117.02
25.02	15.18	2.78	37983.53	147936.66	102332.64
30.01	15.26	2.71	37301.95	138191.11	98256.11
35.01	14.70	2.76	37420.46	144503.89	100498.06
40.01	15.08	2.71	37338.31	138538.47	98144.21
45.02	15.10	2.73	36930.14	139992.70	98096.55
50.00	14.66	2.71	35875.12	134201.02	95035.93
55.01	15.20	2.69	36539.01	133796.95	95908.23
60.04	14.90	2.59	34858.21	118795.41	87844.80
65.05	14.90	2.64	35309.88	125012.53	90735.23
70.01	14.75	2.63	34870.85	122541.41	88793.25
75.02	14.82	2.68	35389.28	128544.73	91416.50
80.03	15.04	2.66	35589.99	128044.15	91735.26
85.05	15.11	2.75	36508.88	141538.02	97837.22
90.05	15.11	2.72	36351.34	137486.19	96247.49
95.02	14.83	2.71	35441.02	131929.45	93282.55
100.00	14.93	2.70	35830.36	132456.00	93690.01
105.02	15.03	2.70	36201.81	134542.75	95085.41
110.01	14.76	2.72	35844.77	135442.73	94911.81
115.03	14.73	2.72	35718.23	134036.52	94510.64
120.01	14.86	2.74	36367.34	138708.84	96906.07
125.01	14.91	2.70	35774.06	132261.16	93625.97
130.01	14.75	2.66	34587.68	125250.05	89914.95
135.03	15.10	2.67	35794.17	129995.00	92606.39
140.00	15.03	2.67	35926.55	130479.53	93474.63
145.03	14.65	2.70	35317.78	131730.27	92673.95
150.02	14.73	2.67	35220.55	128110.42	91683.34
155.01	15.03	2.73	36586.37	139180.20	97533.41
160.01	15.28	2.56	35576.14	119069.16	88845.62
165.00	14.40	2.79	36158.71	143378.94	98928.98
170.01	15.10	2.57	35279.73	117398.12	88137.70
175.01	15.10	2.75	36887.20	141478.16	99044.66
180.01	15.36	2.63	36704.39	128737.63	93494.62

Table 48. Detailed simulation data from [AR= 0.80 / Inlet Length= 60 ft] model.

Time (s)	AreaPlane (m^2)	MeanVeloMag (m/s)	MassFlow (kg/s)	KEFlow (J/s)	MomentumFlow ($kg*m/s^2$)
0.00	17.65	2.00	35180.87	70361.74	70361.74
5.03	17.60	2.46	41183.48	124911.55	98205.75
10.02	17.68	2.36	38583.46	107672.87	87416.78
15.03	17.24	2.54	39812.64	130194.86	97858.95
20.02	17.85	2.31	38796.11	104477.91	85856.88
25.02	17.68	2.50	40409.13	126727.32	96593.12
30.02	17.46	2.61	42177.49	144384.17	106039.44
35.00	16.96	2.40	37420.61	109117.80	86755.38
40.02	17.65	2.44	39581.38	118991.00	93416.23
45.02	17.74	2.41	39426.26	114734.51	90963.51
50.04	17.26	2.46	37998.86	116113.70	89533.52
55.04	17.63	2.39	37659.11	108309.30	87336.93
60.01	17.54	2.26	36125.18	93486.30	78761.05
65.02	17.79	2.35	37845.90	105142.26	84788.55
70.04	17.43	2.38	36988.86	106481.59	84476.75
75.01	17.77	2.39	37707.65	108682.31	86121.17
80.04	17.49	2.38	37468.93	107635.79	85222.99
85.01	17.65	2.42	38566.08	114274.26	90487.41
90.04	17.54	2.41	37473.39	110291.39	86134.66
95.03	17.12	2.40	36794.16	107864.05	84877.95
100.02	17.15	2.45	37554.91	114772.59	89082.51
105.01	17.68	2.45	39312.51	119167.27	92614.63
110.02	17.34	2.45	37934.90	115085.66	88914.90
115.03	17.35	2.49	37954.09	119930.16	91142.80
120.01	17.40	2.40	37426.93	108994.45	86481.14
125.04	17.65	2.47	39407.35	121903.98	93580.39
130.01	17.49	2.51	38731.93	123331.18	93336.51
135.00	17.59	2.49	39440.54	124095.63	94729.41
140.02	17.24	2.46	37850.51	115578.14	89846.06
145.02	17.49	2.49	39002.56	122735.74	93402.45
150.03	17.54	2.50	38958.89	123559.17	93783.80
155.02	17.27	2.49	38569.97	121410.09	92943.38
160.00	17.24	2.43	37934.96	113540.76	88955.85
165.04	17.60	2.49	39597.70	124116.54	95621.42
170.04	17.54	2.46	38408.90	117685.13	90606.59
175.00	17.57	2.55	39553.06	130367.39	96981.70
180.01	17.35	2.42	38637.95	114650.35	90301.62

Table 49. Detailed simulation data from [AR= 0.90 / Inlet Length= 60 ft] model.

Time (s)	AreaPlane (m^2)	MeanVeloMag (m/s)	MassFlow (kg/s)	KEFlow (J/s)	MomentumFlow ($kg*m/s^2$)
0.00	19.86	2.00	39581.14	79162.29	79162.29
5.03	19.86	2.27	42987.83	110962.16	93630.98
10.03	19.82	2.23	41543.28	103517.65	88362.04
15.01	19.86	2.29	42424.61	111977.19	92232.39
20.03	19.90	2.25	41324.72	105618.52	88164.30
25.03	19.99	2.29	42268.52	112317.31	91976.37
30.01	19.73	2.31	42260.15	113826.48	92424.05
35.01	19.69	2.27	40007.79	104981.54	85970.09
40.01	19.99	2.18	39893.90	95912.59	82189.85
45.03	19.86	2.27	41279.19	107350.43	88777.26
50.02	19.82	2.25	40391.66	103941.09	86360.58
55.01	19.86	2.10	37595.49	84141.27	74531.73
60.01	19.69	2.13	38393.82	87869.34	77534.58
65.02	19.86	2.22	40147.39	100970.86	84649.84
70.03	19.82	2.17	38681.57	92812.27	79505.93
75.01	19.73	2.23	39612.18	100504.55	84080.24
80.03	19.86	2.18	39447.32	95330.02	81576.26
85.02	19.82	2.19	39505.16	96917.60	82361.18
90.05	19.90	2.21	39797.98	99087.82	83211.42
95.03	19.65	2.28	39690.87	105463.30	86269.44
100.02	19.52	2.19	38917.84	94901.12	81185.48
105.01	19.69	2.19	38951.90	94725.91	81191.77
110.05	19.57	2.19	39154.40	96007.42	81592.67
115.00	19.73	2.20	39024.53	96109.45	81523.25
120.01	19.69	2.25	40086.29	103186.88	85800.45
125.02	19.56	2.19	38334.81	93999.59	79528.08
130.03	19.82	2.24	40124.75	102028.97	85308.33
135.01	19.78	2.23	39599.41	99894.96	83678.40
140.02	19.36	2.22	38700.30	96921.59	81564.08
145.04	19.94	2.16	38894.48	92751.31	79839.13
150.01	19.44	2.23	39079.02	98392.32	82586.24
155.00	19.77	2.22	39629.03	99368.70	83896.21
160.02	19.65	2.19	39141.58	95630.42	81469.62
165.03	19.94	2.22	40378.91	100895.43	85060.48
170.00	19.82	2.23	40258.12	102212.23	85591.04
175.03	19.82	2.20	39572.24	97012.78	82628.15
180.02	19.82	2.20	40083.92	98202.78	84211.23